Structural Control of Monodisperse Polylactide Microspheres by Microfluidic Emulsification and Solvent Diffusion

Takaichi Watanabe

A thesis submitted in fulfilment of the requirements for the degree of Doctor of Philosophy and the Diploma of Okayama University

Division of Applied Chemistry and Biotechnology, Graduate School of Natural Science and Technology, Okayama University

March 2014

Declaration of Originality

The material presented in this thesis is entirely the result of my own independent research under the supervision of Professor Tsutomu Ono at Okayama University. All published and unpublished material used in this thesis has been given full acknowledgement.

Takaichi Watanabe

Okayama, February 2014

Abstract

The aim of this study is to develop a simple process for preparing monodisperse polylactide (PLA) microparticles and to control their structures by making use of droplet-based microfluidics and solvent diffusion, coupled with physicochemical phenomena. Microfluidics is the fluid analogue of microelectronic circuits, enabling precise handling of pico-liter scale fluids in microchannels and thus generating uniform-sized emulsion droplets with ease. Solvent diffusion method is one of polymer precipitation method using oil-in-water (O/W) emulsions in which the dispersed organic phase is partially miscible with water, such as ethyl acetate (EA) and methylethylketone. Because of high solubility of these solvents in water, microspheres are quickly obtained just by diluting emulsion with a large amount of pure water, which considerably shortens preparation time, compared with the conventional techniques. In addition, EA is a relatively low-toxic organic solvent approved by the Food and Drug Administration in the US, which reduces environmental burden. Therefore, a combinatorial method of microfluidic emulsification and subsequent solvent diffusion is an environmentally friendly process, enabling continuous generation of monodisperse PLA microspheres.

Chapter 1 reviews fundamentals of biocompatible polymers and conventional polymer particle engineering. The classical preparation methods are presented. Especially, fabrication methods of polymer particles from emulsion droplets are introduced. In addition, recent development of microfluidic technology in terms of emulsification and material preparations has been represented. Finally, motivation, objective and brief strategy of this study are mentioned.

Chapter 2 reports the preparation of monodisperse PLA microparticles with a compact structure by combining microfluidic emulsification with solvent diffusion. PLA and amphiphilic poly(ethylene glycol)-*b*-poly(D,L-lactide) (PEG-*b*-PLA) were synthesized *via* ring-opening polymerization of D,L-lactide. The interfacial activity of water-soluble PEG-*b*-PLA (w-PEG-*b*-PLA) between EA and water saturated with EA was measured using a Wilhelmy plate method. The effect of flow rate upon microfluidic emulsification and the initial PLA concentration on the droplet size and the resultant microparticle size was investigated, with theoretical calculations. In addition, structural control of the microspheres by addition of oil-soluble PEG-*b*-PLA (o-PEG-*b*-PLA) in the dispersed phase was exploited.

In chapter 3, the studies relating to preparing monodipserse microcapsules consisting of an oil core and a polymeric shell of PLA by means of internal phase separation between a concentrated polymer phase and a non-solvent phase during solvent diffusion have been demonstrated. The suitable oil core for the preparation of microcapsules with core-shell structures was firstly determined by using spreading coefficient theory based on interfacial tensions in the emulsion system. Preparation of monodisperse PLA microcapsules encapsulating perfluoroocyl bromide (PFOB) has been employed by microfluidic emulsification and internal phase separation during solvent diffusion. The effect of the preparation conditions such as flow rate upon emulsification and concentration of the non-solvent on the diameter of the microcapsules and the core-shell ratio was investigated. In addition, microcapsule formation at a non-equilibrium state during internal phase separation has been developed. Based on *in-situ* observation of solvent diffusion process, the formation mechanism of the microcapsules with distinct morphology was proposed.

Chapter 4 represents the preparation of monodisperse microcapsules encapsulating a single aqueous core by spontaneous emulsification induced by pre-synthesized amphiphilic diblock copolymer, poly(D,L-lactide)-*b*-poly(2-dimethylaminoethyl methacrylate) (PLA-*b*-PDMAEMA) from simple O/W emulsion system during the formulation. The amphiphilic PLA-*b*-PDMAEMA was synthesized through 3-step process, including a synthesis of bifunctional initiator, a ring-opening polymerization of D,L-lactide in the presence of the initiator, and an atom transfer radical polymerization (ATRP) of DMAEMA using the PLA-based macroinitiator, which was used as a co-surfactant. The effect of blend ratio of PLA-*b*-PDMAEMA to PLA into the dispersed phase on the final structure of the microparticles was investigated. Moreover, dual encapsulation of hydrophobic and hydrophilic substances into the microcapsules was demonstrated and confirmed by fluorescence microscopic observation. Furthermore, the microcapsule formation mechanism has been proposed on the basis of sequential optical microscopic observation during solvent diffusion from the droplets.

Chapter 5 concludes this work and establishes prospects for future study.

Acknowledgements

The work hereby presented was carried out successfully owing to direct and indirect contributions from many people. First and foremost, I would like to thank my supervisors: Professor Tsutomu Ono and Professor Yukitaka Kimura for providing many suggestions during the course of the research. Their passion and expertise, as well as their encouragement are truly appreciated. They have inspired my interest in the research area and helped me complete this study.

I would like to offer my thanks to Dr. João Cabral (Imperial College London) for giving me a chance to learn microfluidic processing as well as polymer physics for 1 year. Although the work is not presented in the main chapters, it has contributed importantly to my education in polymer science as well as microfluidic processing.

I thank Professor Seiji Suga (Okayama University), Professor Kuniaki Goto (Okayama University) and Associated Professor Toshinori Shimanouchi (Okayama University) for providing valuable advices during my PhD course. I am also grateful to Dr. Toshiyuki Oshiki (Okayama University) for setting up argon lines in our lab and teaching me a basic skill for controlled radical polymerization.

I appreciate Associate Professor Ken-ichi Ogawara and Mr. Tomoya Araki (Division of Pharmaceutical Sciences, Okayama University) for discussing development of polymer nanoparticles as a joint research.

I am grateful to all past and present colleagues at Interface Process Engineering (at Division of Applied Chemistry and Biotechnology, Okayama University), Environmental Process Engineering (at Division of Material and Energy Science, Okayama University), and Polymers and Microfluidics (at Department of Chemical Engineering, Imperial College London) laboratories for providing very much needed advice during the whole course of the study. My special gratitude is extended to Dr. Makoto Muranaka for teaching me how to precede the research, Dr. Masahiro Yasukawa (Kobe University) for stimulating my interest in PhD course, Dr. Muhammad Moniruzzaman (Universiti Teknologi Petronas) for giving me much attention in biomaterials, Dr. Ana-Maria Oprea (Okayama University) for spending much time to discuss particle formulations and drug release studies, Dr. Joanna Davies (Imperial College London) for teaching me how to fabricate microfluidic devices, Mr. Gonzalez Lopez Carlos (Imperial College London) for teaching me about polymer physics and

polylactide group members, including Mr. Ken Hirota, Ms. Moe Kitanaka, Mr. Tetsuya Inooka, Mr. Kazuhisa Kishimoto, Mr. Yuki Tanaka, and Mr. Yoichiro Ise for intensive contribution to development of solvent diffusion processing in the last 6 years together with me.

I appreciate Associate Professor Yasuhiko Benino (Okayama University), Mr. Nobuyuki Tanaka (Okayama University) and Mr. Toshihiko Tsuneyoshi (Okayama University) for measuring the surface chemical composition on microcapsules by XPS.

I also thank Mr. Yasuji Akiba and Mr. Shin-ichi Onoda for helping me order variety kinds of materials and equipment.

Finally, I am deeply grateful to my family, relatives, and friends whose support was crucial in ensuring the continuity of the research.

Takaichi Watanabe

Okayama, February 17, 2014

Table of Contents

Chapter 1
Introduction and Motivation

1-1 Biocompatible polymers

Since 1950s, polymer microparticles and nanoparticles have been studied in the world because they can steadily disperse in media and exhibit different properties from those bulk polymers. Moreover, it is possible to enhance their properties by controlling the diameter, chemical compositions, internal structures, and surface morphology as well as by introducing different polymers or inorganic compounds into the particles. From these characters, polymer micro/nanoparticles have been widely used in chemical industry such as inks, adhesives, cosmetics, agrochemicals, drug carriers and so on.

In recent decades, there have been increasing interests in global environmental problems. As a result, alternative to polymers from fossil resources such as polystyrene (PS) and poly(methyl methacrylate) (PMMA), much attention has been focused on biodegradable polymers including poly(lactide-*co*-glycolide) (PLGA),[1] polylactide (PLA),[2] and poly(ε-caprolactone) (PCL).[3] Among them, PLGA has been widely used in the biomedical industry as a major component due to its excellent biocompatibility and biodegradability. PLGA has been approved by the Food and Drug Administration (FDA) in the US and has been used as a biodegradable suture material for many years.[4] PLA has gained interests as a biomass-based material with higher mechanical strength than PLGA. PLA can be synthesized from plants such as cone and sugarcane. Protein is extracted from these raw materials and further hydrolyzed, yielding in glucose. Then, glucose undergoes lactic acid fermentation, which results in lactic acid.[5-6] The synthesized lactic acid is converted into the dimer called lactide *via* dehydrated condensation, followed by a ring-closing reaction.[7] PLA is synthesized by a ring-opening polymerization of the lactide in the presence of organo-tin as a catalyst.[8-10] Distinctive properties of PLA are high transparency, high tensile strength, and high modulus of elasticity, being equivalent to PS and PMMA.[11-12] Because of these, PLA-based materials have been already applied to the wide range of chemical products including medical supplies, agrochemical building materials, and household utensils. In

addition, since the used PLA can be easily decomposed by hydrolysis[13-14] or thermal decomposition,[15-20] resulting in lactide, there is possibility to reuse the polymer by chemical recycling. Simultaneously, incineration treatment or act of microorganisms allows to completely decompose the lactide and finally gives carbon dioxide and water, which will be used for the growth of plant *via* photosynthesis. Therefore, considering the whole process, there is no carbon payment, which is so-called “carbon neutral” cycle. This is considered to be an important concept to develop recycling society.

Biocompatible polymer micro/nanoparticles have been considered as a promising drug delivery vehicle for drug targeting and controlled release. The polymer matrix suppresses the burst release of incorporated drugs and enables for the gradual release, relying on diffusion and degradation. Up to now, various techniques have been developed for preparing the biodegradable polymer micro/nanoparticles such spray drying,[21-22] anionic dispersion polymerization,[23-28] and solvent evaporation.[29-38]

1-2 Conventional processes for preparation of biocompatible polymer particles

1-2-1 Spray drying

Spray drying is a technique widely used in food and pharmaceutical industries to obtain dry particles from polymer solution phase. The dispersion solution dissolving pre-synthesized polymer and a drug is sprayed inside a chamber at a fixed temperature, pressure and flow rate by using a nozzle. Inside the chamber, the solvent is immediately evaporated from the droplets and the concentration of polymer in the droplets rapidly increases. The surface of the droplet begins to solidify and eventually the dry particles are formed. In general, this process is carried out under a relatively high temperature in order to facilitate evaporation of the solvent from the droplets. In recent decades, spray drying has been in the limelight to elucidate the evaporation driven self-assembly of colloids at various physicochemical and thermodynamical conditions[39-43] and to synthesize novel nanocomposites,[44-45] colloidal crystals[46] and ordered mesoporous materials.[47-50] The disadvantage of this process is harsh preparation conditions with high temperature. Due to a high operation temperature, there is possibility to denature the encapsulated materials. In addition, rapid gas flow in the chamber makes it difficult to control over the size of particles.

1-2-2 Dispersion polymerization

Dispersion polymerization is a promising one-step process for preparing polymer particles with a narrow size distribution.[51-52] The polymerization is defined as one of bottom-up process. The polymerization of a monomer is carried out in the reaction medium dissolving a suitable polymeric stabilizer. The solvent used in the system is a good solvent for both the monomer and the polymeric stabilizer, but a non-solvent for the polymer that propagates during the process. Therefore, dispersion polymerization is first conducted in a homogeneous solution of monomers with an initiator and a polymeric stabilizer and the polymer particles covered with the stabilizer are generated by precipitation of polymer as a result of competitive reactions of nucleation and growth. Slomkowski *et al.* have reported a series of studies of preparation of PLA microspheres using a dispersion polymerization technique. They have successfully synthesized relatively monodisperse PLA microspheres *via* dispersion polymerization of D,L-lactide using a mixture of 1,4-dioxane/heptane (1:4, v/v) and poly(dodecyl acrylate)-*g*-poly(*ε*-caprolactone) (PDA-*g*-PCL) as a dispersant and a stabilizer, respectively.[27] Muranaka *et al.* have also reported a synthesis of monodisperse PLA microspheres by dispersion polymerization using poly[(dodecyl methacrylate)-*co*-(2-hydroxyethyl methacrylate)] (P(DMA-*co*-HEMA)) in xylene/heptane (1:2, v/v) system. They showed that the synthesized polymeric stabilizer, P(DMA-*co*-HEMA) with hydroxyl groups as initiation sites for a pseudo-anionic dispersion polymerization, produced a graft copolymer *in situ* during the polymerization and formed polymer micelles, which was a contributing factor to producing monodisperse PLA microspheres.[24, 53] Although some research groups have reported to fabricate monodisperse PLA microspheres using a dispersion polymerization method, it is generally challenging to design the polymeric stabilizers with proper molecular structures and to synthesize them. Moreover, this process requires much amount of organic solvent as a dispersion medium; therefore, the handling of unstable drugs, proteins, and vaccines is quite difficult.

1-2-3 Solvent evaporation

Solvent evaporation is the most common preparation procedure for biodegradable polymer particles owing to the ease of operation. In contrast to dispersion polymerization, this is one of top-down process and polymer particles are obtained after

evaporation of solvent from polymer droplets. Relying on the nature of substances entrapped in the particles, the emulsion template can be chosen. Among them, there are many cases to use oil-in-water (O/W) emulsion[29, 32, 36-37, 54-55] and water-in-oil-in-water (W/O/W) emulsion[31, 38, 56-70] as a template. In the case of O/W emulsion system, an organic solution dissolving pre-synthesized polymer and an aqueous surfactant solution are used as a dispersed phase and a continuous phase, respectively. These solutions are poured into the same vessel and emulsified by mechanical stirring using homogenizer or ultra sonication, leading to formation of O/W emulsion. After that the organic solvent evaporates under stirring, thereby inducing precipitation of the polymer. The emulsion system is available for encapsulating lipophilic substances in the particles. On the other hand, when using W/O/W emulsion system, a small amount of water phase containing hydrophilic substances is first mixed with an organic polymer solution, resulting in W/O emulsion. The W/O emulsion is emulsified with a large amount of aqueous surfactant solution, leading to W/O/W emulsion. Then, the W/O/W emulsion is stirred for a long time to evaporate organic solvent and harden the polymer particles. Using the W/O/W emulsion system makes it possible to encapsulate hydrophilic substances in the core of the microparticles, which suppresses undesirable leakage of the substances from the resultant microparticles, thereby achieving a high encapsulation efficiency of the substances. However, the use of mechanical stirring during emulsion formation gives rise to polydispersity in the diameter of the microparticles. Thus, since the last decade, considerable efforts have been devoted to development of preparation technique for uniform-sized droplets and microparticles.

1-3 Microfluidic preparation of biocompatible polymer particles

1-3-1 Microfluidics

Microfluidics is the fluid analogue of microelectronic circuits. The field has emerged in the last decade and deals with the precise handling of pico-liter scale fluids in microchannels using miniature devices as small as a cigarette box. There are many promising applications in microfluidics ranging from medical and biological sciences including implants,[71-72] biological analysis[73-76] and drug analysis[77-78] to channel design[79] and organic chemistry.[80] These implementations and recent advancements have been summarized in a great number of reviews,[81-85] so that only applications of microfluidics for droplet formation are focused in this chapter.

As discussed above, the major preparation techniques of biodegradable polymer particles rely on top-down process using pre-synthesized polymers such as spray drying and solvent evaporation. In terms of top-down process, the common drawbacks are poorly controlled particle size. Considering applications of biodegradable polymer particles as drug delivery carriers, it is of importance to prepare the particles with a narrow size distribution because the release of encapsulated reagents and the dose of administration are considerably affected by the diameter of the particles.[86-87] To improve the polydispersity of the polymer particle size, it is of utmost importance to prepare uniform sized emulsion droplets since monodisperse polymer particles are only obtained from uniform droplets.

The advent of microfluidics has enabled production of emulsion droplets with a narrow size distribution. Moreover, the diameter of droplets can be precisely controlled either by tuning the geometry of microfluidic devices, the properties of two liquid phases (viscosity and interfacial tension) and the operating parameters or by introducing additional energy such as electrical forces,[88] temperature,[89] and acoustic force.[90-91]

1-3-2 Droplet formation in microfluidic devices

In general, droplet-microfluidic processes for fabrication of monodisperse single emulsions (*eg.* W/O and O/W emulsion droplets) involve the pumping of one liquid phase (the dispersed phase) into another immiscible or partially miscible liquid phase (the continuous phase) through a micron-sized channel and the dispersed phase flow is sheared at the junction where the two immiscible phases meet. Regarding the geometry of droplet-microfluidics, Y- or T-junction,[92-96] co-flowing,[97-100] and flow-focusing microfluidic devices[101-103] have been particularly used for droplet generation. For example, T-junction geometries consist of a horizontal channel and a perpendicular channel, resembling “T” shape. In the flow-focusing microfluidic devices, there are many kinds of main channel configurations. The dispersed phase flows in a central channel and the continuous phase goes through two side channels. When the two phases meet at a flow-focused part, the two flows from side squeeze the inner fluid, which induces breakage of the inner fluid into tiny droplets. The geometry of the flow-focusing point affects the shear force for producing droplets and stability of droplet formation. Up to date, not only these 2D microfluidic devices fabricated with various substrates such as silicon, glass,[104] and polydimethylsiloxane (PDMS),[105] but

also 3D microfluidic channels[106] have been developed to achieve more stable droplet formation. The advent of 3D microfluidic devices made of tubes or capillaries has enabled droplet generation without any wetting problems because the dispersed phase in the microfluidic devices is finely aligned in the 3D-centre of the flow and thus completely covered with the continuous phase. On the other hand, terrace-like microchannels are the other type of microfluidic device, which is considered to be superior to mass production of droplets.[107-108]

1-3-3 Important aspects for droplet formation in microfluidics

To achieve successful droplet formation in microfluidic multi-phase systems, it is required to consider dimensionless numbers, including Reynolds number (*R*e), Capillary number (*C*a), Weber Number (*W*e), and flow rate ratio (φ).

$$Re = \frac{\rho d u}{\mu} \tag{1-1}$$

$$Ca = \frac{\mu u}{\sigma} \tag{1-2}$$

$$We = Re \cdot Ca = \frac{\rho u^2 d}{\sigma} \tag{1-3}$$

$$\varphi = \frac{Q_c}{Q_d} \tag{1-4}$$

where ρ is the density of fluids (kg m^{-3}), u is the characteristic velocity (m s^{-1}), d is a hydraulic diameter of the channel (m), μ is the viscosity of fluids (Pa·s), σ is the surface or interfacial tension between the two fluids (mN m^{-1}), Q is the flow rate of fluid (mL h^{-1}) and the subscripts c and d represent the continuous and dispersed phases, respectively.

*R*e number represents the ratio of inertial forces to viscous forces. *C*a number describes the ratio of viscous forces to interfacial tension forces. *W*e number illustrates the ratio of inertial forces to interfacial tension forces. φ shows flow rate ratio of the

continuous phase to the dispersed phase, which is useful to assess flow conditions for production of droplets. Here, it is important to note that in the micrometer length scale in microfluidics, the flow streams in the channels are very slow and have considerably low *R*e number less than 1, meaning laminar flow, so that *C*a and *W*e numbers are more important than *R*e, and especially, the interfacial effects become dominant. In addition, the control of wetting properties of microfluidic channel walls is inevitable to produce desirable type of emulsions and to guarantee stable emulsification. In general, W/O type emulsions can be formed when using microchannels with hydrophobic walls, whereas O/W emulsions can be preferentially produced in hydrophilic microfluidic channels. If a microfluidic channel with undesirable wetting properties or use a microchannel with partially wetting is utilized, the disordered flow patterns will be obtained.

With regard to flow regimes, in T-junction, the flow regimes are classified into 3 types, including dripping, squeezing, and jetting, which have been intensely investigated experimentally[94, 109] and theoretically[110] in recent years. The flow regimes can be dependent of *C*a number. Similarly, three types of flow regimes have been reported in co-flowing and flow-focusing microfluidic devices, including dripping, squeezing, and jetting.[111] In addition, an intriguing flow regime called tip-streaming has also been reported in flow-focusing microchannels, which is considered as a promising breakthrough for producing submicron-sized emulsion droplets.[112-118]

1-3-4 Multiple emulsion formation

The advent of microfluidic technology has also enabled preparation of multiple emulsions with controlled sizes and structures. Monodisperse multiple emulsions have been produced by utilizing a variety of droplet-based microfluidic devices, which is mainly classified into two techniques; two-step emulsification and one-step emulsification method.

In general, monodisperse double emulsions have been fabricated in a two-step emulsification technique by firstly producing inner droplets, followed by second encapsulation of them in an external flow. Two-step emulsification has been widely used for generation of W/O/W double emulsions[119] and oil-in-water-in-oil (O/W/O) double emulsions. The two-step process utilizes two different combinations of simple geometries with opposite wettability such as T-junction, co-flowing, flow-focusing, and cross-flowing and produces discrete double emulsions by forming the internal droplets

at the first geometry and the external droplets at the second, through two T-junctions,[120] two flow-focusing,[121] two co-flowing,[122] and two sequential cross-junctions[123-125]. Moreover, adjusting the microfluidic geometry and the flow rate upon emulsification is important parameters to control over the size of either inner or outer droplets, the thickness of the middle layer, and the number of inner droplets.

For the two-step process, in order for a stable emulsion to form, the surface of microchannel must be tailored to the wettability of the continuous phase. In the case of W/O/W emulsion formation, the surface required to be modified locally to ensure a W/O emulsion at the first junction and a (W/O)/W emulsion at the second junction. For example, hydrophilic glasses are selectively tailored to be hydrophobic using silane coupling reagents to obtain W/O emulsion.[120] On the other hand, hydrophobic PDMS is partly converted to be hydrophilic for O/W emulsion formation.[126] The modification of PDMS is generally employed using plasma treatment, however the treatment does not make PDMS hydrophilic for a long term and the intrinsic hydrophobicity of PDMS can recover within a few days.[127]

Compared with the two-step approaches, the one-step process only requires a single step emulsification to generate double emulsions or multiple emulsions. Utada *et al.* have developed a microcapillary device with a coaxial geometry consisting of cylindrical glass capillary tubes inserted into a square glass tube in order to produce multiple emulsion droplets in a single step emulsification.[128] Although the innermost and the middle phase fluids were pumped from the same direction, through the inner cylindrical capillary tube and the outer capillary region, respectively, the outermost phase fluid was pumped from the outer coaxial region from the opposite direction. The generated co-axial flow breaks into droplets at the exit orifice *via* Rayleigh-Plateau instability,[129] resulting in double emulsions. The device has a 3D geometry and thus the dispersed phases are fully covered with external fluid and do not wet the outer coaxial region.

1-3-5 Microfluidic fabrications of polymer microparticles

Monodisperse PLGA or PLA microparticles have been prepared *via* microfluidic emulsification of O/W emulsions, followed by *ex-situ* solvent evaporation.[86, 130-133] The process has enabled preparation of uniform-sized polymer particles in the range of several tens to hundreds micrometer. The size distribution of the particles is quite

narrow with less than 5% in the coefficient of variation (CV) defined as the ratio of the standard deviation to the mean diameter. For example, Xu *et al.* have reported preparation of amphiphilic drug (bupivacaine)-loaded monodisperse PLGA microparticles by utilizing O/W emulsion produced by a flow-focusing microfluidic device made of PDMS, followed by *ex-situ* solvent evaporation.[86] The prepared monodisperse microparticles exhibited slower drug release than that prepared using the conventional methods with the same average size but with a broader size distribution, and significant suppress of initial burst, presumably because of the uniform distribution of the drug in the particles generated with microfluidic approach. He *et al.* also reported preparation of paclitaxel (PTX) loaded monodisperse poly(*L*-lactic acid) (PLLA) microparticles using a combination of a cross-junction type microfluidic device made of PDMS with surface modification and *ex-situ* solvent evaporation.[131] They prepared monodisperse PTX-loaded PLLA microparticles in the range of 30 to 50 μm, with less than 4% in the CV. Compared to polydisperse microparticles prepared by conventional methods, the monodisperse microparticles generated with the microfluidic technique exhibited considerably slow and sustained release of PTX, continuing for a few weeks.

1-3-6 Microfluidic fabrications of polymer microcapsules

Considerable efforts have been devoted to development of the method for controlling the structures of polymer particles including seeded polymerization,[134] photopolymerization of droplets under confined geometry in microfluidic devices,[135] addition of porogens in the emulsion systems,[136] interfacial instability of droplets in which amphiphilic copolymer is dissolves,[137-138] internal phase separation in droplets,[139-140] and complex emulsion template-photopolymerization.[141] Among them, biocompatible polymer microcapsules consisting of a liquid oil core and a polymeric shell have been prepared by a combination of internal phase separation in O/W emulsion and solvent evaporation. For example, Zhao *et al.* reported preparation of PLLA microcapsules incorporating self-healing reagents in the core *via* internal phase separation in the organic phase and subsequent solvent evaporation.[142] They showed that the microcapsules could encapsulate model hydrophobic self-healing reagents such as alkanes, cycloalkanes, halogenoalkanes, and perfluoroalkanes. Moreover, structural complexity has been introduced on poly(ethylene glycol)-*b*-poly(D,L-lactide) (PEG-*b*-PLA) microcapsules encapsulating perfluorooctyl bromide (PFOB) in the core

by internal phase separation and interfacial instability induced by PEG-*b*-PLA during solvent evaporation.[143] The resultant microcapsules with a PFOB core and PEG-*b*-PLA shell have sponge-like surface morphology, which is advantageous to an increase of surface area. The surface structure was modulated by adjusting the polymer compositions of the dispersed organic phase. Furthermore, Lensen *et al.* prepared relatively monodisperse PLLA microcapsules encapsulating dodecane in the core by making use of a flow-junction type microfluidic device and internal phase separation in the polymer droplets, followed by solvent evaporation.[144] They also showed the release of Oil red-O from the monodisperse microcapsules and prepared hollow microcapsules by removal of dodecane core *via* lyophilization. Duncanson *et al.* reported monodisperse porous PLA microcapsules prepared by a combination of perfluorinated-dendrimer dye complex as a pore-forming agent and O/W emulsion solvent evaporation using a flow-focusing microfluidic device.[132] Using fluorous properties of the pores on the microcapsules, additional guest molecules could be attached into the pores, enabling to employ dual drug delivery.

For microcapsules with aqueous cores, the most common preparation method is W/O/W emulsion solvent evaporation.[145] Lee *et al.* described the preparation of monodisperse PLGA microcapsules with aqueous core and near-infrared (NIR) stimuli responsiveness by W/O/W emulsion formation using a flow-focusing microfluidic device and subsequent solvent evaporation[146]. It was shown that the both composition of PLGA and the organic phase of the W/O/W double emulsions play an important role in determining the final morphology and change of solvent quality of the middle organic phase during solvent evaporation also gave rise to morphological diversity from spherical to “snowman-like”. Introduction of Au nanoparticles in the shell of the microcapsules imparted the NIR sensitivity on the microcapsules, which enabled triggered release of the encapsulated substances. In addition, Amstad *et al.* represented a microfluidic method to produce monodisperse thermo- and photoresponsive polymersomes having high encapsulation efficiency. The polymersomes were composed of thermoresponsive copolymer, poly(*N*-isopropylacrylamide)-*b*-poly(lactide-co-glycolide) (PNIPAM-*b*-PLGA), PEG-*b*-PLA and surface modified Au nanoparticles.[147] The ability to trigger release of encapsulated reagents without changing the overall solution temperature was achieved

by direct incorporating Au nanoparticles into the hydrophobic shell of the polymersomes.

1-4 Motivation, objective and strategy of this study

Microfluidic approach to fabrication of polymer microparticles have gained increasing interest in the last decade because they provide polymeric containers with controllable sizes and structures, which can be applied to various chemical products, including inks, coatings, pharmaceutics, agrochemicals, and cosmetics. Among them, the most common procedure for preparing monodisperse PLGA or PLA microparticles is aforementioned emulsion-solvent evaporation methods. However, requirement of use of organic solvents (especially halogenated solvents) as a dispersed organic phase and the residue of them in the final products actually make it difficult to use the resultant microparticles as drug delivery vehicles for *in vivo* applications due to its high toxicity for human health. In addition, the vapour of the solvents during evaporation also causes environmental problems. Moreover, it takes much time to precipitate the polymers from the droplets *via* evaporation, which leads to limitation in the mass production of them. Furthermore, few studies have been reported in terms of structural control of biocompatible polymer particles, although design of polymer particle structures can improve or enhance properties of polymer particles. Therefore, it is extremely important to construct a simple environmentally friendly process for preparing monodisperse biocompatible polymer particles using microfluidic technologies and to develop a new technique to control the structures by microfluidics coupled with physicochemical phenomena.

In the present study, a novel continuous process for production of monodisperse PLA microparticles by combining microfluidic emulsification with subsequent solvent diffusion has been developed. Solvent diffusion is one of top-down technology using O/W emulsion in which the dispersed organic phase is partially miscible with water such as ethyl acetate (EA) and methylethylketone. Because of high solubility of these solvents in water, the microparticles are quickly obtained just by diluting the emulsion with a large excess amount of pure water, which extensively shortens preparation time. In addition, EA is a relatively low-toxic organic solvent approved by the FDA, which reduces environmental burden.

By utilizing a combinatorial process of microfluidic emulsification and solvent diffusion with physicochemical phenomena based on interfacial chemistry, including internal phase separation and spontaneous emulsification assisted by amphiphilic diblock copolymer, monodisperse PLA microparticles with various controlled structures have been produced. The formation mechanisms of each structure were also discussed in this thesis. In the process, the quick removal of organic solvent from the droplets shortens the preparation time about several hundreds times compared with conventional techniques using halogenated solvents. In addition, all components used in the preparations are biocompatible, which is great advantageous to applications for biomedical field. Furthermore, fine control of flow conditions using a simple Y-shaped microfluidic device has made it possible to prepare monodisperse microspheres as small as 10 μm in the diameter, which has never been achieved by the other groups. The insights gained from this work should stimulate the exploration of novel applications of polymer particles as well as scientific interests in structural control of polymer particles.

References

1. Patrick Jr, C.; Zheng, B.; Johnston, C.; Reece, G. Long-term implantation of preadipocyte-seeded PLGA scaffolds. *Tissue Eng.* **2002,** *8* (2), 283-293.
2. He, Y.; Hu, Z.; Ren, M.; Ding, C.; Chen, P.; Gu, Q.; Wu, Q. Evaluation of PHBHHx and PHBV/PLA fibers used as medical sutures. *J. Mater. Sci. Mater. Med.* **2014**, *25(2)*, 561-571.
3. Williams, J. M.; Adewunmi, A.; Schek, R. M.; Flanagan, C. L.; Krebsbach, P. H.; Feinberg, S. E.; Hollister, S. J.; Das, S. Bone tissue engineering using polycaprolactone scaffolds fabricated via selective laser sintering. *Biomaterials* **2005,** *26* (23), 4817-4827.
4. Lassalle, V.; Ferreira, M. L. PLA nano- and microparticles for drug delivery: an overview of the methods of preparation. *Macromol. Biosci.* **2007,** *7* (6), 767-783.
5. Ohara, H.; Yahata, M. l-Lactic acid production by Bacillus sp. in anaerobic and aerobic culture. *J. Ferment. Bioeng.* **1996,** *81* (3), 272-274.
6. Yin, P.; Nishina, N.; Kosakai, Y.; Yahiro, K.; Pakr, Y.; Okabe, M. Enhanced production of l(+)-lactic acid from corn starch in a culture of Rhizopus oryzae using an air-lift bioreactor. *J. Ferment. Bioeng.* **1997,** *84* (3), 249-253.
7. Yoo, D.; Kim, D.; Lee, D. Synthesis of lactide from oligomeric PLA: Effects

of temperature, pressure, and catalyst. *Macromolecular Research* **2006,** *14* (5), 510-516.

8. Kricheldorf, H. R.; Berl, M.; Scharnagl, N. Poly(lactones). 9. Polymerization mechanism of metal alkoxide initiated polymerizations of lactide and various lactones. *Macromolecules* **1988,** *21* (2), 286-293.

9. Duda, A.; Penczek, S. Thermodynamics of L-lactide polymerization. Equilibrium monomer concentration. *Macromolecules* **1990,** *23* (6), 1636-1639.

10. Kowalski, A.; Duda, A.; Penczek, S. Kinetics and mechanism of cyclic esters polymerization initiated with tin(II) octoate, 1. Polymerization of ε-caprolactone. *Macromol. Rapid Commun.* **1998,** *19* (11), 567-572.

11. Jain, R. A. The manufacturing techniques of various drug loaded biodegradable poly(lactide-co-glycolide) (PLGA) devices. *Biomaterials* **2000,** *21* (23), 2475-2490.

12. Langer, R. Tissue Engineering: A New Field and Its Challenges. *Pharm. Res.* **1997,** *14* (7), 840-841.

13. Tsuji, H.; Nakahara, K.; Ikarashi, K. Poly(L-Lactide), 8. High-Temperature Hydrolysis of Poly(L-Lactide) Films with Different Crystallinities and Crystalline Thicknesses in Phosphate-Buffered Solution. *Macromolecular Materials and Engineering* **2001,** *286* (7), 398-406.

14. Tsuji, H.; Daimon, H.; Fujie, K. A New Strategy for Recycling and Preparation of Poly(l-lactic acid): Hydrolysis in the Melt. *Biomacromolecules* **2003,** *4* (3), 835-840.

15. Gupta, M. C.; Deshmukh, V. G. Thermal oxidative degradation of poly-lactic acid. *Colloid. Polym. Sci.* **1982,** *260* (5), 514-517.

16. Jamshidi, K.; Hyon, S. H.; Ikada, Y. Thermal characterization of polylactides. *Polymer* **1988,** *29* (12), 2229-2234.

17. Wachsen, O.; Platkowski, K.; Reichert, K. H. Thermal degradation of poly-l-lactide—studies on kinetics, modelling and melt stabilisation. *Polym. Degrad. Stab.* **1997,** *57* (1), 87-94.

18. Lee, S.-H.; Hyun Kim, S.; Han, Y.-K.; Kim, Y. H. Synthesis and degradation of end-group-functionalized polylactide. *J. Polym. Sci., Part A: Polym. Chem.* **2001,** *39* (7), 973-985.

19. Aoyagi, Y.; Yamashita, K.; Doi, Y. Thermal degradation of poly[(R)-3-hydroxybutyrate], poly[ε-caprolactone], and poly[(S)-lactide]. *Polym.*

Degrad. Stab. **2002,** *76* (1), 53-59.

20. Tsuji, H.; Fukui, I. Enhanced thermal stability of poly(lactide)s in the melt by enantiomeric polymer blending. *Polymer* **2003,** *44* (10), 2891-2896.

21. Bodmeier, R.; Chen, H. Preparation of Biodegradable Poly(±)lactide Microparticles Using a Spray-Drying Technique. *J. Pharm. Pharmacol.* **1988,** *40* (11), 754-757.

22. Arpagaus, C.; Schafroth, N. Spray dried biodegradable polymers for controlled drug delivery systems. *European Industrial Pharmacy* **2011,** *11*, 10-13.

23. Muranaka, M.; Kitamura, Y.; Yoshizawa, H. Preparation of biodegradable microspheres by anionic dispersion polymerization with PLA copolymeric dispersion stabilizer. *Colloid. Polym. Sci.* **2007,** *285* (13), 1441-1448.

24. Muranaka, M.; Ono, T. Role of dispersion stabilizer with hydroxy groups in preparation of monodisperse polylactide microspheres. *J. Polym. Sci., Part A: Polym. Chem.* **2009,** *47* (20), 5230-5240.

25. Slomkowski, S.; Gadzinowski, M.; Sosnowski, S.; De Vita, C.; Pucci, A.; Ciardelli, F.; Jakubowski, W.; Matyjaszewski, K. Biodegradable Nano- and Microparticles with Controlled Surface Properties. *Macromolecular Symposia* **2005,** *226* (1), 239-252.

26. Sosnowski, S.; Slomkowski, S.; Lorenc, A.; Kricheldorf, H. R. Mechanism of dispersion polymerization of L-lactide initiated with 2,2-dibutyl-2-stanna-1,3-dioxepane. *Colloid. Polym. Sci.* **2002,** *280* (2), 107-115.

27. Slomkowski, S.; Sosnowski, S.; Gadzinowski, M. Latexes and microspheres by ring-opening polymerization. Polymerization of cyclic esters. *Colloids Surf. Physicochem. Eng. Aspects* **1999,** *153* (1–3), 111-118.

28. Jakubowski, W.; Lutz, J.-F. o.; Slomkowski, S.; Matyjaszewski, K. Block and random copolymers as surfactants for dispersion polymerization. I. Synthesis via atom transfer radical polymerization and ring-opening polymerization. *J. Polym. Sci., Part A: Polym. Chem.* **2005,** *43* (7), 1498-1510.

29. Bodmeier, R.; McGinity, J. W. Solvent selection in the preparation of poly(dl-lactide) microspheres prepared by the solvent evaporation method. *Int. J. Pharm.* **1988,** *43* (1–2), 179-186.

30. Chung, T.-W.; Huang, Y.-Y.; Liu, Y.-Z. Effects of the rate of solvent evaporation on the characteristics of drug loaded PLLA and PDLLA microspheres. *Int.*

J. Pharm. **2001,** *212* (2), 161-169.

31. Rosca, I. D.; Watari, F.; Uo, M. Microparticle formation and its mechanism in single and double emulsion solvent evaporation. *J. Control. Release* **2004,** *99* (2), 271-280.

32. Heslinga, M. J.; Mastria, E. M.; Eniola-Adefeso, O. Fabrication of biodegradable spheroidal microparticles for drug delivery applications. *J. Control. Release* **2009,** *138* (3), 235-242.

33. Yoshizawa, H.; Nishino, S.; Shiomori, K.; Natsugoe, S.; Aiko, T.; Kitamura, Y. Surface morphology control of polylactide microspheres enclosing irinotecan hydrochloride. *Int. J. Pharm.* **2005,** *296* (1-2), 112-116.

34. Nishino, S.; Kitamura, Y.; Kishida, A.; Yoshizawa, H. Preparation and interfacial properties of a novel biodegradable polymer surfactant: poly(ethylene oxide monooleate-block-DL-lactide). *Macromol. Biosci.* **2005,** *5* (11), 1066-1073.

35. Nishino, S.; Kishida, A.; Yoshizawa, H. Morphology control of polylactide microspheres enclosing irinotecan hydrochloride with polylactide based polymer surfactant for reduction of initial burst. *Int. J. Pharm.* **2007,** *330* (1-2), 32-36.

36. Jang, J.; Sah, H. Nonhalogenated solvent-based solvent evaporation process useful in preparation of PLGA microspheres. *J. Microencapsul.* **2011,** *28* (6), 490-498.

37. Kwon, S.; Joo, J.-r.; Lee, W.-k.; Jeong, Y.; Choi, J. Polymeric Nano-half-shells Prepared by Simple Solvent Evaporation Method. *Bull. Korean Chem. Soc.* **2009**. *30* (2), 486-488.

38. Uchida, T.; Yoshida, K.; Goto, S. Preparation and characterization of polylactic acid microspheres containing water-soluble dyes using a novel w/o/w emulsion solvent evaporation method. *J. Microencapsulation* **1996,** *13* (2), 219-228.

39. Tsapis, N.; Dufresne, E.; Sinha, S.; Riera, C.; Hutchinson, J.; Mahadevan, L.; Weitz, D. Onset of Buckling in Drying Droplets of Colloidal Suspensions. *Phys. Rev. Lett.* **2005,** *94* (1), 018302.

40. Okuyama, K.; Wuled Lenggoro, I. Preparation of nanoparticles via spray route. *Chem. Eng. Sci.* **2003,** *58* (3–6), 537-547.

41. Iskandar, F.; Gradon, L.; Okuyama, K. Control of the morphology of nanostructured particles prepared by the spray drying of a nanoparticle sol. *J. Colloid Interface Sci.* **2003,** *265* (2), 296-303.

42. Bahadur, J.; Sen, D.; Mazumder, S.; Paul, B.; Bhatt, H.; Singh, S. G. Control

of Buckling in Colloidal Droplets during Evaporation-Induced Assembly of Nanoparticles. *Langmuir* **2011,** *28* (3), 1914-1923.

43. Suhendi, A.; Nandiyanto, A. B. D.; Munir, M. M.; Ogi, T.; Gradon, L.; Okuyama, K. Self-Assembly of Colloidal Nanoparticles Inside Charged Droplets during Spray-Drying in the Fabrication of Nanostructured Particles. *Langmuir* **2013,** *29* (43), 13152-13161.

44. Bian, H.-m.; Yang, Y.; Wang, Y.; Tian, W. Preparation of nanostructured alumina–titania composite powders by spray drying, heat treatment and plasma treatment. *Powder Technol.* **2012,** *219*, 257-263.

45. Bippus, L.; Jaber, M.; Lebeau, B. Laponite and hybrid surfactant/laponite particles processed as spheres by spray-drying. *New J. Chem.* **2009,** *33* (5), 1116-1126.

46. Ventosa, E.; Mei, B.; Xia, W.; Muhler, M.; Schuhmann, W. TiO2(B)/Anatase Composites Synthesized by Spray Drying as High Performance Negative Electrode Material in Li-Ion Batteries. *ChemSusChem* **2013,** *6* (8), 1312-1315.

47. Melnyk, I. V.; Zub, Y. L.; Veron, E.; Massiot, D.; Cacciaguerra, T.; Alonso, B. Spray-dried mesoporous silica microspheres with adjustable textures and pore surfaces homogenously covered by accessible thiol functions. *J. Mater. Chem.* **2008,** *18* (12), 1368-1382.

48. Majano, G.; Restuccia, A.; Santiago, M.; Perez-Ramirez, J. Assembly of a hierarchical zeolite-silica composite by spray drying. *CrystEngComm* **2012,** *14* (18), 5985-5991.

49. Waldron, K.; Wu, W. D.; Wu, Z.; Liu, W.; Selomulya, C.; Zhao, D.; Chen, X. D. Formation of monodisperse mesoporous silica microparticles via spray-drying. *J. Colloid Interface Sci.* **2014,** *418* (0), 225-233.

50. Boissiere, C.; Grosso, D.; Chaumonnot, A.; Nicole, L.; Sanchez, C. Aerosol Route to Functional Nanostructured Inorganic and Hybrid Porous Materials. *Adv. Mater.* **2011,** *23* (5), 599-623.

51. Zhang, X.; Shen, S.; Fan, L. Uniform Polystyrene Particles by Dispersion Polymerization in Different Dispersion Medium. *Polym. Bull.* **2008,** *61* (1), 19-26.

52. Kawaguchi, S.; Ito, K. Dispersion polymerization. In *Polymer Particles*; Springer, *2005*, 299-328.

53. Muranaka, M.; Ono, T. Preparation of monodisperse polylactide microspheres by dispersion polymerization using a polymeric stabilizer with hydroxy groups.

Macromol. Rapid Commun. **2009,** *30* (3), 152-156.

54. Yeo, Y.; Park, K. Control of encapsulation efficiency and initial burst in polymeric microparticle systems. *Arch. Pharmacal Res.* **2004,** *27* (1), 1-12.

55. Park, S. J.; Kim, S. H. Preparation and characterization of biodegradable poly(l-lactide)/poly(ethylene glycol) microcapsules containing erythromycin by emulsion solvent evaporation technique. *J. Colloid Interface Sci.* **2004,** *271* (2), 336-341.

56. Fu, K.; Pack, D.; Klibanov, A.; Langer, R. Visual Evidence of Acidic Environment Within Degrading Poly(lactic-co-glycolic acid) (PLGA) Microspheres. *Pharm. Res.* **2000,** *17* (1), 100-106.

57. Uchida, Y.; Fukuda, K.; Murakami, Y. The hydrogel containing a novel vesicle-like soft crosslinker, a “trilayered” polymeric micelle, shows characteristic rheological properties. *J. Polym. Sci., Part B: Polym. Phys.* **2013,** *51* (2), 124-131.

58. Hong, X.; Wei, L.; Ma, L.; Chen, Y.; Liu, Z.; Yuan, W. Novel preparation method for sustained-release PLGA microspheres using water-in-oil-in-hydrophilic-oil-in-water emulsion. *Int. J. Nanomed.* **2013,** *8*, 2433-2441.

59. Qian, L.; Zhang, H. One-step synthesis of protein-encapsulated microspheres in a porous scaffold by freeze-drying double emulsions and tuneable protein release. *Chem. Commun.* **2013,** *49* (78), 8833-8835.

60. Herzi, S.; Essafi, W.; Bellagha, S.; Leal-Calderon, F. Influence of the inner droplet fraction on the release rate profiles from multiple W/O/W emulsions. *Colloids Surf. Physicochem. Eng. Aspects* **2014,** *441* (0), 489-495.

61. Jiménez-Colmenero, F. Potential applications of multiple emulsions in the development of healthy and functional foods. *Food Res. Int.* **2013,** *52* (1), 64-74.

62. Campardelli, R.; Della Porta, G.; Gomez, L.; Irusta, S.; Reverchon, E.; Santamaria, J. Au-PLA nanocomposites for photothermally controlled drug delivery. *Journal of Materials Chemistry B* **2014,** *2* (4), 409-417.

63. Schmitz-Hertzberg, S.-T.; Mak, W. C.; Lai, K. K.; Teller, C.; Bier, F. F. Multifactorial design of poly(d,l-lactic-co-glycolic acid) capsules with various release properties for differently sized filling agents. *J. Appl. Polym. Sci.* **2013,** *130* (6), 4219-4228.

64. Bao, M.; Zhou, Q.; Dong, W.; Lou, X.; Zhang, Y. Ultrasound-modulated shape memory and payload release effects in a biodegradable cylindrical rod made of

chitosan-functionalized PLGA microspheres. *Biomacromolecules* **2013,** *14* (6), 1971-1979.

65. Jin, Y.; Wang, J.; Ke, H.; Wang, S.; Dai, Z. Graphene oxide modified PLA microcapsules containing gold nanoparticles for ultrasonic/CT bimodal imaging guided photothermal tumor therapy. *Biomaterials* **2013,** *34* (20), 4794-4802.

66. Samadi, N.; van Nostrum, C. F.; Vermonden, T.; Amidi, M.; Hennink, W. E. Mechanistic Studies on the Degradation and Protein Release Characteristics of Poly(lactic-co-glycolic-co-hydroxymethylglycolic acid) Nanospheres. *Biomacromolecules* **2013,** *14* (4), 1044-1053.

67. Meng, F. T.; Ma, G. H.; Liu, Y. D.; Qiu, W.; Su, Z. G. Microencapsulation of bovine hemoglobin with high bio-activity and high entrapment efficiency using a W/O/W double emulsion technique. *Colloids Surf. B. Biointerfaces* **2004,** *33*, 177-183.

68. Li, M.; Rouaud, O.; Poncelet, D. Microencapsulation by solvent evaporation: State of the art for process engineering approaches. *Int. J. Pharm.* **2008,** *363*, 26-39.

69. Wei, Y.; Wang, Y.-X.; Wang, W.; Ho, S. V.; Wei, W.; Ma, G.-H. mPEG-PLA microspheres with narrow size distribution increase the controlled release effect of recombinant human growth hormone. *J. Mater. Chem.* **2011,** *21* (34), 12691-12699.

70. Xu, B.; Dou, H.; Tao, K.; Sun, K.; Ding, J.; Shi, W.; Guo, X.; Li, J.; Zhang, D.; Sun, K. "Two-in-one" fabrication of Fe3O4/MePEG-PLA composite nanocapsules as a potential ultrasonic/MRI dual contrast agent. *Langmuir* **2011,** *27* (19), 12134-12142.

71. Andersson, H.; Berg, A. v. d. Microfabrication and microfluidics for tissue engineering: state of the art and future opportunities. *Lab Chip* **2004,** *4* (2), 98-103.

72. Chung, A. J.; Erickson, D. Engineering insect flight metabolics using immature stage implanted microfluidics. *Lab Chip* **2009,** *9* (5), 669-676.

73. Song, H.; Tice, J. D.; Ismagilov, R. F. A Microfluidic System for Controlling Reaction Networks in Time. *Angew. Chem. Int. Ed.* **2003,** *42* (7), 768-772.

74. Zheng, B.; Tice, J. D.; Roach, L. S.; Ismagilov, R. F. A droplet-based, composite PDMS/glass capillary microfluidic system for evaluating protein crystallization conditions by microbatch and vapor-diffusion methods with on-chip X-ray diffraction. *Angew. Chem. Int. Ed. Engl.* **2004,** *43* (19), 2508-11.

75. Zheng, B.; Tice, J. D.; Ismagilov, R. F. Formation of droplets of alternating composition in microfluidic channels and applications to indexing of concentrations in

droplet-based assays. *Anal. Chem.* **2004,** *76* (17), 4977-4982.

76. Chen, D. L.; Gerdts, C. J.; Ismagilov, R. F. Using microfluidics to observe the effect of mixing on nucleation of protein crystals. *J. Am. Chem. Soc.* **2005,** *127* (27), 9672-9673.

77. Toh, Y.-C.; Lim, T. C.; Tai, D.; Xiao, G.; van Noort, D.; Yu, H. A microfluidic 3D hepatocyte chip for drug toxicity testing. *Lab Chip* **2009,** *9* (14), 2026-2035.

78. James, D.; Oag, B.; Rushworth, C. M.; Lee, J. W. L.; Davies, J.; Cabral, J. T.; Vallance, C. High-sensitivity online detection for microfluidics via cavity ringdown spectroscopy. *RSC Advances* **2012,** *2* (12), 5376-5384.

79. Comina, G.; Suska, A.; Filippini, D. PDMS lab-on-a-chip fabrication using 3D printed templates. *Lab Chip* **2014,** *14* (2), 424-430.

80. Nagaki, A.; Ichinari, D.; Yoshida, J.-i. Reactions of organolithiums with dialkyl oxalates. A flow microreactor approach to synthesis of functionalized [small alpha]-keto esters. *Chem. Commun.* **2013,** *49* (31), 3242-3244.

81. Song, H.; Chen, D. L.; Ismagilov, R. F. Reactions in Droplets in Microfluidic Channels. *Angew. Chem. Int. Ed.* **2006,** *45* (44), 7336-7356.

82. Huebner, A.; Sharma, S.; Srisa-Art, M.; Hollfelder, F.; Edel, J. B.; deMello, A. J. Microdroplets: A sea of applications? *Lab Chip* **2008,** *8* (8), 1244-1254.

83. Kelly, B. T.; Baret, J.-C.; Taly, V.; Griffiths, A. D. Miniaturizing chemistry and biology in microdroplets. *Chem. Commun.* **2007,** (18), 1773-1788.

84. Whitesides, G. M. The origins and the future of microfluidics. *Nature* **2006,** *442* (7101), 368-373.

85. Watts, P.; Haswell, S. J. The application of micro reactors for organic synthesis. *Chem. Soc. Rev.* **2005,** *34* (3), 235-246.

86. Xu, Q.; Hashimoto, M.; Dang, T. T.; Hoare, T.; Kohane, D. S.; Whitesides, G. M.; Langer, R.; Anderson, D. G. Preparation of monodisperse biodegradable polymer microparticles using a microfluidic flow-focusing device for controlled drug delivery. *Small* **2009,** *5* (13), 1575-1581.

87. Huang, K.-S.; Lu, K.; Yeh, C.-S.; Chung, S.-R.; Lin, C.-H.; Yang, C.-H.; Dong, Y.-S. Microfluidic controlling monodisperse microdroplet for 5-fluorouracil loaded genipin-gelatin microcapsules. *J. Controlled Release* **2009,** *137* (1), 15-19.

88. Link, D. R.; Grasland-Mongrain, E.; Duri, A.; Sarrazin, F.; Cheng, Z.; Cristobal, G.; Marquez, M.; Weitz, D. A. Electric Control of Droplets in Microfluidic

Devices. *Angew. Chem. Int. Ed.* **2006,** *45* (16), 2556-2560.

89. Nguyen, N.-T.; Ting, T.-H.; Yap, Y.-F.; Wong, T.-N.; Chai, J. C.-K.; Ong, W.-L.; Zhou, J.; Tan, S.-H.; Yobas, L. Thermally mediated droplet formation in microchannels. *Appl. Phys. Lett.* **2007,** *91* (8), 084102.

90. Martz, T. D.; Bardin, D.; Sheeran, P. S.; Lee, A. P.; Dayton, P. A. Microfluidic generation of acoustically active nanodroplets. *Small* **2012,** *8* (12), 1876-1879.

91. Harada, T.; Kanda, T.; Suzumori, K.; Ono, T.; Iwabuchi, S.; Ito, K.; Ogawara, K.-i.; Higaki, K. Emulsion Generating Microchannel Device Oscillated by 2.25 MHz Ultrasonic Vibrator. *Jpn. J. Appl. Phys.* **2010,** *49* (7), 07HE13.

92. Thorsen, T.; Roberts, R. W.; Arnold, F. H.; Quake, S. R. Dynamic Pattern Formation in a Vesicle-Generating Microfluidic Device. *Phys. Rev. Lett.* **2001,** *86* (18), 4163-4166.

93. Atencia, J.; Beebe, D. J. Controlled microfluidic interfaces. *Nature* **2005,** *437* (7059), 648-655.

94. Christopher, G. F.; Noharuddin, N. N.; Taylor, J. A.; Anna, S. L. Experimental observations of the squeezing-to-dripping transition in T-shaped microfluidic junctions. *Physical Review E* **2008,** *78* (3), 036317.

95. De Menech, M.; Garstecki, P.; Jousse, F.; Stone, H. A. Transition from squeezing to dripping in a microfluidic T-shaped junction. *J. Fluid Mech.* **2008,** *595*, 141-161.

96. Steegmans, M. L.; Warmerdam, A.; Schroen, K. G.; Boom, R. M. Dynamic interfacial tension measurements with microfluidic Y-junctions. *Langmuir* **2009,** *25* (17), 9751-9758.

97. Guillot, P.; Ajdari, A.; Goyon, J.; Joanicot, M.; Colin, A. Droplets and jets in microfluidic devices. *Comptes Rendus Chimie* **2009,** *12* (1-2), 247-257.

98. Utada, A.; Fernandez-Nieves, A.; Stone, H.; Weitz, D. Dripping to Jetting Transitions in Coflowing Liquid Streams. *Phys. Rev. Lett.* **2007,** *99* (9), 094502.

99. Utada, A.; Fernandez-Nieves, A.; Gordillo, J.; Weitz, D. Absolute Instability of a Liquid Jet in a Coflowing Stream. *Phys. Rev. Lett.* **2008,** *100* (1), 014502.

100. Shao, T.; Feng, X.; Jin, Y.; Cheng, Y. Controlled production of double emulsions in dual-coaxial capillaries device for millimeter-scale hollow polymer spheres. *Chem. Eng. Sci.* **2013,** *104* (0), 55-63.

101. Bauer, W. A.; Fischlechner, M.; Abell, C.; Huck, W. T. Hydrophilic PDMS

microchannels for high-throughput formation of oil-in-water microdroplets and water-in-oil-in-water double emulsions. *Lab Chip* **2010,** *10* (14), 1814-1819.

102. Nie, Z.; Seo, M.; Xu, S.; Lewis, P. C.; Mok, M.; Kumacheva, E.; Whitesides, G. M.; Garstecki, P.; Stone, H. A. Emulsification in a microfluidic flow-focusing device: effect of the viscosities of the liquids. *Microfluid. Nanofluid.* **2008,** *5* (5), 585-594.

103. Roberts, C. C.; Rao, R. R.; Loewenberg, M.; Brooks, C. F.; Galambos, P.; Grillet, A. M.; Nemer, M. B. Comparison of monodisperse droplet generation in flow-focusing devices with hydrophilic and hydrophobic surfaces. *Lab Chip* **2012,** *12* (8), 1540-1547.

104. Deng, N. N.; Meng, Z. J.; Xie, R.; Ju, X. J.; Mou, C. L.; Wang, W.; Chu, L. Y. Simple and cheap microfluidic devices for the preparation of monodisperse emulsions. *Lab Chip* **2011,** *11* (23), 3963-3969.

105. Duffy, D. C.; McDonald, J. C.; Schueller, O. J.; Whitesides, G. M. Rapid prototyping of microfluidic systems in poly (dimethylsiloxane). *Anal. Chem.* **1998,** *70* (23), 4974-4984.

106. Anton, N.; Bally, F.; Serra, C. A.; Ali, A.; Arntz, Y.; Mely, Y.; Zhao, M.; Marchioni, E.; Jakhmola, A.; Vandamme, T. F. A new microfluidic setup for precise control of the polymer nanoprecipitation process and lipophilic drug encapsulation. *Soft Matter* **2012,** *8* (41), 10628-10635.

107. Sugiura, S.; Nakajima, M.; Tong, J.; Nabetani, H.; Seki, M. Preparation of Monodispersed Solid Lipid Microspheres Using a Microchannel Emulsification Technique. *J. Colloid Interface Sci.* **2000,** *227* (1), 95-103.

108. Sugiura, S.; Nakajima, M.; Seki, M. Preparation of monodispersed emulsion with large droplets using microchannel emulsification. *J. Am. Oil Chem. Soc.* **2002,** *79* (5), 515-519.

109. Garstecki, P.; Fuerstman, M. J.; Stone, H. A.; Whitesides, G. M. Formation of droplets and bubbles in a microfluidic T-junction-scaling and mechanism of break-up. *Lab Chip* **2006,** *6* (3), 437-446.

110. Baroud, C. N.; Gallaire, F.; Dangla, R. Dynamics of microfluidic droplets. *Lab Chip* **2010,** *10* (16), 2032-2045.

111. Seo, M.; Nie, Z.; Xu, S.; Mok, M.; Lewis, P. C.; Graham, R.; Kumacheva, E. Continuous Microfluidic Reactors for Polymer Particles. *Langmuir* **2005,** *21* (25),

11614-11622.

112. Eggleton, C. D.; Tsai, T.-M.; Stebe, K. J. Tip Streaming from a Drop in the Presence of Surfactants. *Phys. Rev. Lett.* **2001,** *87* (4), 048302.

113. Anna, S. L.; Mayer, H. C. Microscale tipstreaming in a microfluidic flow focusing device. *Phys. Fluids* **2006,** *18* (12), 121512.

114. Moyle, T. M.; Walker, L. M.; Anna, S. L. Predicting conditions for microscale surfactant mediated tipstreaming. *Phys. Fluids* **2012,** *24* (8), 082110.

115. Moyle, T. M.; Walker, L. M.; Anna, S. L. Controlling thread formation during tipstreaming through an active feedback control loop. *Lab on a Chip* **2013,** *13* (23), 4534-4541.

116. Sherwood, J. Tip streaming from slender drops in a nonlinear extensional flow. *J. Fluid Mech.* **1984,** *144* (1), 281-295.

117. Ward, T.; Faivre, M.; Stone, H. A. Drop production and tip-streaming phenomenon in a microfluidic flow-focusing device via an interfacial chemical reaction. *Langmuir* **2010,** *26* (12), 9233-9239.

118. Jeong, W. C.; Lim, J. M.; Choi, J. H.; Kim, J. H.; Lee, Y. J.; Kim, S. H.; Lee, G.; Kim, J. D.; Yi, G. R.; Yang, S. M. Controlled generation of submicron emulsion droplets via highly stable tip-streaming mode in microfluidic devices. *Lab Chip* **2012,** *12* (8), 1446-1453.

119. Teh, S. Y.; Khnouf, R.; Fan, H.; Lee, A. P. Stable, biocompatible lipid vesicle generation by solvent extraction-based droplet microfluidics. *Biomicrofluidics* **2011,** *5* (4), 44113-44113-12.

120. Okushima, S.; Nisisako, T.; Torii, T.; Higuchi, T. Controlled Production of Monodisperse Double Emulsions by Two-Step Droplet Breakup in Microfluidic Devices. *Langmuir* **2004,** *20* (23), 9905-9908.

121. Chen, C. H.; Abate, A. R.; Lee, D.; Terentjev, E. M.; Weitz, D. A. Microfluidic assembly of magnetic hydrogel particles with uniformly anisotropic structure. *Adv. Mater.* **2009,** *21* (31), 3201-3204.

122. Perro, A.; Nicolet, C. l.; Angly, J.; Lecommandoux, S. b.; Le Meins, J.-F. o.; Colin, A. Mastering a Double Emulsion in a Simple Co-Flow Microfluidic to Generate Complex Polymersomes. *Langmuir* **2010,** *27* (14), 9034-9042.

123. Thiele, J.; Abate, A. R.; Shum, H. C.; Bachtler, S.; Forster, S.; Weitz, D. A. Fabrication of polymersomes using double-emulsion templates in glass-coated stamped

microfluidic devices. *Small* **2010,** *6* (16), 1723-1727.

124. Abate, A. R.; Thiele, J.; Weitz, D. A. One-step formation of multiple emulsions in microfluidics. *Lab Chip* **2011,** *11* (2), 253-258.

125. Thiele, J.; Chokkalingam, V.; Ma, S.; Wilson, D. A.; Huck, W. T. S. Vesicle budding from polymersomes templated by microfluidically prepared double emulsions. *Materials Horizons* **2014,** *1* (1), 96-101.

126. Barbier, V.; Tatoulian, M.; Li, H.; Arefi-Khonsari, F.; Ajdari, A.; Tabeling, P. Stable Modification of PDMS Surface Properties by Plasma Polymerization: Application to the Formation of Double Emulsions in Microfluidic Systems. *Langmuir* **2006,** *22* (12), 5230-5232.

127. Bodas, D.; Khan-Malek, C. Hydrophilization and hydrophobic recovery of PDMS by oxygen plasma and chemical treatment—An SEM investigation. *Sensors Actuators B: Chem.* **2007,** *123* (1), 368-373.

128. Utada, A. S.; Lorenceau, E.; Link, D. R.; Kaplan, P. D.; Stone, H. A.; Weitz, D. A. Monodisperse double emulsions generated from a microcapillary device. *Science* **2005,** *308* (5721), 537-541.

129. Rayleigh, L. On the Capillary Phenomena of Jets. *Proc. R. Soc. London* **1879,** *29* (196-199), 71-97.

130. Häfeli, U. O.; Saatchi, K.; Elischer, P.; Misri, R.; Bokharaei, M.; Labiris, N. R. e.; Stoeber, B. Lung perfusion imaging with monosized biodegradable microspheres. *Biomacromolecules* **2010,** *11* (3), 561-567.

131. He, T.; Liang, Q.; Zhang, K.; Mu, X.; Luo, T.; Wang, Y.; Luo, G. A modified microfluidic chip for fabrication of paclitaxel-loaded poly(l-lactic acid) microspheres. *Microfluid. Nanofluid.* **2011,** *10* (6), 1289-1298.

132. Duncanson, W. J.; Zieringer, M.; Wagner, O.; Wilking, J. N.; Abbaspourrad, A.; Haag, R.; Weitz, D. A. Microfluidic synthesis of monodisperse porous microspheres with size-tunable pores. *Soft Matter* **2012,** *8* (41), 10636-10640.

133. Vladisavljevic, G. T.; Duncanson, W. J.; Shum, H. C.; Weitz, D. A. Emulsion templating of poly(lactic acid) particles: droplet formation behavior. *Langmuir* **2012,** *28* (36), 12948-12954.

134. Shi, S.; Zhou, L.; Wang, T.; Bian, L.; Tang, Y.; Kuroda, S.-i. Preparation of raspberry-like poly(methyl methacrylate) particles by seeded dispersion polymerization. *J. Appl. Polym. Sci.* **2011,** *120* (1), 501-508.

135. Xu, S.; Nie, Z.; Seo, M.; Lewis, P.; Kumacheva, E.; Stone, H. A.; Garstecki, P.; Weibel, D. B.; Gitlin, I.; Whitesides, G. M. Generation of monodisperse particles by using microfluidics: control over size, shape, and composition. *Angew. Chem. Int. Ed. Engl.* **2005,** *44* (5), 724-728.

136. Bae, S. E.; Son, J. S.; Park, K.; Han, D. K. Fabrication of covered porous PLGA microspheres using hydrogen peroxide for controlled drug delivery and regenerative medicine. *J. Control. Release* **2009,** *133* (1), 37-43.

137. Zhu, J.; Hayward, R. C. Hierarchically structured microparticles formed by interfacial instabilities of emulsion droplets containing amphiphilic block copolymers. *Angew. Chem. Int. Ed. Engl.* **2008,** *47* (11), 2113-2116.

138. Zhu, J.; Hayward, R. C. Interfacial tension of evaporating emulsion droplets containing amphiphilic block copolymers: effects of solvent and polymer composition. *J. Colloid Interface Sci.* **2012,** *365* (1), 275-279.

139. Atkin, R.; Davies, P.; Hardy, J.; Vincent, B. Preparation of Aqueous Core/Polymer Shell Microcapsules by Internal Phase Separation. *Macromolecules* **2004,** *37* (21), 7979-7985.

140. Kim, M. R.; Lee, S.; Park, J. K.; Cho, K. Y. Golf ball-shaped PLGA microparticles with internal pores fabricated by simple O/W emulsion. *Chem. Commun. (Camb.)* **2010,** *46* (39), 7433-7435.

141. Choi, C. H.; Weitz, D. A.; Lee, C. S. One step formation of controllable complex emulsions: from functional particles to simultaneous encapsulation of hydrophilic and hydrophobic agents into desired position. *Adv. Mater.* **2013,** *25* (18), 2536-2541.

142. Zhao, Y.; Fickert, J.; Landfester, K.; Crespy, D. Encapsulation of self-healing agents in polymer nanocapsules. *Small* **2012,** *8* (19), 2954-2958.

143. Pisani, E.; Ringard, C.; Nicolas, V.; Raphaël, E.; Rosilio, V.; Moine, L.; Fattal, E.; Tsapis, N. Tuning microcapsules surface morphology using blends of homo- and copolymers of PLGA and PLGA-PEG. *Soft Matter* **2009,** *5* (16), 3054-3060.

144. Lensen, D.; van Breukelen, K.; Vriezema, D. M.; van Hest, J. C. Preparation of biodegradable liquid core PLLA microcapsules and hollow PLLA microcapsules using microfluidics. *Macromol. Biosci.* **2010,** *10* (5), 475-480.

145. Shum, H. C.; Kim, J.-W.; Weitz, D. A. Microfluidic fabrication of monodisperse biocompatible and biodegradable polymersomes with controlled

permeability. *J. Am. Chem. Soc.* **2008,** *130* (29), 9543-9549.

146. Lee, M. H.; Hribar, K. C.; Brugarolas, T.; Kamat, N. P.; Burdick, J. A.; Lee, D. Harnessing Interfacial Phenomena to Program the Release Properties of Hollow Microcapsules. *Adv. Funct. Mater.* **2012,** *22* (1), 131-138.

147. Amstad, E.; Kim, S. H.; Weitz, D. A. Photo- and thermoresponsive polymersomes for triggered release. *Angew. Chem. Int. Ed. Engl.* **2012,** *51* (50), 12499-12503.

Chapter 2
Preparation of monodisperse PLA microparticles using microfluidics

2-1 Introduction

Microparticles consisting of biodegradable polymers have been developed for use in chemical industry such as in coatings, inks, foods, cosmetics, agrichemicals and drug delivery carriers.[1-3] Especially, PLA and PLGA have been intensely studied all over the world in recent decades because they can be synthesized from renewable resources. In addition, they also have excellent biodegradability and biocompatibility. Because of this, when they are taken into our body, they undergo hydrolysis reaction under acidic or alkali conditions, which gives rise to secession of the polymer chains and provides their monomer molecules that are non-toxic to the human body and environment.

In general, PLA/PLGA microparticles are prepared by emulsion-solvent evaporation technique.[4-7] In this technique, O/W emulsion is employed as a template, in which the dispersed organic phase consists of the polymer with a volatile solvent. As the volatile solvent evaporates from the polymer droplets, the droplets shrink and the concentration of polymer in the droplets increases and eventually reaches the saturation concentration, thereby precipitating the polymer and yielding the polymer particles with a spherical form. It is considered that these microparticles are promising candidates as a drug delivery carrier to employ sustained release of drugs. However the technique has some drawbacks to be addressed such as the presence of toxic organic solvent residues and a surfactant in the end products, requirement for multi-step preparation and minimal control of the size of the microparticles.

During the emulsion preparation, dichloromethane (DCM) or chloroform are commonly used as an organic solvent due to the good solubility of polyesters and its high volatility, which facilitates the evaporation from the emulsion droplets, however, the remaining solvents in the end products are severely toxic to human health, especially for their organs such as liver and kidney when the microparticles are used as

a drug carrier[8]. In addition, surfactant residues after the microparticle preparation are the other impurity and make it difficult to obtain fine end products. Therefore, the complete removal of them from the products is required to improve the quality of the products.

From the point of view of chemical industry, the multi-step preparation of the microparticles increases the equipment investment and the total production cost. Considering solvent evaporation process after the emulsion preparation, it takes several tens minutes to hours to remove the organic solvent from the system, depending on the volume of reaction vessel even if volatile organic solvents discussed above are employed. This evaporation process is the rate-determining step to obtain the microparticles.

Regarding microparticle size, uniformity in the diameter enhances the quality of the final products in all applications and saves further separation processes. Especially for drug delivery applications, monodisperse carriers decrease undesirable side effects and achieve precise control of drug release kinetics and encapsulation efficiency.[9-10] In the last decade, extrusion emulsification using a Shirasu porous glass membrane, followed by emulsion-solvent evaporation has been developed to produce uniform microparticles.[11-15] However, in fact, the polydispersity of the droplets is higher around CV = 7-15% than that in microchannel emulsification. In addition, it is difficult to control over the diameter of the microparticles because the diameter and the monodispersity are strongly dependent on the pore size distribution of the membrane that is used. Furthermore, the intrinsic surface anion charge of the membrane also affects the droplet production, which gives limitation in the choice of surfactant regardless of stability of the emulsion. On the other hand, microfluidic approaches have enabled the fabrication of monodisperse microparticles with well-defined sizes and structures.[16-18] For example, using a coaxial microcapillary fluidic device, monodisperse PEG-*b*-PLA polymersomes have been prepared *via* W/O/W emulsion-solvent evaporation method by Weitz group.[19] In the preparation of W/O/W emulsion, however, a mixture of toluene and chloroform, toxic to human health, was still used as the middle organic phase. In addition, the prepared emulsion was required to be stored in a vessel for a few hours until the polymersomes were obtained by evaporation of the organic solvent from the dispersed phase. To employ microfluidic technology for industrial production of functional microspheres, it is desirable to construct a simple and

environmentally friendly continuous process for the preparation of monodisperse microspheres.

In this chapter, a novel, environmentally friendly method to fabricate monodisperse PLA microparticles with controlled sizes through combining microfluidic emulsification and subsequent emulsion-solvent diffusion is described. The microfluidic emulsification technique is used to fabricate monodisperse O/W single emulsions. During the preparation, alternative to DCM and chloroform, EA, an organic solvent approved by the FDA, is used as an organic phase because of its low toxicity and its high solubility in water (8.7%, w/w). The high solubility of water in EA allows polymer droplets to solidify by solvent diffusion process. On the other hand, although almost all conventional reports have employed poly(vinyl alcohol) or sodium dodecyl sulfate to produce stable O/W emulsions, as discussed earlier, the remaining surfactant on the surface of microparticles is not always good for the clinical applications. Thus, instead of these commercial surfactants, w-PEG-*b*-PLA is applied to the emulsion preparation since the whole diblock copolymer is an environmentally friendly nature, meaning that there is no need to consider the residue in the end products. The PEG segment is hydrophilic and biocompatible, whilst the PLA segment is hydrophobic and biocompatible. In addition, EA is a good solvent for only the PLA segment, though DCM dissolves both the PEG and the PLA segments. For this selective solubility of the copolymer, w-PEG-*b*-PLA plays a role in a surfactant in EA/water emulsion system.[20]

PLA and PEG-*b*-PLA with different compositions were firstly synthesized by a ring-opening polymerization. The surface activity of w-PEG-*b*-PLA between EA and water saturated with EA was evaluated by using a Wilhelmy plate method. Then the optimal conditions for preparing monodisperse O/W emulsion by microfluidic emulsification were investigated. The effect of the continuous flow rate on the diameter of polymer droplets was also investigated. Monodisperse PLA droplets were then mixed with excess amount of pure water, which facilitated the solvent diffusion of EA from the droplets to the external aqueous phase and resulted in precipitation of PLA microparticles. The effect of the flow rate of continuous phase and the concentration of PLA in the organic phase on the diameter of the microparticles was investigated. In addition, the diameters of the microparticles obtained in the experiments were in comparison with those theoretical values in order to evaluate the compactness of the resulting microparticles. Moreover, the effect of addition of o-PEG-*b*-PLA on the final

morphology was investigated.

2-2 Experimental procedures

2-2-1 Materials

D,L-lactide was purchased from Purac (Netherland), which was used as a monomer for a ring-opening polymerization after recrystallization using toluene. Poly(ethylene glycol) monomethyl ether (PEG, *M*n = 4,000, *M*w/*M*n = 1.06) was kindly supplied from NOF (Japan) and used as a macromoinitiator for the polymerization. Tin(II) 2-ethylhexanoate ($Sn(Oct)_2$), *n*-hexane, 2-propanol and EA were obtained from Wako Pure Chemical Industries, Ltd. (Japan). All reagents are of the finest grade available and used as received. Ultra pure water was produced by a Millipore Milli-Q purification system (EMD Millipore Corporation, USA).

2-2-2 Syntheses of PLA and PEG-*b*-PLA

PLA and PEG-*b*-PLA were synthesized by a ring-opening polymerization of D,L-lactide using lauryl alcohol and PEG as an initiator, respectively in the presence of $Sn(Oct)_2$ as a catalyst (**Scheme 2-1**).[21] D,L-lactide, the initiator and a toluene solution of tin(II) 2-ethylhexanoate at 80 mg mL^{-1} were introduced into a glass ampule, which was sealed in vacuo and immersed in an oil bath at 130°C. The polymerization was carried out for 24 hours. After the reaction, the ampule was broken and the reaction mixture was dissolved in 50 mL of chloroform, which was reprecipitated in 400 mL of *n*-hexane through a cotton filter. The precipitated polymer was recovered by decantation and washed with 2-propanol, after which the product was dried in an oven at 40°C under reduced pressure. The molecular weight distributions (*M*w/*M*n) of the polymers were measured by Gel Permeation Chromatography (GPC, HLC-8220GPC, TOSOH, Japan) at 40°C, equipped with a refractive index detector and columns (TSKguardcolumn SuperH-H, TSKgel SuperHM-H, and TSKgel SuperH2000, TOSOH, Japan). THF was used as the eluent at a flow rate of 0.6 mL min^{-1}. The calibration curve was prepared by using polystyrene standards. The chemical structures of the polymers were confirmed from ^{1}H NMR spectra. The analysis was carried out using a JEOL FT NMR System (300 MHz, JMN-AL300, JEOL, Japan) at room temperature in $CHCl_3$-*d*. The number average molecular weights (*M*n) of the polymers were calculated from ^{1}H NMR spectra. With regard to PEG-*b*-PLA diblock copolymers, they were characterized using

hydrophilic-lipophile balance (HLB) calculated by Griffin's method using the equation as follow.[22]

$$\boldsymbol{HLB = 20 \times \frac{M_n(PEG)}{M_n(PEG-b-PLA)}} \qquad (2\text{-}1)$$

Scheme 2-1 Synthesis of PLA and PEG-*b*-PLA *via* ring opening polymerization of D,L-lactide.

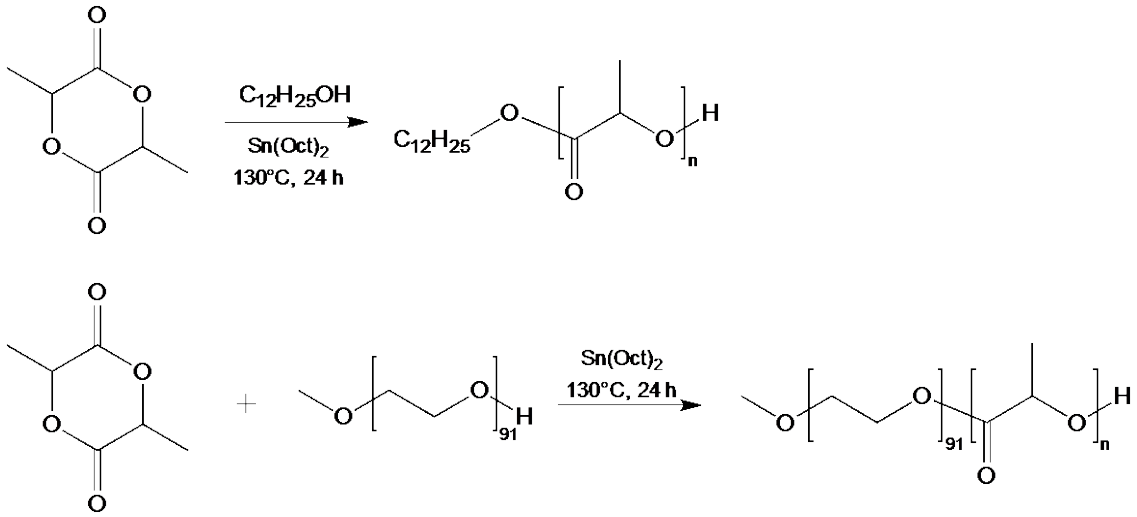

2-2-3 Interfacial tension measurement

The interfacial tensions between EA and EA-saturated aqueous solutions dissolving w-PEG-*b*-PLA at various concentrations were measured using a Wilhelmy plate interfacial tension meter (K100, Krüss, Germany). The aqueous solution containing w-PEG-*b*-PLA (*M*n=4,400, *M*w/*M*n= 1.05, HLB= 18.2) at various concentrations (5 mL) was poured into a 50 mL vessel, and then EA (20 mL) was gently added into the aqueous solution. The measurements were performed at 20°C. The interfacial tension was accepted as an equilibrium value when it reached constant value regardless of time.

2-2-4 Fabrication of PLA microparticles using microfluidics

The schematic illustration of the preparation process of PLA microparticles is shown in **Scheme 2-2**. Poly(D,L-lactide) (PLA, *M*n= 3,200, *M*w/*M*n = 1.12) was dissolved in EA, which was served as a dispersed organic phase. The concentrations of the PLA were 1.0, 2.5 and 5.0 wt%, depending on the conditions. Aqueous solution saturated with EA, dissolving 1 wt% of w-PEG-*b*-PLA (*M*n= 4,400, *M*w/*M*n =18.2) was used as a continuous aqueous phase. After complete dissolution of polymers in the solvents, each solution was placed in a glass microsyringe (1000 series, Hamilton Company, RN). The microsyringes were mounted on syringe pumps (BS-MD1001, ISIS Co., Ltd) and syringe pump controller (BS-MD 1020, ISIS Co., Ltd) that can synchronously operate two syringes at various flow rates. The solutions were separately fed into a simple Y-shaped microfluidic device (Kasen Nozzle Co. Ltd., Japan). The organic phase flow channel (ϕ 126 μm wide x 75 μm depth) meets the aqueous phase flow channel (ϕ 136 μm wide x 75 μm depth) at an angle of 44°. The flow rate of the organic phase (Q_d) was kept constant at 1 μL min^{-1}, whilst that of the aqueous phase (Q_c) was controlled from 5 to 100 μL min^{-1}. Prepared O/W emulsion droplets were directly poured into 100 mL of ultrapure water *via* Teflon tubing (ϕ = 0.5 mm, *L* = 20 cm), which was connected to the outlet of the microfluidic device. The tip of the tubing was immersed into the ultrapure water in a vessel (100 mL). EA was rapidly removed from the polymer droplet (organic phase) by solvent diffusion to the water phase, inducing volume reduction in the droplets and eventually precipitating PLA as a spherical form. The system was run for more than 15 minutes, after which solidified microparticles were collected in a 15 mL of centrifugation tube, centrifuged at 11,000 rpm for 3 minutes, and washed with

ultrapure water three times so as to remove excess w-PEG-*b*-PLA. Then, the microparticle dispersion was lyophilized over night.

Scheme 2-2 Schematic illustration of the procedure to fabricate monodisperse PLA microparticles by combining microfluidic emulsification and solvent diffusion.

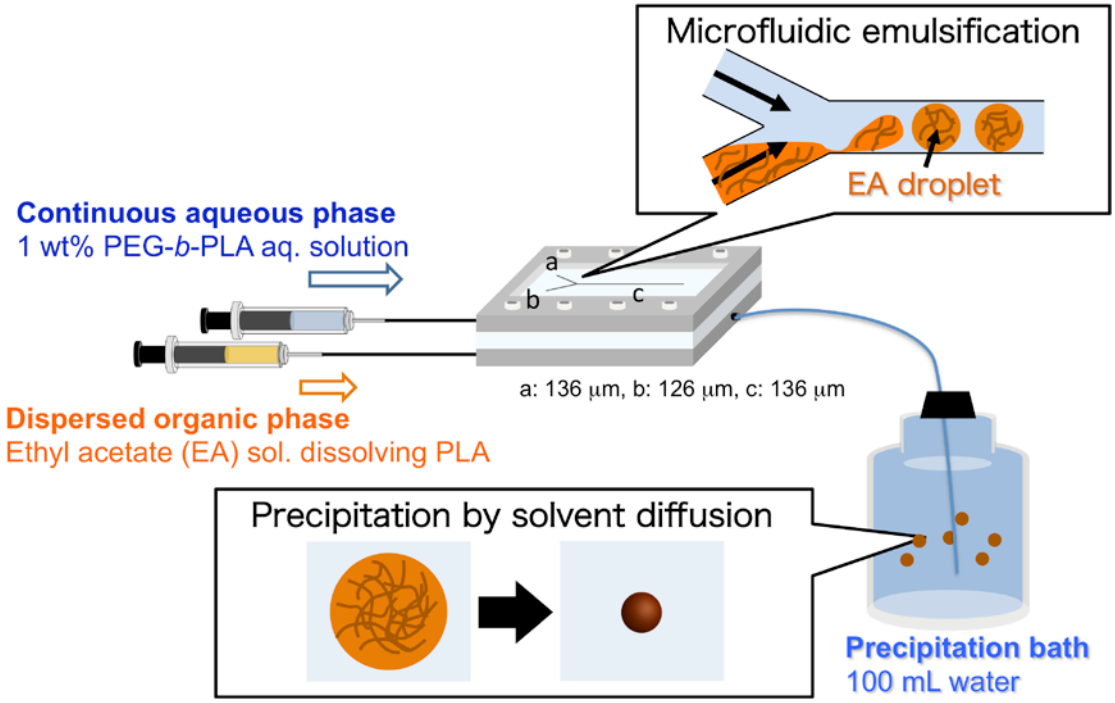

2-2-5 Observation of the microparticle morphology

Prepared O/W emulsion droplets in the Teflon tubing were observed using an optical microscope (OLYMPUS BX50). The microparticles after freeze-drying were observed by a scanning electron microscope (SEM, S-4700, Hitachi, Ltd.) at an intensity of 1 kV under various magnifications. Prior to observation, the samples were coated with Pt-Pd using a sputter-coater (E-1030 Ion Sputter, Hitachi, Ltd.). From optical microscopy images and SEM microphotographs, polydispersity of the droplets and the microparticles was characterized as the coefficient of variation (CV), CV = σ / D, where σ is the standard deviation of droplet diameter (μm) and D is the mean diameter of the droplets (μm). To obtain D and CV of droplets and microparticles, the dimensions of 200 samples were measured.

2-2-6 Calculation of theoretical microparticle size

Theoretical final particle size (D_{th}) was estimated from the initial emulsion droplet size and the dispersed phase compositions using the following equation.

$$\boldsymbol{D_{th} = [x_{PLA}/(1-\varepsilon)\cdot(\rho_d/\rho_{PLA})]^{1/3}\cdot D_{drop}} \quad (2\text{-}2)$$

where D_{drop}; emulsion droplet size [μm], x_{PLA}; mass fraction of PLA in EA [-], ε; particle porosity [-], ρ_{EA}; density of EA [g mL^{-1}], and ρ_{PLA}; density of PLA [g mL^{-1}].

2-3 Results and discussion

2-3-1 Syntheses of PLA and PEG-*b*-PLA

Both PLA and amphiphilic PEG-*b*-PLA were synthesized *via* ring-opening polymerization of D,L-lactide initiated by initiators having a hydroxide group. Figure 2-1 shows ^{1}H NMR spectra of representative PLA and PEG-*b*-PLA. In Figure 2-1 (A), peaks a (δ = 1.57), b (δ = 5.15) and c (δ = 1.35) were assigned to methine proton of the PLA block, methyl protons of the PLA block and dodecyl protons relating to the initiator, respectively. From these peaks, the synthesis of PLA was confirmed. In Figure 2-1 (B), a successful synthesis of PEG-*b*-PLA was also confirmed from the peaks derived from the PEG block ((d) δ = 3.65 and (e) δ = 3.35) and the PLA block ((a) δ = 1.60 and (b) δ = 5.10).

The molecular weights and the molecular weight distributions of PLA and PEG-*b*-PLA were summarized in **Table 2-1**. The molecular weights of PLA were determined from the spectrum by comparing the relative intensity of dodecyl groups of lauryl alcohol and the methine groups of the PLA block. In the case of PEG-*b*-PLA, the molecular weight was calculated by comparing the ratio of methine protons of the PLA block to methylene protons of the PEG block. In the polymerization, the molecular weights of PLA and PEG-*b*-PLA were finely controlled by changing the molar ratio of monomer to initiator. As shown in **Table 2-1**, the molecular weight distributions of polymers were narrow (Mw/Mn ~ 1.3), implying that the ring-opening polymerization proceeded with a pseudo-controlled living process. With regard to PEG-*b*-PLA diblock copolymers, two kinds of them with different solubility were synthesized. One is water-soluble PEG-*b*-PLA with HLB value at 18.2, which was used as a polymeric surfactant when preparing the O/W emulsion. The other one is oil-soluble PEG-*b*-PLA with HLB lower than 10, which is soluble in EA but poorly soluble in water. The oil-soluble PEG-*b*-PLA was used as a matrix of microparticles.

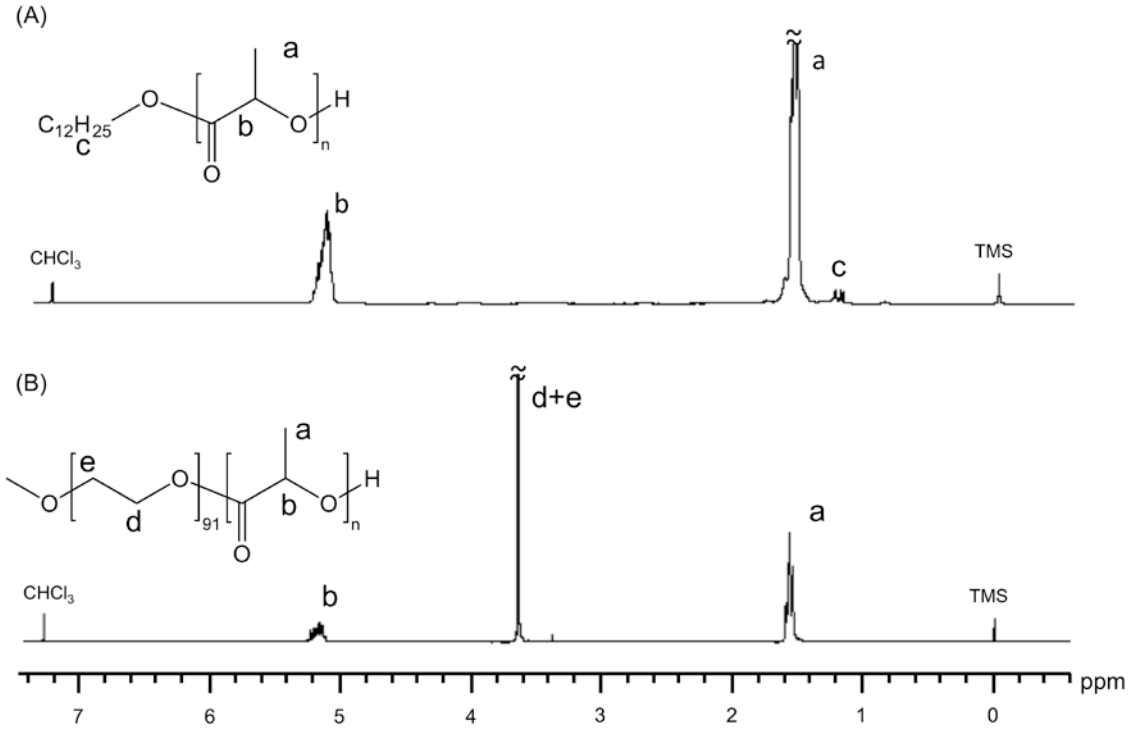

Figure 2-1 ^{1}H NMR spectra of (A) PLA and (B) PEG-*b*-PLA. (Solvent; $CHCl_3$-*d*).

Table 2-1 Synthesis results of PLA and PEG-*b*-PLA.

Sample	*M*n[a]		*M*w/*M*n[b]	HLB[c]
	PEG-PLA	PLA		
PLA-1	-	3,200	1.12	-
PLA-2	-	7,300	1.31	-
o-PEG-*b*-PLA	14,200	10,200	1.20	5.6
w-PEG-*b*-PLA	4,400	400	1.06	18.2

[a] Calculated from ^{1}H NMR spectra. [b] Determined by GPC.
[c] Calculated by Griffin's method. HLB = 20 x Mn_{PEG} / $Mn_{PEG\text{-}b\text{-}PLA}$

2-3-2 Interfacial tension measurement

In order to obtain stable emulsions without coalescence, it is important to use a surfactant with a high surface activity. As discussed above, in the previous study, EA/water (O/W) nanoemulsion has been successfully prepared using w-PEG-*b*-PLA.[20] However, the surface activity of w-PEG-*b*-PLA such as critical micellar concentration (CMC) that is a concentration above which the surfactant molecules start to form micelles has never been determined. Therefore, the interfacial activity of w-PEG-*b*-PLA between the given emulsion system was firstly assessed by measuring the interfacial tensions.

Figure 2-2 depicts interfacial tensions between EA and water-saturated with EA as a function of w-PEG-*b*-PLA concentration in aqueous phase. The interfacial tension without the surfactant was 5.3 mN m^{-1} (data not shown), which is relatively lower interfacial tension than the other typical O/W systems.[23] This lower interfacial tension comes from high miscibility of EA in water. In Figure 2-2, the interfacial tension decreased with increasing the concentration of w-PEG-*b*-PLA and reached plateau value around 2.6 mN m^{-1} above 0.01 wt% although it showed a slight decrease at higher concentration. From the kink in Figure 2-2, the CMC of w-PEG-*b*-PLA was determined at 0.01 wt%. These results showed that w-PEG-*b*-PLA had a strong surface activity at an interface between EA and water saturated with EA. Considering the results, when preparing O/W emulsion in the following experiments, the concentration of w-PEG-*b*-PLA in the continuous phase was fixed at 1 wt%, which is approximately 100 folds of the CMC.

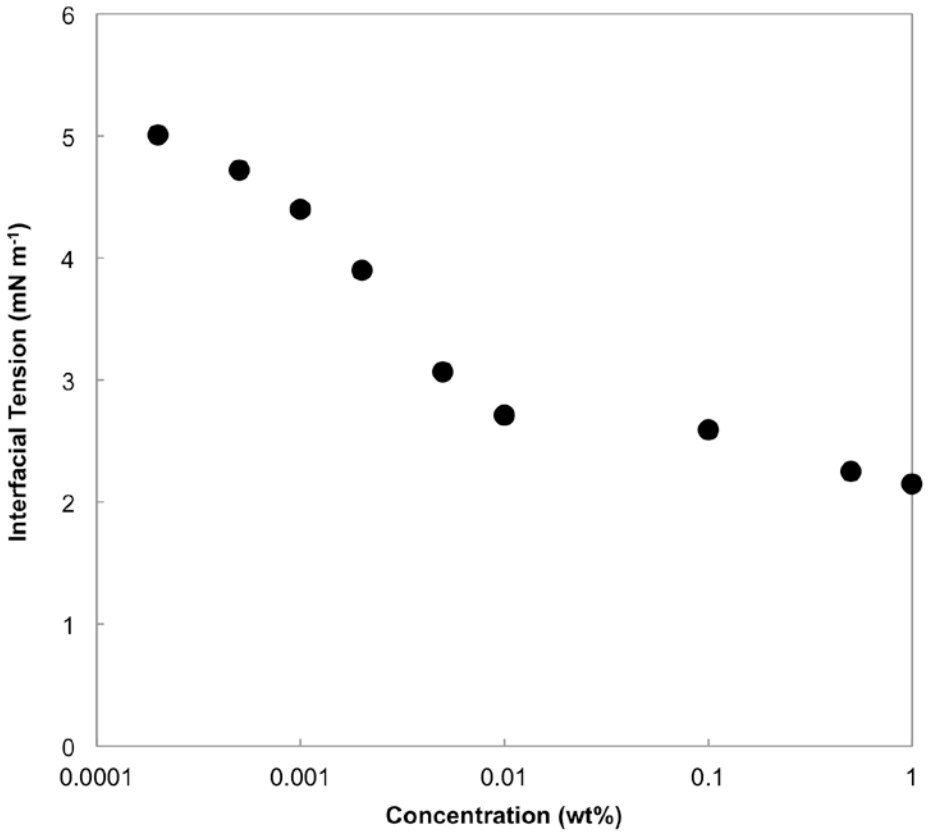

Figure 2-2 Interfacial tensions between EA and water saturated with EA as a function of w-PEG-*b*-PLA concentration in the continuous phase. The interfacial tension between them in the absence of w-PEG-*b*-PLA was 5.3 mN m^{-1}.

After successful synthesis of polymers in this study, the design of microfluidic device used for producing monodisperse emulsion droplets was considered. In order to prepare O/W emulsion in microchannel, it is inevitable to use a microfluidic device with hydrophilic surface to circumvent undesirable wetting of the dispersed organic phase on the channel. In this study, a commercial microfluidic device with a simple Y-shaped geometry was chosen to generate O/W emulsions, which was made from SUS that was covered with a thick glass plate. The advantage of SUS for a material of the channel is to have not only hydrophilic surface but also high chemical resistance.

On the emulsion preparation, an EA solution dissolving 1 wt% of PLA (Mn = 3,200, Mw/Mn = 1.12) was used as a dispersed organic phase. For the continuous aqueous phase, an aqueous solution containing 1 wt% of w-PEG-*b*-PLA (Mn = 4,400, Mw/Mn = 1.05, HLB = 18.2), with saturated amount of EA or not was utilized. These solutions were separately fed into a Y-shaped microfluidic device using a syringe pump. The flow rates of the dispersed phase (Q_d) and the continuous phase (Q_c) were fixed at 1 μL min^{-1} and 10 μL min^{-1}, respectively. At the Y-junction, the dispersed organic phase was periodically emulsified by the continuous aqueous phase, resulting in O/W emulsion droplets. The polymer droplets travelled towards the downstream of the channel, Teflon tubing, and eventually were mixed with excess amount of pure water outside of the tubing. Then EA was rapidly removed from the polymer droplets by solvent diffusion to the external aqueous phase, leading to volume shrinkage of the droplets and an increase of the polymer concentration in the droplets. Within a few seconds after the emulsion was mixed with pure water, polymer molecules that were no longer dissolved in the droplets started to precipitate and finally formed hardened microparticles.

2-3-3 Effect of EA in the continuous phase on droplet formation

Figure 2-3 shows optical microscopic images of the prepared O/W emulsion in which the continuous aqueous phase was saturated (A) without and (B) with EA. It was found that when using an aqueous solution without EA as the continuous phase, the droplet formation was stable, however the resultant emulsion became polydisperse at the downstream due to partial diffusion of EA into the neighbouring aqueous phase. On the contrary, it was found that droplet formation periodically occurred in the case with using an aqueous solution saturated with EA. As a result, monodisperse O/W emulsion was successfully generated as shown in Figure 2-3 (B). Obviously, the prepared

emulsion droplets were bigger than those in Figure 2-3 (A), indicating that the suppression of quick diffusion of EA into the continuous aqueous phase enabled production of monodisperse droplets. It was also found that the droplets did not coalesce in the tube at all but they collapsed when the emulsion was dropped onto a slide glass at the outlet of the tube. This result indicates that the droplets are stabilized by w-PEG-*b*-PLA at the interface between EA and EA-saturated aqueous solution. However, since EA is a volatile organic solvent, it readily evaporates when the emulsion solution is exposed to air on a slide glass, leading to the breakup of the droplets.

Consequently, in order to fabricate stable and monodisperse O/W emulsion, it is very important that the emulsion solution should not be exposed to the air before solvent diffusion and that the continuous phase should be saturated with EA.

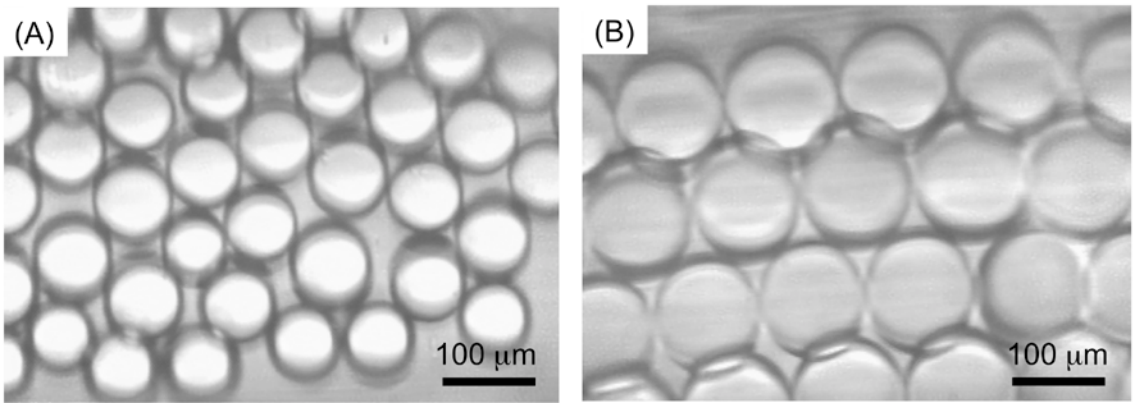

Figure 2-3 Optical microscopic images of O/W emulsions prepared by microfluidic emulsification. The continuous aqueous phase was (A) an aqueous solution dissolving 1 wt% w-PEG-*b*-PLA and saturated amount of EA and (B) an aqueous solution dissolving 1 wt% w-PEG-*b*-PLA. The pictures depicted in Teflon tubing connected to the exit of the microfluidic device (Q_d = 1 μL min^{-1}, Q_c = 10 μL min^{-1}).

2-3-4 Effect of flow rate upon emulsification on droplet size

Secondly, an important parameter to consider, mainly for microfluidic emulsification, is the droplet size and the monodispersity at different flow conditions. Relying on the flow conditions such as viscosity ratios of the both phases and flow rate ratios, there may be possible that the emulsification behaviour would change, which results in polydisperse emulsion droplets. It is important to obtain monodisperse droplets in the wide range of the emulsification conditions in order to produce the microparticles that can be useful for ubiquitous applications. To investigate the flow feasibility on emulsification, emulsion droplets were prepared by altering the flow rate of the continuous phase whilst maintaining that of the dispersed phase constant at 1 μL min^{-1}. In Figure 2-4, the optical micrographs illustrate the resultant O/W emulsion droplets prepared by different flow rates. The images show that regardless of the flow conditions, monodisperse emulsion droplets are successfully formed within the experimental conditions investigated and as the continuous flow rate raises, the diameter of the droplets dramatically decreases. It is also important to note that the mean diameter of the emulsion droplets is smaller than the width of the channel as shown in Figure 2-5. The result means that microfluidic emulsification can produce smaller droplets than the width of the channel, which is superior to SPG membrane emulsification that can only produce emulsion droplets with the diameter as small as the pore size. In terms of the flow rate, it was also found that successful feeding of both solutions was achieved at the flow rate ratio of the continuous phase to the dispersed phase at 100 holds, which gave smallest emulsion droplets that were difficult to observe in Teflon tubing during flowing (data not shown here).

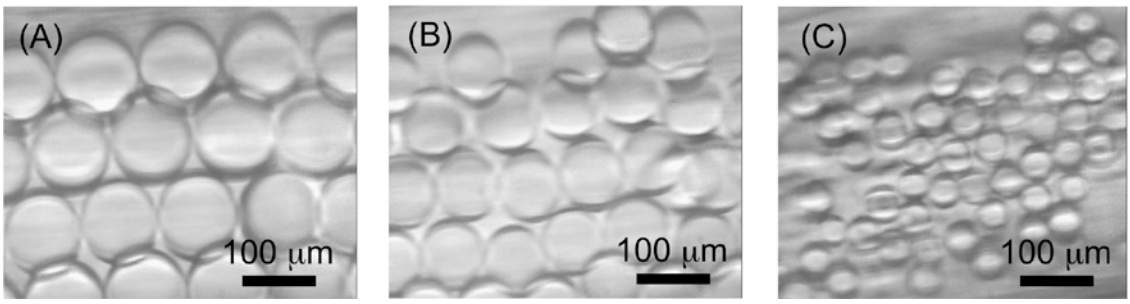

Figure 2-4 Optical micrographs of monodisperse emulsion droplets prepared by changing the Q_c at a fixed flow rate of the Q_d. The Q_c = (A) 5 μL min^{-1}, (B) 10 μL min^{-1} and (C) 20 μL min^{-1}. The Q_d was constant at 1 μL min^{-1}.

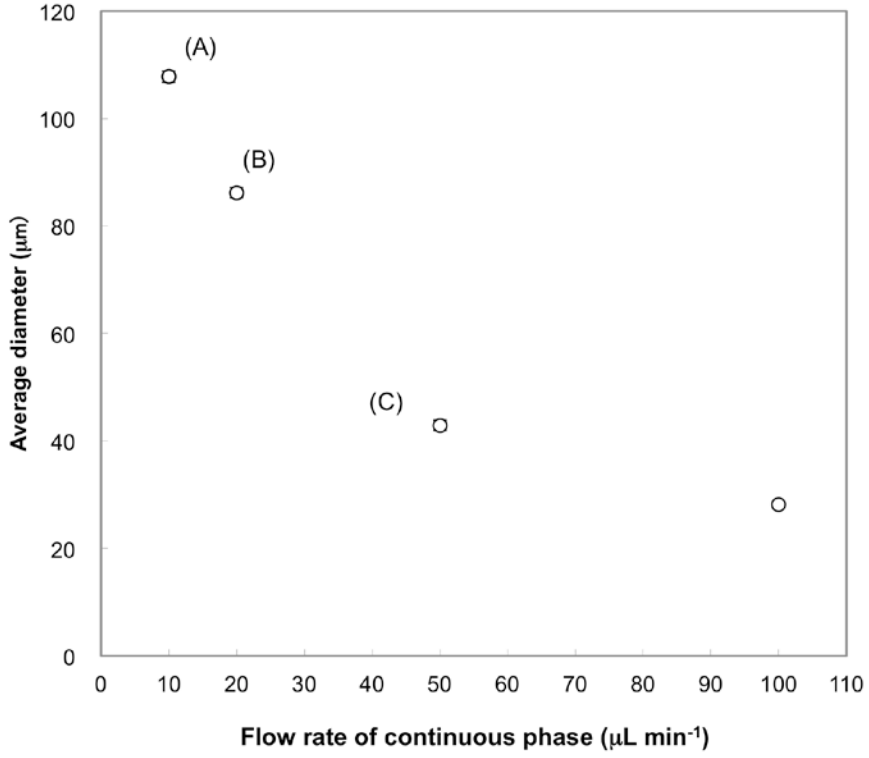

Figure 2-5 Effect of the flow rate of the continuous phase whilst keeping that of the dispersed phase at constant (Q_d = 1 μL min^{-1}) on the mean diameters of droplets.

2-3-5 Effect of flow rate upon emulsification on particle size

Following the optimization of microfluidic emulsification, the preparation of monodisperse PLA microparticle was employed by O/W emulsion-solvent diffusion. The monodisperse O/W emulsion was poured into water (more than 50 times of the volume of the O/W emulsion) in order to trigger the diffusion of EA from the emulsion, resulting in the rapid solidification of droplets. After freeze-drying of the particle dispersion overnight, the prepared microparticles were observed by SEM.

Figure 2-6 shows SEM images of the resultant PLA microparticles prepared by changing the flow rate of the continuous phase upon emulsification. It was shown that monodisperse PLA microparticles with a smooth surface were obtained regardless of the emulsification conditions. Figure 2-7 describes the diameter difference between the emulsion droplets and the particles after solvent diffusion as a function of the flow rate of the continuous phase in the preparation. In Figure 2-7 (A), the results clearly show that the diameter of the final microparticles declines with an increase of the continuous phase flow rate. In addition, each particle diameter is highly monodisperse with less than 5% in CV and about 5 times smaller than that of the original droplets before solvent diffusion as shown in Figure 2-7 (B). These are because the shear force at the Y-junction in the microfluidic device is increased with increasing the continuous phase flow rate, leading to the production of smaller droplets. These droplets are then finally shrunken by solvent diffusion. Therefore, the diameter of the microspheres is smaller than that of the droplets. It is worth mentioning that the minimal diameter of the microparticles obtained in this study is 6.3 μm. As far as I know, this is the smallest PLA microparticles prepared *via* microfluidic emulsification, thus it is evident that this technology is advantageous to preparing monodisperse microparticles with smaller diameter.

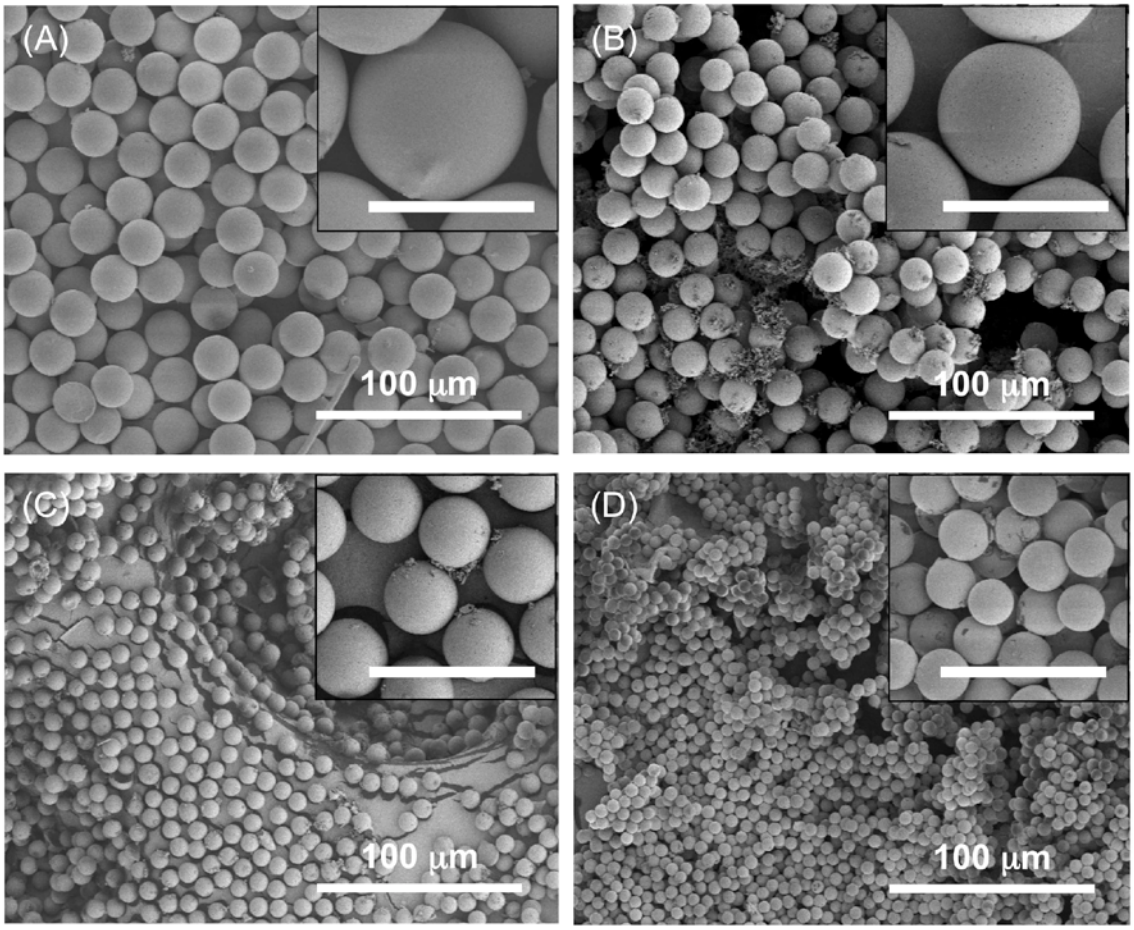

Figure 2-6 SEM images of PLA microparticles prepared by microfluidic emulsification, followed by solvent diffusion. The Q_c was (A) 10 (B) 20, (C) 50 and (D) 100 μL min^{-1} at a fixed Q_d of 1 μL min^{-1}. The concentration of PLA and w-PEG-*b*-PLA were 1 wt%. The obtained microparticles were freeze-dried before SEM observation. The inset is magnified view with a scale bar corresponding to 20 μm.

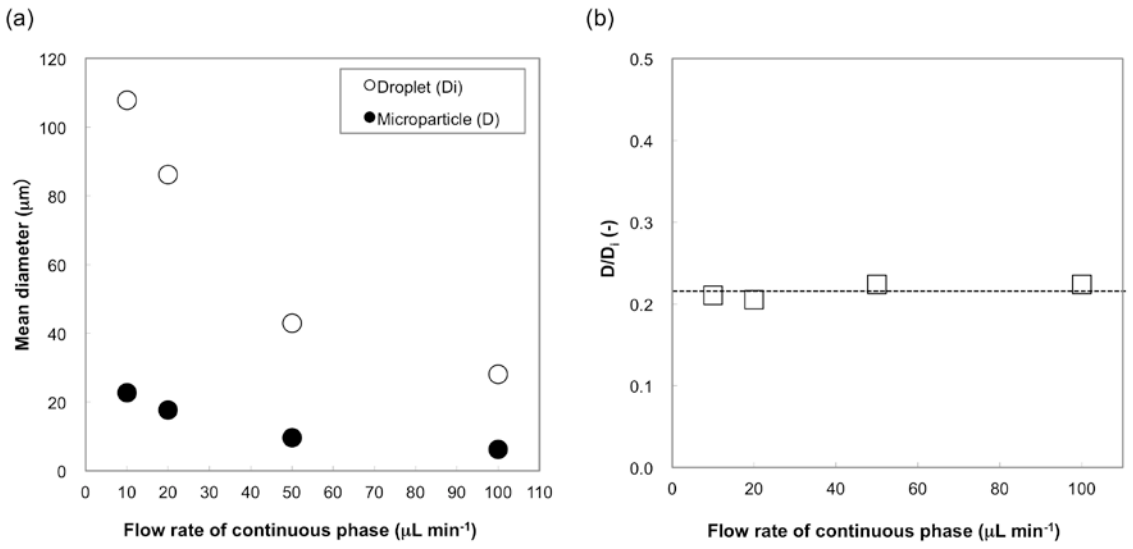

Figure 2-7 (a) Diameter difference between emulsion droplets and the resultant microparticles. (b) Shrink ratio of particle to droplet as a function of the Q_c (at a given Q_d = 1 μL min^{-1}).

2-3-6 Effect of PLA concentration on particle size

In addition, it was found that the initial PLA concentration in the dispersed phase also affected the diameter of the microparticles. The microparticles were prepared by altering the original PLA concentration (1.0, 2.5, and 5.0 wt%). Figure 2-8 shows the diameter change of the microparticles prepared by varying the initial PLA concentration in the dispersed phase as a function of the flow rate of the continuous phase. Comparing with the microparticles prepared with different PLA concentrations and with a fixed flow rate of the continuous phase, the final diameter of the microparticles became bigger as an increment of the initial PLA concentration although the diameter of the emulsion droplets were almost same. This must be caused by a difference in the solidification rate of the microparticles. As the polymer concentration is increased, the polymer concentration in a droplet easily reaches the supersaturation concentration in the time course of solvent diffusion, thereby decreasing the size difference between the droplets and the particles, which results in bigger microspheres. Regardless of the initial PLA concentration, the diameter decreased with raising the flow rate as shown in Figure 2-8. The size distributions of the microparticles were relatively monodisperse (CV~8%). In Figure 2-9, SEM observation clearly revealed that the microparticles had a smooth surface. Figure 2-10 shows the dependence of the original PLA concentration in the

dispersed phase on the diameter of PLA microparticles. The results were plotted in the graph with a double logarithmic axis of the mean diameter versus the initial concentration. The slope of the proportional line was 0.38, which is in good agreement with the proportional to third root of PLA concentration. The result implies that a single PLA microparticle can be produced from a single EA droplet dissolving PLA and that the final diameter of PLA microparticle is proportional in relation to the third root of the concentration of the PLA in EA droplets. Therefore, the final PLA microparticle size would be represented as the following equation.[24]

$$\boldsymbol{r = a\sqrt[3]{C}} \qquad (2\text{-}3)$$

where *r* denotes the mean particle size determined from SEM images, *a* is a constant, and *C* represents the concentration of the initial PLA in the solution. With regard to internal structure of the microparticles, the compactness was assessed by estimating the theoretical diameter of the microparticles without any pores inside using the mean droplet sizes and the equation describing in section 2-2-6. Solid lines in Figure 2-8 illustrate the theoretical particle diameters calculated using the equation (2-2) at porosity (ε) = 0. The results show that all solid lines are in good accordance with the experimental results, indicating that the microparticles have a highly compact structure without pores. These results suggests that this approach can easily produce monodisperse PLA microparticles with a compact structure and the size can be controlled by changing the flow rates and the concentration of the PLA in the dispersed organic phase.

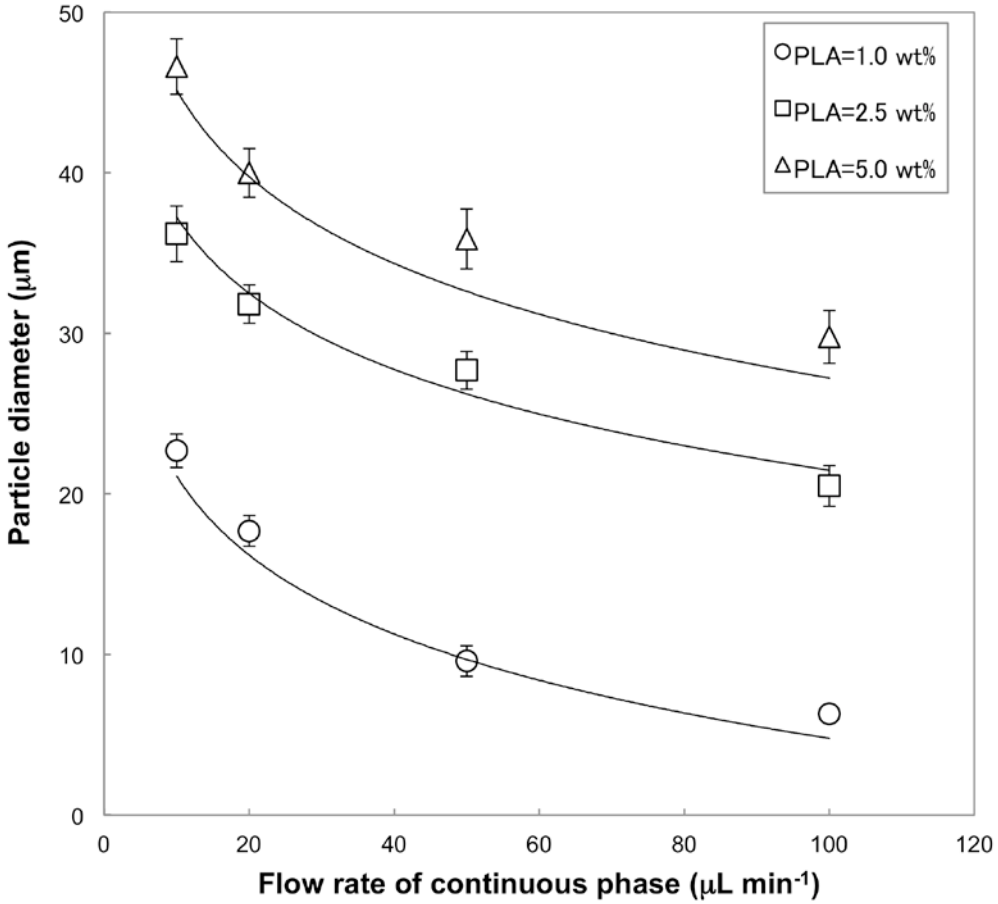

Figure 2-8 Effect of the flow rate of the continuous phase and the original PLA concentration on the diameter of the resultant microparticles after solvent diffusion.

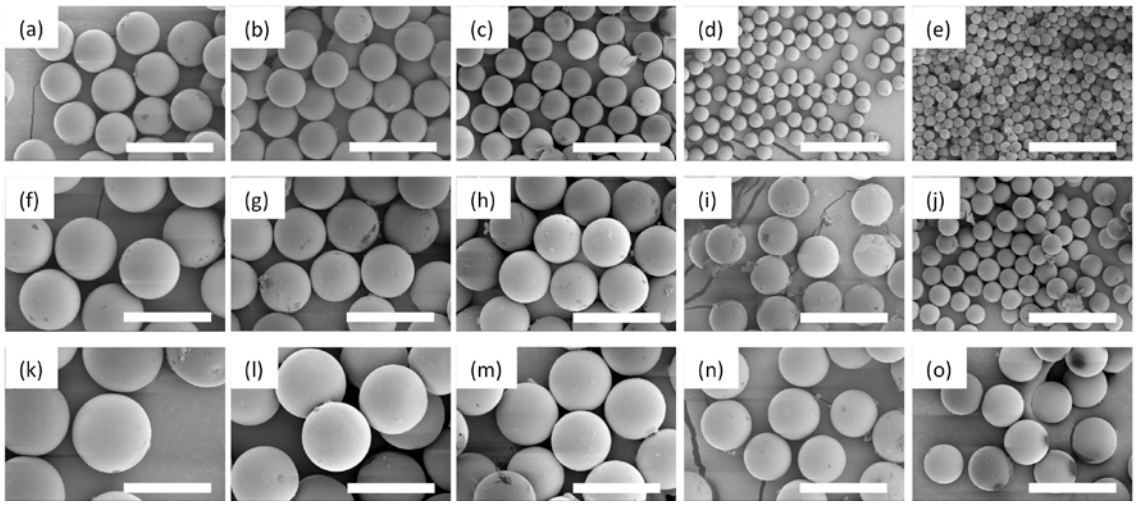

Figure 2-9 SEM images of PLA microspheres prepared by varying the flow rate of the continuous phase and the PLA concentration. The flow rates of the continuous phase were fixed at 5 (a, f, k), 10 (b, g, l), 20 (c, h, m), 50 (d, i, n), and 100 μL h^{-1} (e, j, o). The PLA concentrations in the dispersed phase were 1.0 (a, b, c, d, e), 2.5 (f, g, h, i, j), and 5.0 wt% (k, l, m, n, o). The flow rate of the dispersed phase and the w-PEG-*b*-PLA concentration in the continuous phase were kept constant at 1 μL h^{-1} and 1 wt%, respectively. Scale bars represent 50 μm.

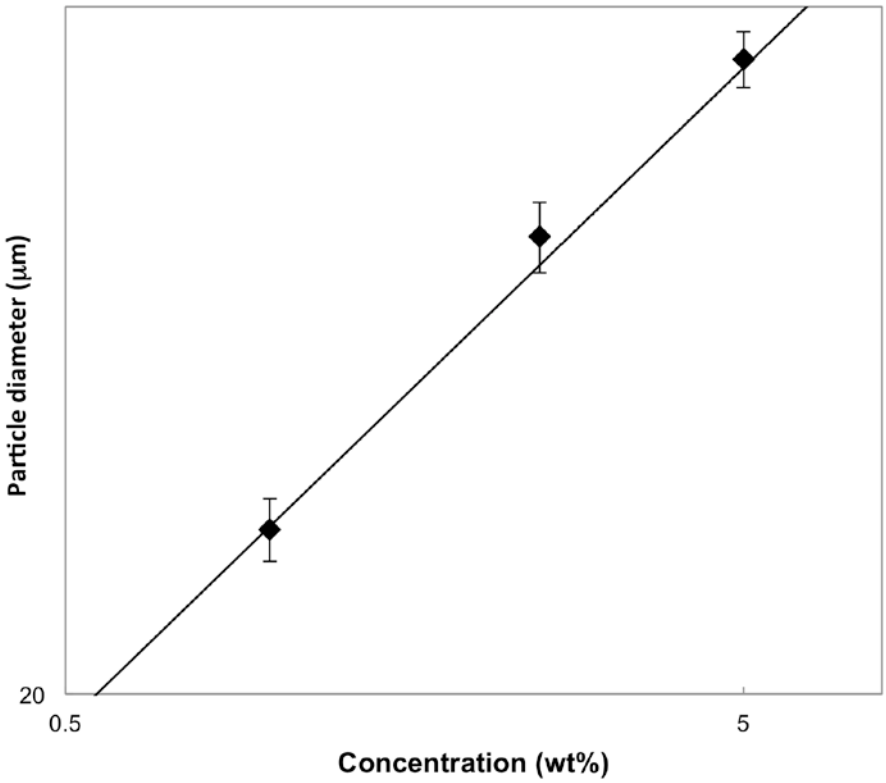

Figure 2-10 Dependence of PLA concentration in EA on the diameter of PLA microparticles.

2-3-7 Effect of o-PEG-*b*-PLA on the microparticle structure

Moreover, it was found that when using oil-soluble PEG-*b*-PLA (o-PEG-PLA, *M*n = 14,200, *M*w/*M*n = 1.20, HLB = 5.6) instead of PLA as a matrix for the microparticles, structural complexity of the microparticles occurred inside the emulsion droplets during solvent diffusion, leading to microparticles with porous structures (Figure 2-11).

With the aid of a microfluidic device, monodisperse PEG-*b*-PLA microparticles were fabricated likewise and the microspheres had a highly porous surface. The diameter and the CV value were 33.2 μm and 5.5%, respectively (Figure 2-12 (A)). From the point of view of polymer affinity to the solvent, o-PEG-*b*-PLA dissolved in a dispersed phase would form a reverse micelle structure with a small amount of water. Fabricated monodisperse oil droplets containing o-PEG-*b*-PLA are subsequently solidified by solvent diffusion. Therefore, the polymer matrix of o-PEG-*b*-PLA contains small water droplets in the PEG domains[25]. After freeze drying, porous microparticles are obtained by the evaporation of water from the microparticle matrix.

Furthermore, the porosity of the microparticles was controlled by blending o-PEG-*b*-PLA and PLA. As the blend ratio of PLA to o-PEG-*b*-PLA was increased, the surface porosity of the microparticles decreased and the microparticles finally showed a smooth surface when the ratio was 50/40 (w/w) (Figure 2-12). These results suggest that this simple fabrication method can readily control the morphology of the microparticles with a narrow diameter distribution by altering the polymer composition in the dispersed phase.

2-4 Conclusions

A facile and environmentally friendly process for production of monodisperse microparticles composed of PLA or PEG-*b*-PLA by combining microfluidic emulsification and O/W emulsion-solvent diffusion method was developed. The diameter of the microparticles was easily tuned by the flow rate of the continuous phase during the microfluidic emulsification and the polymer concentration of the feed solution. In addition, the morphology was controlled by the polymer composition comprising the matrix. These results suggest that this simple fabrication technique has great potential to produce PLA microparticles with a well-defined diameter and morphology for use in cosmetics, agrichemicals, and drug delivery applications.

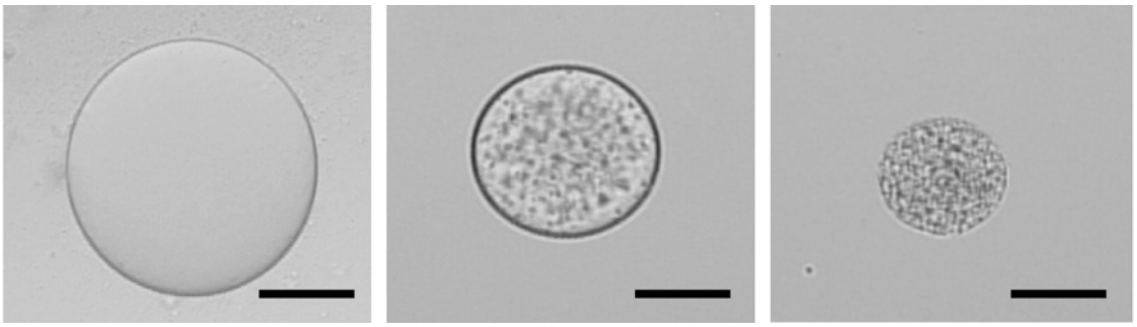

Figure 2-11 Structural complexity inside the emulsion droplets during solvent diffusion when using o-PEG-*b*-PLA as a matrix instead of PLA. The scale bars represent 50 μm. (left) An initial droplet (middle) A droplet during solvent diffusion, showing a phase separated structure (right) A final particle after solvent diffusion.

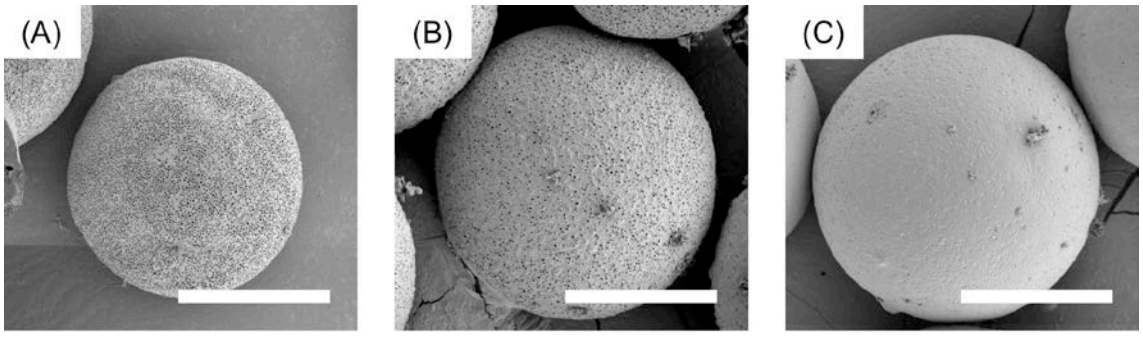

Figure 2-12 SEM images of magnified view of o-PEG-*b*-PLA/PLA microsphere prepared by changing the blend ratios of PLA to o-PEG-PLA in the dispersed phase. The blend ratios were (A) 50/0, (B) 50/20, and (C) 50/40 (w/w). Scale bars represent 25 μm.

References

1. Sawalha, H.; Purwanti, N.; Rinzema, A.; Schroën, K.; Boom, R. Polylactide microspheres prepared by premix membrane emulsification—Effects of solvent removal rate. *J. Membr. Sci.* **2008,** *310* (1-2), 484-493.

2. Vila, A.; Sanchez, A.; Perez, C.; Alonso, M. J. PLA-PEG nanospheres: new carriers for transmucosal delivery of proteins and plasmid DNA. *Polym. Adv. Technol.* **2002,** *13*, 851-858.

3. Wei, Q.; Wei, W.; Tian, R.; Wang, L. Y.; Su, Z. G.; Ma, G. H. Preparation of uniform-sized PELA microspheres with high encapsulation efficiency of antigen by premix membrane emulsification. *J. Colloid Interface Sci.* **2008,** *323* (2), 267-273.

4. Rosca, I. D.; Watari, F.; Uo, M. Microparticle formation and its mechanism in single and double emulsion solvent evaporation. *J. Controlled Release* **2004,** *99* (2), 271-280.

5. Kim, T. K.; Yoon, J. J.; Lee, D. S.; Park, T. G. Gas foamed open porous biodegradable polymeric microspheres. *Biomaterials* **2006,** *27* (2), 152-159.

6. Ruan, G.; Feng, S.-S. Preparation and characterization of poly(lactic acid)–poly(ethylene glycol)–poly(lactic acid) (PLA–PEG–PLA) microspheres for controlled release of paclitaxel. *Biomaterials* **2003,** *24* (27), 5037-5044.

7. Heslinga, M. J.; Mastria, E. M.; Eniola-Adefeso, O. Fabrication of biodegradable spheroidal microparticles for drug delivery applications. *J. Controlled Release* **2009,** *138* (3), 235-242.

8. Hu, J.; Tang, Z.; Qiu, X.; Pang, X.; Yang, Y.; Chen, X.; Jing, X. Formation of Flower-or Cake-Shaped Stereocomplex Particles from the Stereo Multiblock Copoly (r ac-lactide) s. *Biomacromolecules* **2005,** *6* (5), 2843-2850.

9. Huang, K.-S.; Lu, K.; Yeh, C.-S.; Chung, S.-R.; Lin, C.-H.; Yang, C.-H.; Dong, Y.-S. Microfluidic controlling monodisperse microdroplet for 5-fluorouracil loaded genipin-gelatin microcapsules. *J. Controlled Release* **2009,** *137* (1), 15-19.

10. Berkland, C.; Pollauf, E.; Raman, C.; Silverman, R.; Kim, K.; Pack, D. W. Macromolecule release from monodisperse PLG microspheres: Control of release rates and investigation of release mechanism. *J. Pharm. Sci.* **2007,** *96* (5), 1176-1191.

11. Liu, R.; Ma, G.; Meng, F. T.; Su, Z. G. Preparation of uniform-sized PLA microcapsules by combining Shirasu porous glass membrane emulsification technique

and multiple emulsion-solvent evaporation method. *J. Controlled Release* **2005,** *103* (1), 31-43.

12. Ito, F.; Honnami, H.; Kawakami, H.; Kanamura, K.; Makino, K. Preparation and properties of PLGA microspheres containing hydrophilic drugs by the SPG (shirasu porous glass) membrane emulsification technique. *Colloids Surf. B. Biointerfaces* **2008,** *67* (1), 20-25.

13. Ito, F.; Fujimori, H.; Honnami, H.; Kawakami, H.; Kanamura, K.; Makino, K. Effect of polyethylene glycol on preparation of rifampicin-loaded PLGA microspheres with membrane emulsification technique. *Colloids Surf. B. Biointerfaces* **2008,** *66* (1), 65-70.

14. Ito, F.; Kanakubo, Y.; Murakami, Y. Rapid preparation of monodisperse biodegradable polymer nanospheres using a membrane emulsification technique under low gas pressure. *J. Polym. Res.* **2011,** *18* (6), 2077-2085.

15. Liu, R.; Ma, G. H.; Wan, Y. H.; Su, Z. G. Influence of process parameters on the size distribution of PLA microcapsules prepared by combining membrane emulsification technique and double emulsion-solvent evaporation method. *Colloids Surf. B. Biointerfaces* **2005,** *45* (3-4), 144-153.

16. Kim, J.-W.; Utada, A. S.; Fernández-Nieves, A.; Hu, Z.; Weitz, D. A. Fabrication of Monodisperse Gel Shells and Functional Microgels in Microfluidic Devices. *Angew. Chem. Int. Ed.* **2007,** *46* (11), 1819-1822.

17. Yu, Y. L.; Xie, R.; Zhang, M. J.; Li, P. F.; Yang, L.; Ju, X. J.; Chu, L. Y. Monodisperse microspheres with poly(N-isopropylacrylamide) core and poly(2-hydroxyethyl methacrylate) shell. *J. Colloid Interface Sci.* **2010,** *346* (2), 361-369.

18. Nisisako, T.; Torii, T.; Higuchi, T. Novel microreactors for functional polymer beads. *Chem. Eng. J.* **2004,** *101*, 23-29.

19. Shum, H. C.; Kim, J.-W.; Weitz, D. A. Microfluidic fabrication of monodisperse biocompatible and biodegradable polymersomes with controlled permeability. *J. Am. Chem. Soc.* **2008,** *130* (29), 9543-9549.

20. Muranaka, M.; Hirota, K.; Ono, T. PEG–PLA nanoparticles prepared by emulsion solvent diffusion using oil-soluble and water-soluble PEG–PLA. *Mater. Lett.* **2010,** *64* (8), 969-971.

21. Bazile, D.; Prud'homme, C.; Bassoullet, M. T.; Marlard, M.; Spenlehauer, G.;

Veillard, M. Stealth Me. PEG‐PLA nanoparticles avoid uptake by the mononuclear phagocytes system. *J. Pharm. Sci.* **1995,** *84* (4), 493-498.

22. Griffin, W. C. Classification of surface active agents by "HLB". *J. Soc. Cosmetic Chem.* **1949,** *1*, 311–326.

23. Pisani, E.; Fattal, E.; Paris, J.; Ringard, C.; Rosilio, V.; Tsapis, N. Surfactant dependent morphology of polymeric capsules of perfluorooctyl bromide: influence of polymer adsorption at the dichloromethane-water interface. *J. Colloid Interface Sci.* **2008,** *326* (1), 66-71.

24. Ishizaka, T.; Ishigaki, A.; Chatterjee, M.; Suzuki, A.; Suzuki, T. M.; Kawanami, H. Continuous process for fabrication of size controlled polyimide nanoparticles using microfluidic system. *Chem. Commun.* **2010,** *46* (38), 7214-7216.

25. Ruan, G.; Feng, S.-S.; Li, Q.-T. Effects of material hydrophobicity on physical properties of polymeric microspheres formed by double emulsion process. *J. Controlled Release* **2002,** *84* (3), 151-160.

Chapter 3
Preparation of monodisperse PLA microcapsules with core shell structures by internal phase separation

3-1 Introduction

As elaborated in chapter 2, “droplet-to-particle technology” consisting of microfluidic emulsification and subsequent solvent diffusion has enabled production of monodisperse PLA microparticles with controlled sizes. The diameter can be precisely predicted from the composition of the dispersed organic phase and the diameter of the droplets. Moreover, morphology of the microparticles can be controlled by using o-PEG-*b*-PLA diblock copolymer as a matrix for the microparticles, resulting in microparticles with a porous structure. However, when utilizing the process, the internal structure of the microparticles is mainly hydrophobic polymer matrix, which is challenging to encapsulate liquid substances in the microparticles. To overcome the limitation and to extend the range of the applications, a simple process to fabricate the microparticles consisting of an oil core and a polymeric shell is required.

Generally, liquid-filled microcapsules are produced by adding a non-solvent for a matrix polymer to the dispersed phase when preparing O/W or W/O emulsion[1-6] or by using water-in-oil-in-water (W/O/W) emulsions[7-10] as a template for a solvent evaporation process. These techniques have been shown as a promising way to successfully produce core-shell polymeric microcapsules encapsulating lipophilic or hydrophilic compounds in the core and control their release behaviour.

In terms of microcapsule size, monodisperse microcapsules are preferable in several applications, especially in drug delivery carriers because they can decrease undesirable side effects and exhibit controlled drug release kinetics and encapsulation efficiency.[11-12] Since monodisperse microcapsules can only be produced from precision emulsion droplets, generation of uniform droplets is of utmost importance process in fabrication of microcapsules upon using top-down techniques. To date, several methods

have been developed to produce monodisperse polymeric microcapsules using flow dynamics such as membrane emulsification,[13] microfluidic emulsification,[14-18] and jet acoustic excitation.[19] Among them, droplet-based microfluidic system is considered as one of the most effective ways to prepare monodisperse microcapsules. Pioneer work by Utada *et al*. has been achieved to fabricate monodisperse W/O/W double emulsion using a coaxial microcapillary fluidic device.[20] Since then, there have been many reports regarding fabrication of monodisperse microcapsules using a method combining microfluidics with solvent evaporation. For example, Tu *et al.* have successfully controlled the stability and the size of monodisperse PLGA microcapsules by tuning osmotic pressure between the internal and the external aqueous phase during W/O/W double emulsion formation.[21] Amstad *et al.* have developed monodisperse polymersomes with thermo- and photoresponsive by introducing thermoresponsive diblock copolymer, poly(*N*-isopropylacrylamide)-*b*-poly(lactide-*co*-glycolide) and photosensitive gold naoparticles into the shell of the polymersomes.[22] For oil-filled microcapsules, Lensen *et al.* have employed to prepare monodisperse dodecane-filled poly(*L*-lactide) (PLLA) microcapsules using a combination of O/W emulsion-solvent evaporation and internal phase separation.[23] However, these methods require toxic organic solvents and much time to form microcapsules, and difficult to tailor microcapsule structures. On the emulsion preparation, DCM or chloroform are commonly used as the organic solvent due to a good solvent for biodegradable polyesters and their high volatile properties that facilitate evaporation of the solvent from the emulsion droplets, although the vapour or residue are considered to be harmful to environment and human body. In addition, even when using volatile organic solvents as the dispersed phase, the rate-determining step for the microcapsule formation is the solvent evaporation process, which actually takes a few minutes to several hours, depending on the volume of the continuous phase. That is why, the emulsion is required to be stored in a vessel until the solvent evaporates from the system and the microcapsules are formed. Moreover, despite the fact that the morphology of microparticles plays a crucial role in determining the behaviour in the fluid, controlling loading efficiency and release kinetics of the ingredients, tuning the structure of polymeric microparticles at a micrometre scale is still challenging. Hence, developing a simple and environmentally friendly process for production of monodisperse

microcapsules with controllable size and tailored architecture is in great demand to expand their functionalities.

In this chapter, a facile straightforward method to continuously produce monodisperse PLA microcapsules with controlled structures by a modified "droplet-to-particle technology" is represented, which includes microfluidic emulsification, emulsion-solvent diffusion, and internal phase separation. In this process, for a dispersed organic phase, PLA and a non-solvent for PLA, were dissolved in EA. Monodisperse O/W emulsion droplets were produced by using a commercial Y-shaped microfluidic device that was used in chapter 2, which were directly poured into an excess amount of water, inducing rapid extraction of EA from the droplets and internal phase separation between a non-solvent phase and a concentrated PLA/EA phase. Within a few seconds, PLA precipitated at the surface of each droplet, resulting in forming monodisperse PLA microcapsules encapsulating liquid non-solvent. Different from conventional techniques, this approach for forming robust microcapsules takes only a few seconds to precipitate the polymer after onset of solvent diffusion, enabling not only to produce uniform microcapsules in a continuous manner, but also to solidify microcapsules at a non-equilibrium state and to tailor their structures. In addition, similar to the system utilized in chapter 2, all components used in the microcapsule formation are biocompatible, which is great advantageous to applications for biomedical fields. This is the first demonstration to continuously fabricate monodisperse core-shell PLA microcapsules with tuneable sizes and structures using solvent diffusion from simple O/W emulsion droplets.

3-2 Experimental procedures

3-2-1 Materials

PLA and PEG-*b*-PLA were synthesized by a ring-opening polymerization of D,L-lactide in the presence of $Sn(Oct)_2$ as a catalyst using lauryl alcohol and PEG (Mn= 4,000, Mw/Mn= 1.06) as an initiator, respectively as previously reported in chapter 2. The D,L-lactide was purchased from Purac (Netherland). The PEG was kindly supplied from NOF (Japan). $Sn(Oct)_2$, EA and perfluorooctyl bromide (PFOB) were obtained from Wako Pure Chemical Industries, Ltd. (Japan). Porphyrin derivative was kindly supplied from porphyrin laboratory (Japan). The ultra pure water was produced by a Millipore

Milli-Q purification system (EMD Millipore Corporation, USA). All reagents are of the finest grade available and used as received.

3-2-2 Interfacial tension measurement

Interfacial tension measurements were carried out by a pendant drop method using DSA10 (Krüss, Germany). An EA droplet containing 25 mg mL^{-1} PLA and a pure PFOB droplet were formed in an aqueous solution of 1 wt% w-PEG-*b*-PLA (*M*n=4,400, *M*w/*M*n= 1.05, HLB= 18.2) saturated with EA. The interfacial tensions were calculated from the droplet images using image analysis software. The measurements were carried out at 20°C.

3-2-3 Fabrication of monodisperse PLA microcapsules

A schematic illustration of the preparation procedure of monodisperse PLA microcapsules is shown in **Scheme 3-1**. The microfluidic device that was used for the microcapsule fabrication consisted of a Y-shaped channel (126 μm- and 136 μm-width channels with 75 μm in depth) made of a SUS basement and a glass cover plate, fabricated by Kasen Nozzle Mfg. Co., Ltd, Japan. The continuous aqueous phase and the dispersed organic phase were pumped independently at adjustable flow rates using syringe pumps connected to the device *via* Teflon tubing. An aqueous solution saturated with EA containing 1 wt% of w-PEG-*b*-PLA (*M*n= 4,400, *M*w/*M*n= 1.05, HLB= 18.2) was used as the continuous phase and an EA solution composed of 25 mg mL^{-1} of PLA (*M*n= 13,600, *M*w/*M*n= 1.14 or *M*n= 52,000, *M*w/*M*n= 1.29) and 1.25-15 μL mL^{-1} of PFOB was used as the dispersed phase. In the case of confocal laser scanning microscopic observation, a trace amount of porphyrin derivative was added to the dispersed phase before the feeding. The obtained O/W emulsion was transferred to a bath filled with 100 mL of ultra pure water through Teflon tubing (Φ= 0.5 mm, *L*= 20 cm) whose exit tip was submerged in the water. The EA was then rapidly removed from the droplet to the massive amount of pure water by solvent diffusion with or without gentle stirring, leading to precipitation of PLA microcapsules. The microcapsules were washed with ultra pure water three times by centrifugation (himac CF 15R, Hitachi, Japan) (3,000 rpm, 3 min) to remove the surfactant, followed by lyophilization overnight, yielding dried PLA microcapsules.

Scheme 3-1 Schematic illustration of the process used to continuously produce monodisperse PLA microcapsules encapsulating liquid non-solvent in the core through microfluidic emulsification and solvent diffusion, coupled with internal phase separation.

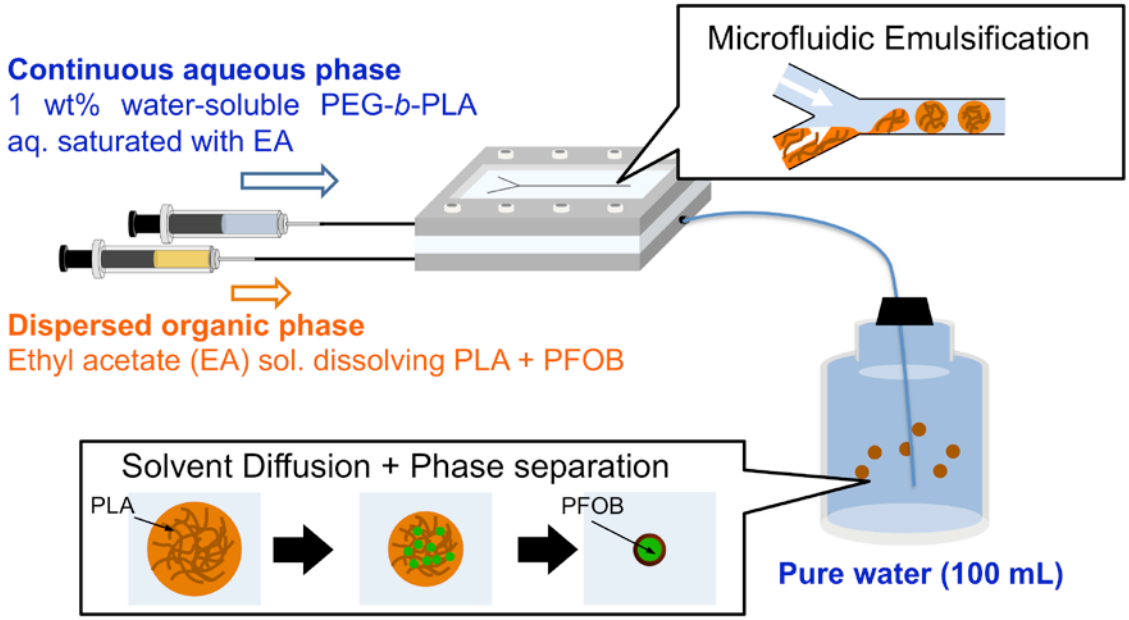

3-2-4 Observation of the microparticle morphology

Prepared O/W emulsion droplets in the Teflon tubing were observed using an optical microscope (OLYMPUS BX50). The microparticles after freeze-drying were observed by a scanning electron microscope (SEM, S-4700, Hitachi, Ltd.) at an intensity of 1 kV under various magnifications. Prior to observation, the samples were coated with Pt-Pd using a sputter-coater (E-1030 Ion Sputter, Hitachi, Ltd.). A porphyrin derivative-labelled microcapsule dispersion was observed with a confocal laser scanning microscope (CLSM) equipped with a 1 mW helium-neon laser (Zeiss LSM-510, Japan). The red fluorescence was observed with a long-pass 560 nm emission filter under 543 nm laser illumination. The microcapsule sizes and the size distributions were evaluated by using an image analysis software (Winroof, Mitanishoji Co., Ltd., Japan). In the analysis, the size distributions were expressed by the coefficient of variation (CV) that is defined as the ratio of the standard deviation to the mean diameter. Each calculation used 200 microcapsules.

3-2-5 Theoretical calculation of the shell thickness of the microcapsules

The theoretical shell thickness of the microcapsules was calculated by the following equation.

$$T_{theore.} = R\left(1 - \sqrt[3]{\frac{1}{1 + \frac{m_{PLA} \cdot \rho_{PFOB}}{m_{core} \cdot \rho_{PLA}}}}\right) \quad (3\text{-}1)$$

where $T_{\text{theore.}}$, R, m_{PLA}, ρ_{PFOB}, m_{PFOB}, and ρ_{PLA} are the shell thickness of the microcapsule, the radius of the microcapsule, mass of PLA, density of PFOB (= 1,930 kg m^{-3}), mass of PFOB, and density of PLA (= 1,210 kg m^{-3}), respectively.

3-2-6 Observation of formation of microcapsules with a dimpled surface

The dispersed organic phase (100 μL) and the continuous aqueous phase (1 mL) were mixed and then emulsified by homogenizer at 1,500 rpm, for 1 minute to prepare O/W emulsion. The dispersed phase was an EA solution containing 25 mg mL^{-1} of PLA (*M*n = 52,000, *M*w/*M*n = 1.29) and 15 μL mL^{-1} of PFOB. The continuous phase was 1 wt% w-PEG-*b*-PLA (*M*n = 4,400, *M*w/*M*n = 1.05, HLB = 18.2) aqueous solution saturated with EA. After emulsification, a small portion of the emulsion was placed on a glass plate and covered with thin cover slip in order to suppress evaporation of EA. The sample was set up on the stage of optical microscope. To induce solvent diffusion of EA into aqueous phase, pure water was introduced into the gap between the glass slide and the cover slip using a disposal syringe. Using an optical microscope, internal phase separation in the droplet and the following microcapsule formation process were observed.

3-2-7 Confirmation of the encapsulation of liquid oil inside the microcapsules

To confirm the encapsulation of liquid oil within the microcapsules, differential scanning calorimetry (DSC) measurements were performed using a PYRIS Diamond DSC (PerkinElmer, the UK). The samples were placed in an aluminum pan with 5-10 mg of sample. Empty aluminum pan was used as a reference. The samples were heated

at a ramping rate of 5°C min^{-1} under a nitrogen atmosphere. The first scans were recorded.

3-3 Results and discussion

Continuous preparation of monodisperse microcapsules with a liquid oil core and a biocompatible polymeric shell of PLA *via* emulsion-solvent diffusion has been exploited in this chapter. The process is based on the method for preparing monodisperse compact PLA microparticles using a combined method of microfluidic emulsification and subsequent solvent diffusion discussed in chapter 2. This method does not need any toxic materials and a time-consuming solidification process like the conventional emulsion-solvent evaporation method. The dispersed oil phase is a mixture of PLA, EA, and perfluorooctyl bromide (PFOB) unless specifically mentioned. EA is a good solvent for PLA with high solubility in water, whereas PFOB that is used as a model-encapsulated reagent acts as a non-solvent for PLA. Another reason why PFOB is chosen as the non-solvent is to be a fluorocarbon with higher hydrophobicity than normal hydrocarbons such as hexadecane and decane, which makes much easier to prepare the microcapusles with an oil-core and a polymer shell. The continuous phase is an aqueous solution saturated with EA containing biocompatible w-PEG-*b*-PLA as a surfactant.

3-3-1 Interfacial tension measurements

Before the preparation of microcapsules, interfacial tensions of the emulsion system were measured to achieve successful encapsulation of liquid oil in the microcapsules. When using internal phase separation mechanism between a polymer phase and a non-solvent phase to prepare polymer microcapsules with core-shell structures, it is well known that the equilibrium structure of the microcapsules can be predicted by using a spreading coefficient theory established by Torza and Mason, which is based on the interfacial energy of the O/W interface.[24] Following the theory, if droplets of two immiscible liquids (phase 1 and 3) are brought into contact with the third mutually immiscible liquid (phase 2), then the equilibrium conformation can be predicted by calculating spreading coefficient values using each interfacial tension (γ_{12}, γ_{23}, and γ_{31}). The spreading coefficients S_i for each phase are defined as

$$S_i = \gamma_{jk} - (\gamma_{ij} + \gamma_{ik}) \quad (3\text{-}2)$$

$$S_j = \gamma_{ik} - (\gamma_{jk} + \gamma_{ij}) \quad (3\text{-}3)$$

$$S_k = \gamma_{ij} - (\gamma_{ik} + \gamma_{jk}) \quad (3\text{-}4)$$

In this case, two immiscible droplets correspond to pure liquid PFOB (phase 1) and EA dissolving 25 mg mL^{-1} of PLA (phase 3), and the third immiscible phase is an aqueous solution of 1 wt% w-PEG-*b*-PLA saturated with EA (phase 2) as shown in Figure 3-1. Two initial interfacial tension values; (1) between phases 1 and 2 and (2) between phases 2 and 3 were thus measured in this experiment. It should be noted that it was impossible to measure the interfacial tension between pure liquid PFOB (phase 1) and the EA solution dissolving PLA (phase 3) because these solutions were completely miscible under the initial experimental condition and there was therefore no interface, which expects that the interfacial tension would be significantly smaller than that of the other two interfaces. The interfacial tension values were γ_{12} = 8.51 mN m^{-1} and γ_{23} = 2.53 mN m^{-1} (**Table 3-1**). Assuming that the interfacial tension value between phases 1 and 3, corresponding to γ_{13}, is close to 0 mN m^{-1}, spreading coefficient values of this system will be $S_1 < 0$, $S_2 < 0$, and $S_3 > 0$, indicating that the equilibrium configuration of the microcapsules is the core-shell morphology (Figure 3-1 (B)).

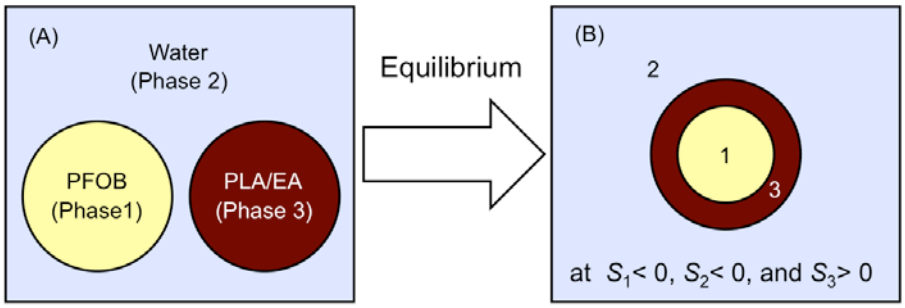

Figure 3-1 (A) Designation of each phase for the calculation of spreading coefficients. (B) Expected equilibrium core-shell configuration obtained at $S_1 < 0$, $S_2 < 0$, and $S_3 > 0$.

Table 3-1 Interfacial tensions measured by Pendant drop method.

Entry	Interfacial tension (mN m^{-1})
PFOB - Water (γ_{12})	8.51
PLA/EA - Water (γ_{23})	2.53
PFOB - PLA/ EA (γ_{13})	*NA

*The interfacial tension was assumed to be almost 0 mN m^{-1} when calculating spreading coefficients

3-3-2 Effect of stirring during solvent diffusion on microcapsule formation

The Y-shaped microfluidic device continuously generated monodisperse O/W emulsion droplets in which the dispersed organic phase dissolved PLA and PFOB. As shown in Figure 3-2, highly monodisperse emulsion droplets without any satellite droplets were successfully produced, indicating that the droplets were stabilized by w-PEG-*b*-PLA molecules at the interface of the emulsion droplets even if PFOB was contained in the dispersed phase. The emulsion droplets were then transferred into a water bath with or without stirring at 120 rpm in order to induce solvent diffusion of EA and the subsequent precipitation of the polymer. Figure 3-3 (A) depicts an optical microscopic image of the resultant microcapsules after solvent diffusion when using a water bath without stirring for the precipitation. Highly monodisperse PLA microcapsules (d = 35.8 μm, CV = 4.2%) with a core-shell structure were obtained, indicating that internal phase separation occurred during solvent diffusion. Figure 3-3 (B) shows SEM image of a cross sectional view of the microcapsules after freeze-drying. The SEM image revealed that the microcapsule had a big empty core where the PFOB oil core existed before freeze-drying. However it was found that the PFOB oil core was not always located at the radial centre of the microcapsules and some of them existed nearby the interface between the shell and the external aqueous phase although they were covered with a polymeric shell. This result would be caused by change of interfacial tension in the course of polymer precipitation. To predict the final morphology of the microcapsules, the interfacial tensions of the initial stage of the emulsion before solvent diffusion were utilized. However, in fact, the interfacial tension between the concentrated PLA phase and the PFOB is not constant in this system and it varies as the

volume fraction of PLA increases as a function of time after onset of the solvent diffusion. It is expected that the concentrated PLA phase becomes more hydrophobic with an increment of the concentration because of intrinsic hydrophobicity of the polymer. Therefore, the interfacial tension between the concentrated PLA phase and the external aqueous phase at the latter stage of solvent diffusion should become higher than the original value (γ_{23} = 2.53 mN m^{-1}). Because of this, the core position within the microcapsules was not at the radial centre of the microcapsules although the final conformation was a core-shell structure, which was in good agreement with the structure expected from the calculation using spread coefficient theory.

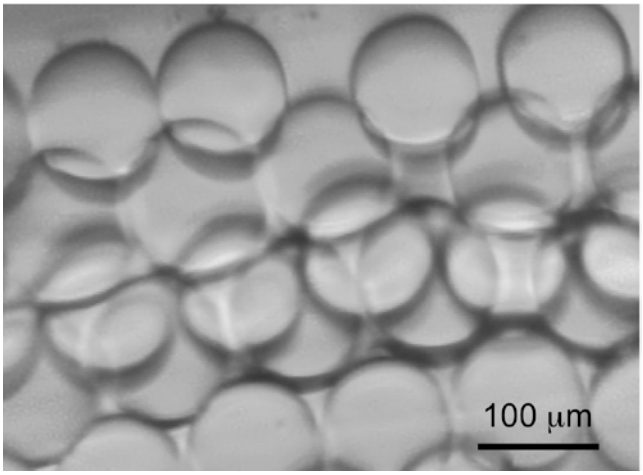

Figure 3-2 Optical microscopic image of the emulsion droplets flowing in the Teflon tubing after emulsification (Q_d = 1 μL min^{-1} and Q_c = 20 μL min^{-1}).

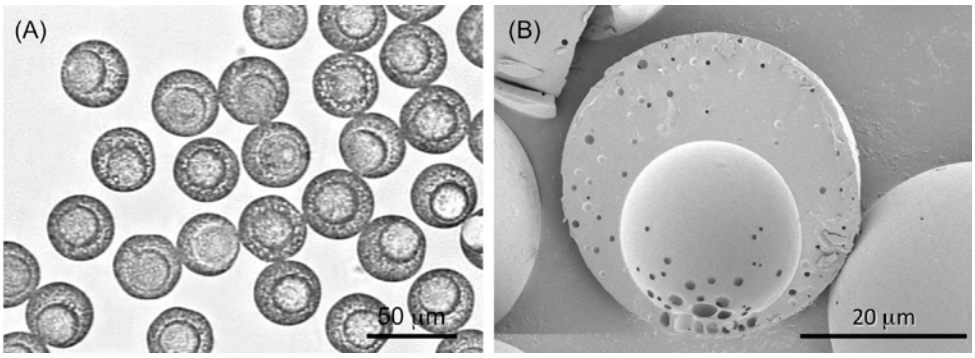

Figure 3-3 (A) Optical microscopic image and (B) SEM of monodisperse PLA microcapsules with a core-shell structure. The microcapsules were prepared without stirring during solvent diffusion (Q_d = 1 μL min^{-1} and Q_c = 20 μL min^{-1}). The SEM image was captured after freeze-drying of the microcapsule dispersion overnight.

Considering the result, in order to fabricate the microcapsules with controlled core-shell structures, it is important to precipitate the microcapsules from the emulsion droplets after complete of the internal phase separation. Thus, the microcapsule preparation under gentle magnetic stirring at 120 rpm during the solvent diffusion was employed. In the case of which the microcapsules were prepared under the stirring condition, monodisperse PLA microcapsules (d = 35.0 μm, CV = 4.0%) with core-shell structures were obtained, as shown in Figure 3-4, which indicates that the gentle stirring during solvent diffusion does not affect the polydispersity of the emulsion droplets within the experimental conditions. To understand the internal microcapsule structure, the microcapsules with a trace amount of porphyrin-derivative as a fluorescent maker were prepared using the same process. Before the experiment, it was confirmed that the reagent coloured hydrophobic PLA red but did not do PFOB, and it also did not have any adverse effect on the stability of the emulsion. In Figure 3-5, the CLSM image has proven that microcapsules possess a relatively uniform shell thickness and a large cavity located at the radial centre of the microcapsules. Moreover, it is also important to note that the shell of microcapsules has small pores although the configuration is roughly relevant to the theoretical prediction estimated from spreading coefficient theory. It is considered that the small cavities would be derived from small droplets of the PFOB phase before coalescence. Since the diffusion of EA to the outer aqueous phase is a much faster process than the evaporation of DCM reported by the other groups, due to higher solubility of EA in water, the microcapsules are obtained even at a non-equilibrium configuration. Precipitation of polymer begins from the surface of EA droplets; therefore, some of the phase-separated small PFOB droplets before coalescence where it is located near the surface would be kinetically entrapped in the polymer matrix, forming the shell of the microcapsules during the precipitation process.

Figure 3-6 represents SEM images of the resultant microcapsules after lyophilization. It is evidently shown that most of the microcapsules maintain a spherical shape with a smooth surface. In addition, it was found that the microcapsules had a hollow internal structure at the radial centre of the microcapsules as a result of the evaporation of the PFOB core during freeze-drying as shown in Figure 3-6 (right). The dimples are another clue that the rapid solidification of polymer droplets provides a kinetically “locked” non-equilibrium structure of microcapsules. From these results, it was concluded that this simple process was capable of the continuous production of well-defined

monodisperse PLA microcapsules with a hydrophobic oil core as well as hollow microcapsules.

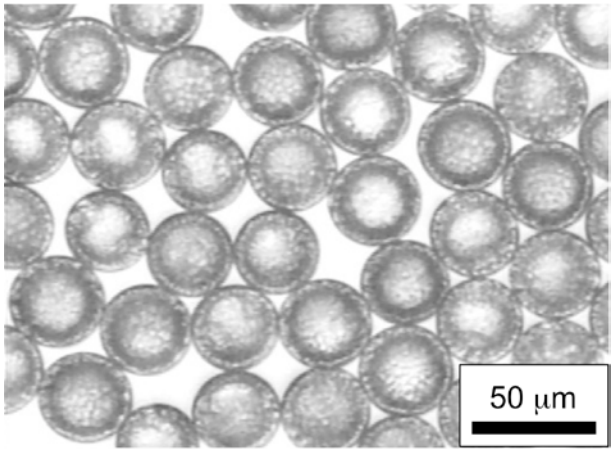

Figure 3-4 Optical microscopic image of monodisperse PLA microcapsules with a core-shell structure. The microcapsules were prepared with stirring at 120 rpm whilst the precipitation (Q_d = 1 μL min^{-1} and Q_c = 20 μL min^{-1}).

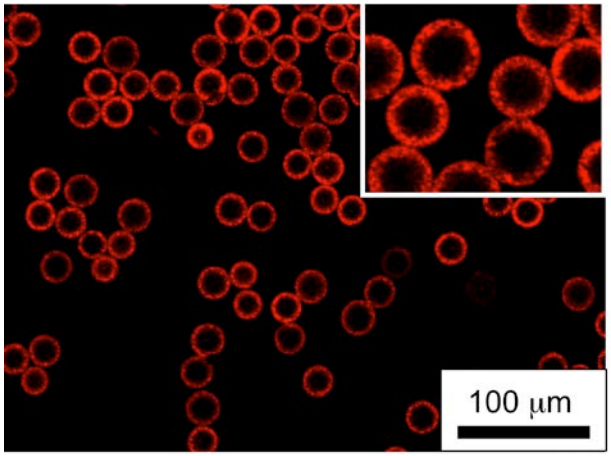

Figure 3-5 Confocal laser scanning microscopic image of porphyrin-derivative-labelled monodisperse PLA microcapsules. The inset is the magnified image (Q_d = 1 μL min^{-1} and Q_c = 100 μL min^{-1})

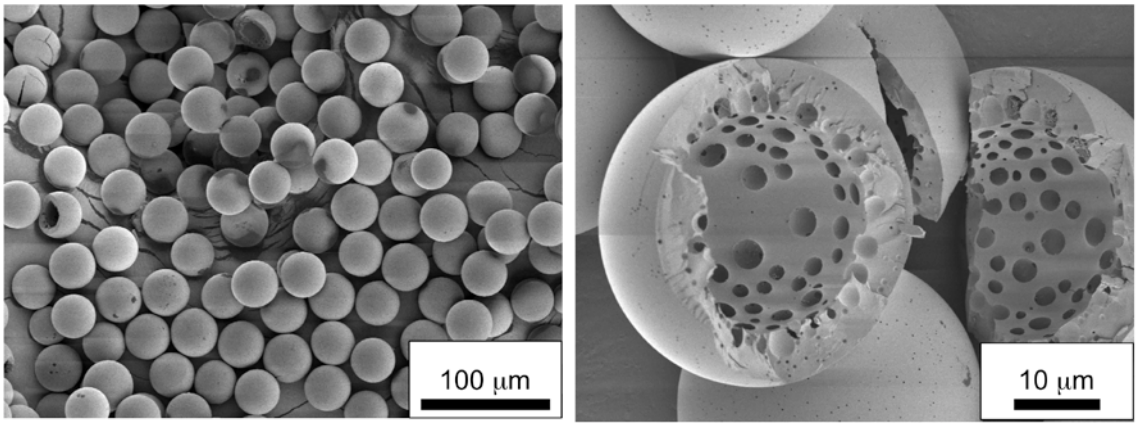

Figure 3-6 SEM images of the microcapsules after freeze-drying. The right image is the magnified cross-sectional view of the microcapsules (Q_d = 1 μL min^{-1} and Q_c = 20 μL min^{-1})

3-3-3 Effect of drying process on encapsulation of liquid oil in microcapsules

To investigate encapsulation property of the microcapsules, DSC measurements of the core-shell microcapsules encapsulating PFOB were demonstrated. The samples were washed with pure water 3 times, followed by freeze-drying overnight or drying under reduced pressure at room temperature for 1 day. As shown in Figure 3-7 (upper graph), although the thermograph showed undulation at the temperature above 100°C, the boiling point of PFOB around 142°C was not clearly confirmed. On the contrary, in the case of the sample being washed with pure water, followed by drying under reduced pressure for 1 day, the boiling point derived from PFOB was detected, with slightly lower shift around 138°C (in Figure 3-7, lower graph). The peak was apparently broad due to evaporation of the oil and encapsulated in the microcapsules. On the other hand, both peaks appeared between 40 and 50°C were T_g of PLA. From these results, it was concluded that the encapsulated substances were completely removed by freeze-drying, although they still existed in the microcapsules after drying in open air under the experimental condition.

Table 3-2 Thermal property of PLA and PFOB.

Sample	T_g *1 (°C)	T_{bp} *2 (°C)
PLA	40-55	-
PFOB	-	141-143

*1 T_g; glass transition temperature, *2T_{bp}; boiling temperature.

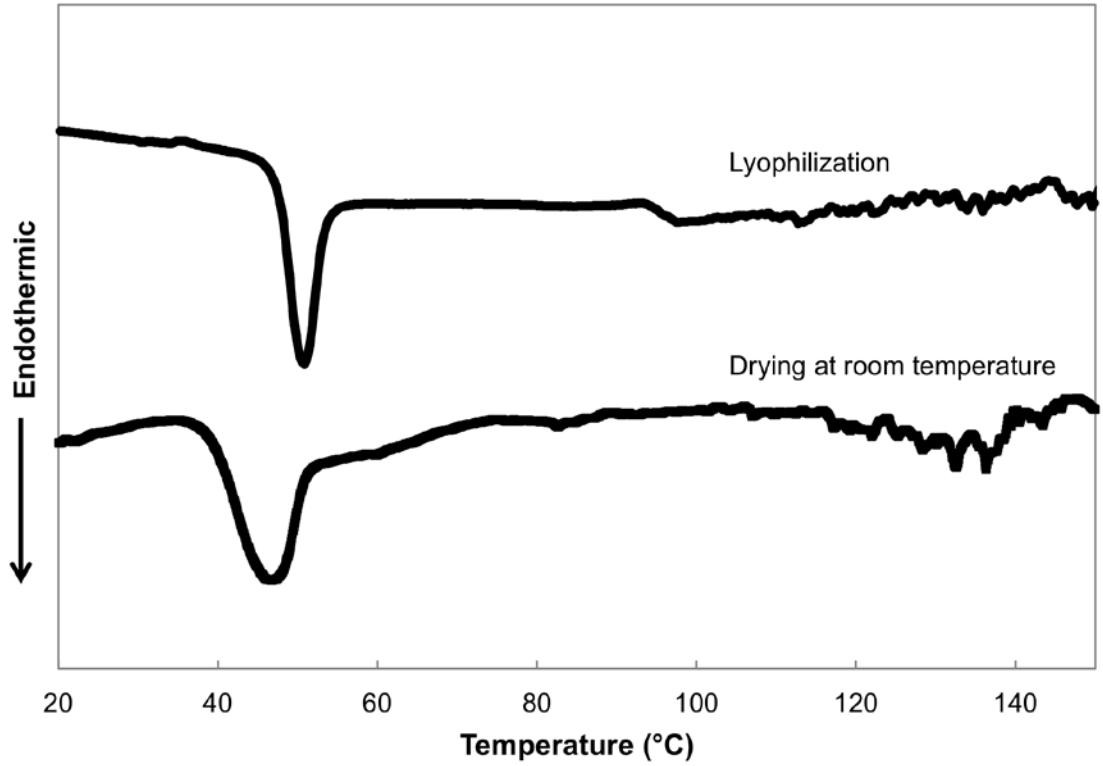

Figure 3-7 DSC thermographs of PLA microcapsules with a core shell structure, encapsulating PFOB oil. The ramping rate was 5°C min^{-1}. The microcapsules were dried with different processes (upper; lyophilization, lower; drying at room temperature).

3-3-4 Effect of flow rate upon emulsification on microcapsule size

After construction of the preparation procedure for monodisperse PLA microcapsules using internal phase separation, the effect of the flow rate of the continuous phase on the diameter of the microcapsules was investigated. The microcapsules were prepared by varying the flow rate of the continuous phase from 20 to 100 μL min^{-1} whilst keeping the disperse phase flow rate constant at 1 μL min^{-1}. Figure 3-8 depicts the optical microphotographs of the microcapsules prepared by changing the flow rate of

the continuous phase upon microfluidic emulsification. As shown in Figure 3-8, the diameter of the resultant microcapsules declined with increasing Q_c, which was precisely tuned from 20.8 to 34.6 μm in which the CV values of the core and the microcapsule size kept below 7%. It was also found that the shell thickness to radius (T/R) ratio was approximately constant at 0.28 regardless of the diameter of the microcapsules (**Table 3-3**). From these results, it was concluded that this process enabled producing monodisperse PLA microcapsules with tuneable sizes without any effect on the T/R ratio of the core-shell structure.

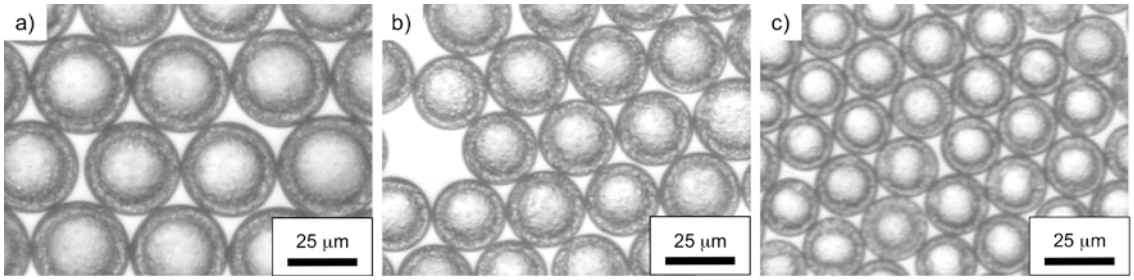

Figure 3-8 Optical microscopic images of monodisperse PLA microcapsules prepared by changing Q_c at a fixed Q_d (1 μL min^{-1}). The Q_c was (a) 20, (b) 50, and (c) 100 μL min^{-1}. C_{PFOB} was constant at 15 μL mL^{-1}.

Table 3-3 Effect of Q_c on the diameter of microcapsule, the inner core size and the shell thickness to radius ratio.

Q_c [μL min^{-1}]	20	50	100
Microcapsule size [μm] (CV)	34.6 (4.0%)	26.8 (6.8%)	20.8 (4.0%)
Inner core size [μm] (CV)	25.0 (4.4%)	19.2 (6.1%)	15.0 (5.2%)
Shell thickness to radius ratio (T/R [-])	0.28	0.28	0.28

3-3-5 Effect of PFOB concentration on the core size of the microcapsules

Following control over the diameter of the microcapsules, the effect of the PFOB concentration in the dispersed organic phase on the T/R ratio of the core-shell structures was investigated. Using the same process, the microcapsules were prepared by altering the concentration of PFOB in the original dispersed phase from 1.25 to 15 μL mL^{-1}. Figure 3-9 shows the optical microphotographs of the microcapsules with different PFOB content. It was found that monodisperse PLA microcapsules with core-shell structures were successfully obtained in different to the PFOB concentration within the experimental conditions. The images obviously show that the T/R ratio decreases with an increment of the PFOB concentration and that it can be tuned from 0.28 to 0.61 as summarized in **Table 3-4**.

Moreover, the experimental results of the shell thickness were compared with the theoretical shell thickness. The values and the calculation results were summarized in **Table 3-5**. It was found that each shell thickness was in good accordance with the theoretical calculation results, supporting that this process can produce monodisperse PLA microcapsules with core-shell structures with desirable shell thickness.

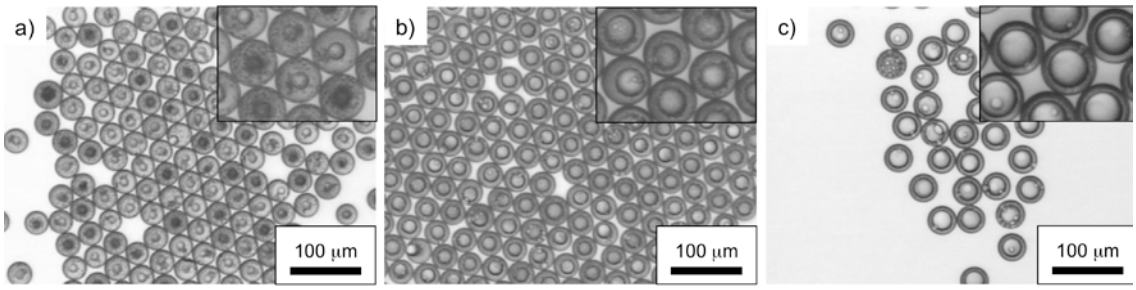

Figure 3-9 Optical microscopic images of monodisperse PLA microcapsules prepared by varying the concentration of PFOB in the dispersed phase whilst keeping each flow rate constant (C_{PFOB} = (d) 1.25, (e) 5, and (f) 15 μL mL^{-1} at Q_d = 1 μL mL^{-1} and Q_c = 20 μL min^{-1}).

Table 3-4 Effect of the PFOB concentration in the dispersed phase on the diameter of microcapsule, the inner core size and the shell thickness to radius ratio.

ϕ_{PFOB} [μL mL^{-1}]	1.25	5	15
Microcapsule size [μm] (CV)	33.8 (3.1%)	35.5 (3.3%)	38.4 (3.1%)
Inner core size [μm] (CV)	13.1 (9.2%)	20.5 (3.4%)	27.6 (4.6%)
Shell thickness to radius ratio (T/R [-])	0.61	0.42	0.28

Table 3-5 Comparison between the shell thickness of the microcapsules and that of theoretical values.

Run	C_{PFOB} (μL mL^{-1})	Microcapsule diameter (μm)	Core diameter (μm)	Shell thickness (μm)	$T_{theore.}$ (μm)
1	15	34.6	25.0	4.8	4.3
2	15	26.8	19.2	3.9	3.4
3	15	20.8	15.0	2.9	2.6
4	1.25	33.8	13.1	10.4	10.4
5	10	35.5	20.5	7.5	7.5
6	15	38.4	27.6	5.4	4.8

3-3-6 Effect of PLA molecular weight on the microcapsule structure

The effect of molecular weight of PLA on the final structure of the microcapsules was investigated. In this experiment, as an alternative to lower molecular weight PLA (Mn = 13,600, Mw/Mn = 1.14), the microcapsules were prepared using PLA with a relatively higher molecular weight (Mn = 52,000, Mw/Mn = 1.29) as a shell-forming material. Figure 3-10 shows the optical microphotograph of the prepared microcapsules after solvent diffusion. Surprisingly, it was found that monodisperse microcapsules covered with many small droplets were obtained, which looks like a Pickering emulsion or a colloidsome.[25] In addition, it was observed that there was contrast between the core and the shell, indicating that the microcapsules had a core-shell structure. Understanding the internal structure of the microcapsules, the microcapsules were observed by CLSM. For the CLSM observation, the microcapsules with a porphyrin-derivative as a fluorescence marker were prepared through the same process. Figure 3-11 describes the CLSM image of the microcapsules after solvent diffusion. It was revealed that the microcapsules covered with small droplets also had a single oil core. Although there were some microcapsules with multiple cores, most of the microcapsules had a single core. In addition, it was found that the microcapsules had a dark rough surface, which indicated the existence of the PFOB phase, forming small droplets. To observe the detailed surface morphology of the microcapsules, the microcapsules after freeze-drying were observed by SEM. As shown in Figure 3-12, monodisperse hollow PLA microcapsules with dimpled surfaces were obtained, which resembles Golf-ball. Apparently, the size of the dimples is polydisperse, and the dimples just form patch structure on the surface and they do not penetrate the shell of the microcapsules.

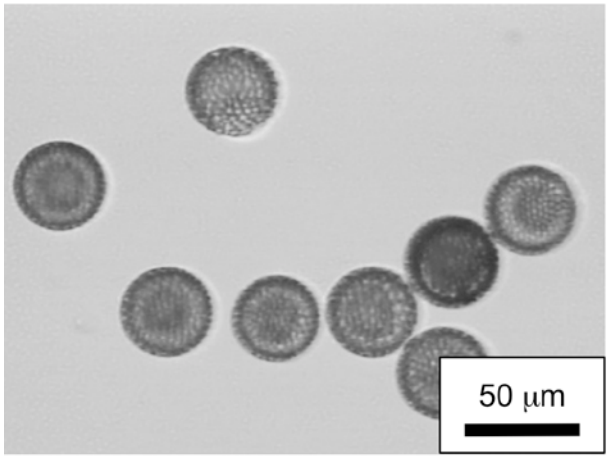

Figure 3-10 Optical photograph of monodisperse PLA microcapsules prepared using relatively higher molecular weight of PLA as a shell forming material.

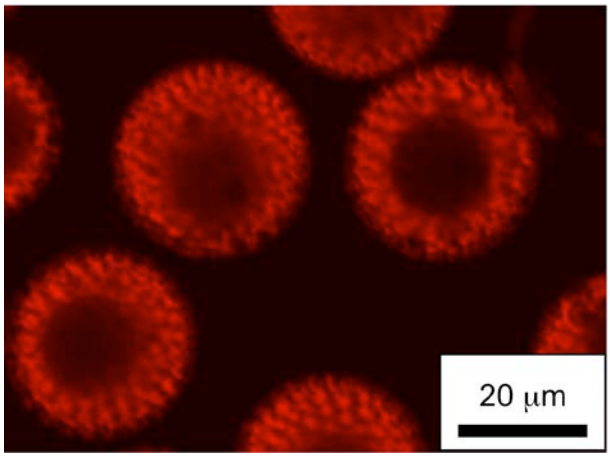

Figure 3-11 CLSM image of monodisperse PLA microcapsules covered with small droplets after solvent diffusion. The PLA matrix was dyed with porphyrin-derivative in red.

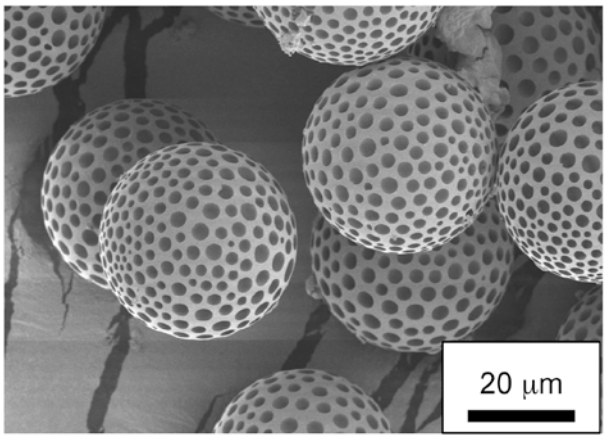

Figure 3-12 SEM image of monodisperse PLA microcapsules with a dimpled surface, which was prepared using a relatively higher molecular weight of PLA as a shell forming material.

3-3-7 Formation mechanisms of the microcapsules

To elucidate the formation mechanisms of the dimpled surface structure on the core-shell microcapsules, the time course of the microcapsule formation during solvent diffusion was observed by an optical microscope. However, it was found that due to several limitations on the volatility of EA, the quick diffusion of EA into the aqueous phase, and the rapid change in the density of the droplets within a few seconds, it was impossible to observe the microcapsule formation process under typical experimental conditions. Therefore, instead of the experiment, the model experiment using polydisperse emulsion droplets prepared with a mechanical stirring by homogenizer was carried out on a slide glass covered with a coverslip on a microscope stage. Then, the solvent diffusion of EA was induced by adding a small amount of pure water into the system from the gap between the slide glass and the coverslip. It is important to note that because of step-by-step addition of pure water from one side of the sample, the diffusion time scale is longer than that of the typical microfluidic process and the diffusion occurs heterogeneously in the sample, depending on the difference of the local EA concentration in pure water, which gave the resultant microcapsules with irregular shapes. Figure 3-13 depicts the optical microphotographs of time course of microcapsule formation with (A) a smooth surface and (B) a dimpled surface. When using relatively low molecular weight of PLA as a matrix of the microcapsules, as

shown in Figure 3-13 (A), it was observed that as soon as pure water was added into the system, the droplet began to shrink and the internal phase separation was induced, resulting in small PFOB droplets inside the emulsion droplets. The small droplets subsequently migrated towards the centre region of the emulsion droplet and microcapsules with multiple cores were finally obtained. In contrast, in the case of which PLA with high molecular weight was used as a matrix of the microcapsules, the same event was observed however, the migration of small PFOB droplets was considerably slower than the case with a low molecular weight of PLA. As a result, microcapsules with an irregular shape were obtained (Figure 3-13 (B)).

The morphological difference must be caused by the increase in the viscosity of the PLA solution. In **Scheme 3-2**, the formation mechanisms of these microcapsules were proposed. Under the preparation condition in which monodisperse PLA microcapsules with smooth surfaces were obtained, the viscosity of the dispersed organic phase during internal phase separation was low. That is why, small PFOB droplets arising from the emulsion droplets in the course of internal phase separation can easily move in the polymer droplet and smoothly migrate towards the centre so as to minimize the higher interfacial tension between the PFOB phase and the continuous phase, whilst small PFOB droplets coalesce with each other before precipitating polymer as shown in **Scheme 3-2A**. On the contrary, when using a higher molecular weight PLA, the viscosity of the solution was relatively high as a result of the increase in the degree of polymer entanglement in the solution. By increasing the viscosity, the small PFOB droplets formed by internal phase separation become to move and to migrate towards the centre Moreover, it is much easier for the emulsion composition to reach the bimodal boundary in the droplets as a result of solvent diffusion, which leads to rapid solidification of the polymer droplets from the surface. Therefore, the part of PFOB droplets is kinetically locked on the surface. Since the volume shrinkage of the polymer droplets is much faster and PFOB is immiscible with water and a non-solvent for PLA, partially phase-separated small PFOB droplets that escaped from the solidification front migrate to the centre of the polymer droplets, coupled with coalescence prior to complete solidification. Consequently, monodisperse core-shell microcapsules covered with a number of small PFOB droplets are formed in the collection bath (**Scheme 3-2B**). In order to slow down the rate of solvent diffusion, a small amount of pure water was introduced into the system from one side of the glass plate step by step. Thus, the time

scale of the microcapsule formation was quite longer than the typical experimental conditions using microfluidics (t ~3 sec.) and the final morphology of the microcapsules was different from that prepared by microfluidic approach because of heterogeneous solvent diffusion from only one side of the sample.

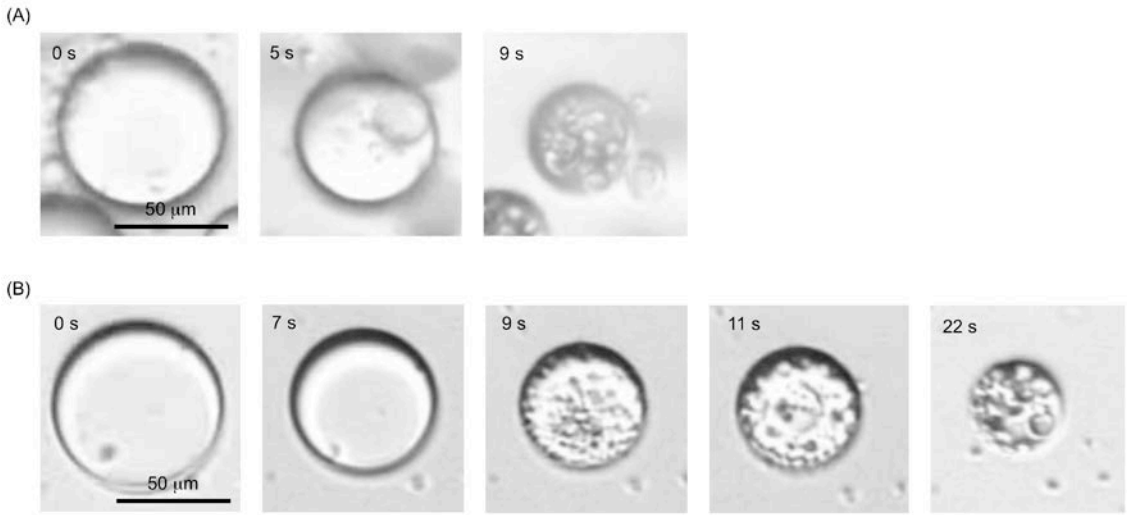

Figure 3-13 Time course of microcapsule formation during solvent diffusion. (A) Microcapsules with a smooth surface (B) Microcapsules with a dimpled surface.

Scheme 3-2 Schematic illustration of the proposed formation mechanism of PLA microcapsules with (A) a smooth surface and (B) a dimpled surface during solvent diffusion.

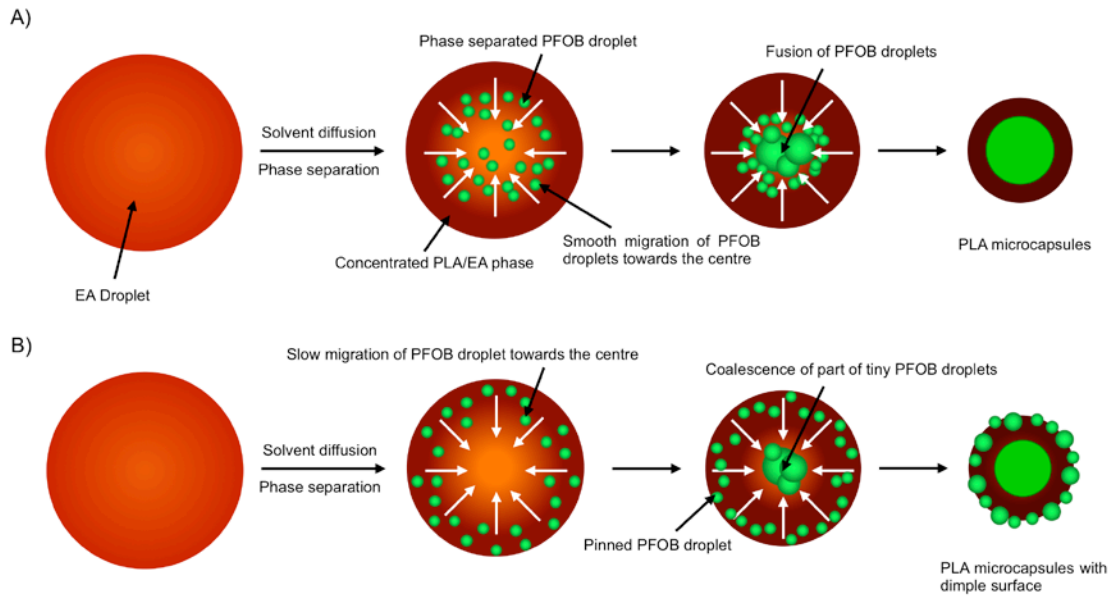

3-3-8 Effect of flow rate on the microcapsules with a dimpled surface

The diameters of the microcapsules with a dimpled surface were also tuned by changing the conditions of microfluidic emulsification likewise. Figure 3-15 shows the effect of the flow rate of the continuous phase on the diameter of the microcapsules and the mean diameter of surface dimples. Regardless of the continuous flow rate, dimpled PLA microcapsules were generated and the diameter was controlled from 11.7 to 40.6 μm. It was found that the dimple size decreased with decreasing the diameter of the microcapsules. In addition, it should be noted that the dimple size prepared with gentle stirring is smaller than that prepared without stirring, although there is no difference in the microcapsule diameter. These results indicate that the stirring during solvent diffusion facilitates polymer precipitation and hinders the fusion of small PFOB droplets until some of them are stabilized on the surface by w-PEG-*b*-PLA.

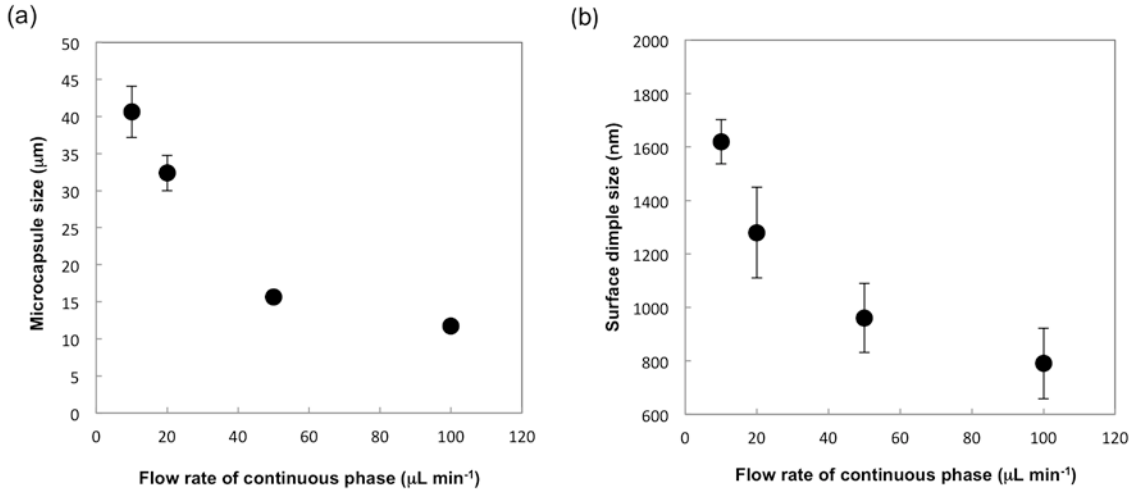

Figure 3-14 Effect of Q_c on (a) the diameter and (b) the surface dimple diameter of the microcapsules.

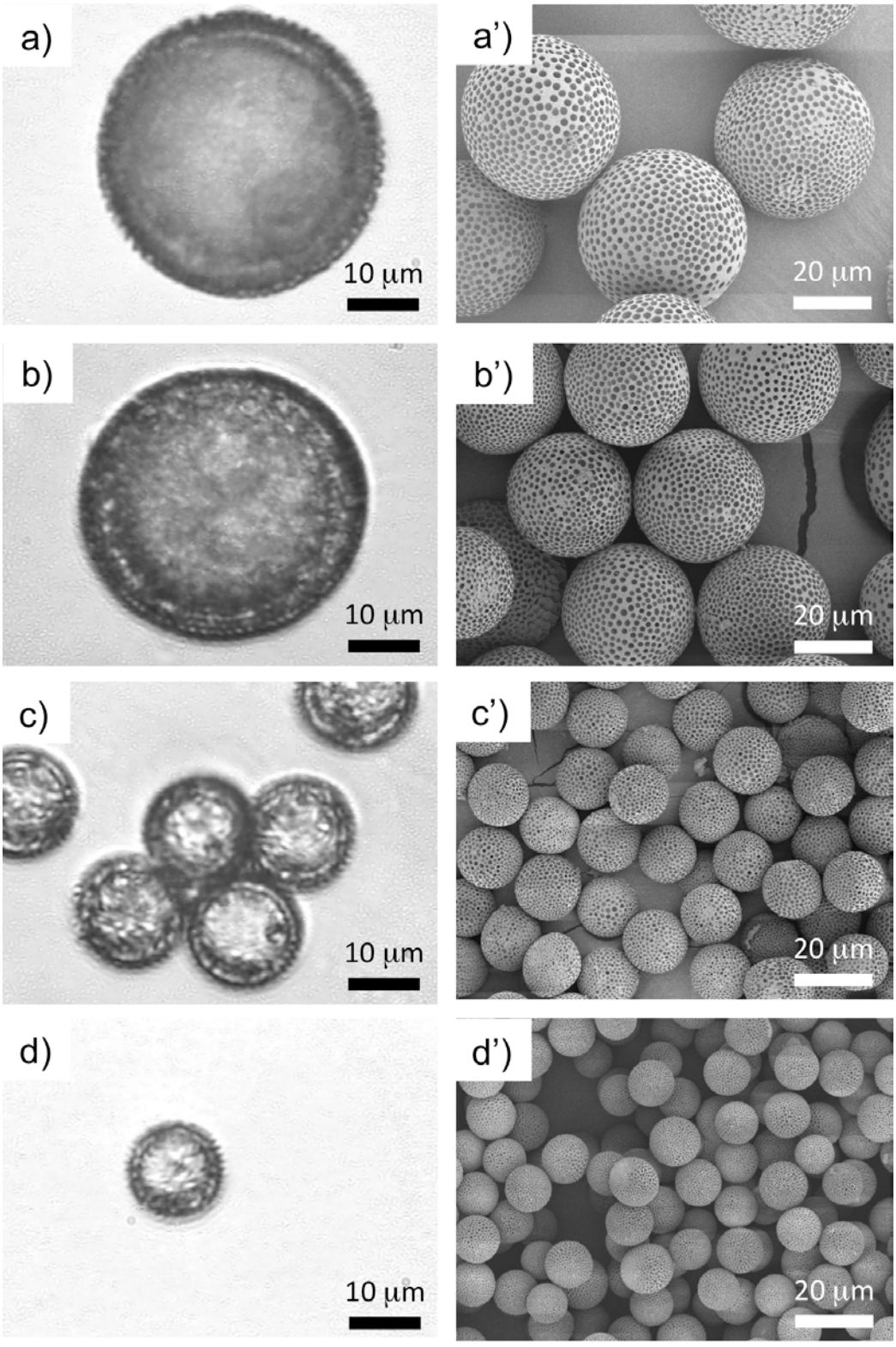

Figure 3-15 (a-d) Optical micrographs and (a'-d') SEM images of the PLA microcapsules before freeze-drying. Q_c = (a, a') 10, (b, b') 50, and (c, c') 100 μL min^{-1} at Q_d = 1 μL min^{-1}. C_{PFOB} = 15 μL mL^{-1}.

3-4 Conclusions

Monodisperse PLA microcapsules encapsulating a liquid oil (PFOB) core were successfully produced by simply diluting a monodisperse O/W emulsion with pure water under stirring. The rapid extraction of EA from the droplets into outer aqueous phase led to internal phase separation between the concentrated PLA/EA phase and the PFOB phase and rapid solidification of the droplets, resulting in core shell microcapsules with non-equilibrium structures. The core shell ratios and the diameter of the microcapsules could be modulated by varying the compositions of the dispersed phase and flow rates upon emulsification. This process has enabled to prepare monodisperse PLA microcapsules having a hydrophobic oil core and a hollow structure with either a smooth or a dimpled surface. Such PLA microcapsules with controllable structures have great potential for carriers of functional molecules used in biomedical fields such as cosmetics, pharmaceutics, and contrast imaging.

References

1. Dowding, P. J.; Atkin, R.; Vincent, B.; Bouillot, P. Oil Core−Polymer Shell Microcapsules Prepared by Internal Phase Separation from Emulsion Droplets. I. Characterization and Release Rates for Microcapsules with Polystyrene Shells. *Langmuir* **2004,** *20* (26), 11374-11379.
2. Dowding, P. J.; Atkin, R.; Vincent, B.; Bouillot, P. Oil Core/Polymer Shell Microcapsules by Internal Phase Separation from Emulsion Droplets. II: Controlling the Release Profile of Active Molecules. *Langmuir* **2005,** *21* (12), 5278-5284.
3. Wang, Y.; Guo, B.-H.; Wan, X.; Xu, J.; Wang, X.; Zhang, Y.-P. Janus-like polymer particles prepared via internal phase separation from emulsified polymer/oil droplets. *Polymer* **2009,** *50* (14), 3361-3369.
4. Jiang, Y.; Wang, D.; Zhao, T. Preparation, characterization, and prominent thermal stability of phase-change microcapsules with phenolic resin shell and n-hexadecane core. *J. Appl. Polym. Sci.* **2007,** *104* (5), 2799-2806.
5. Dai, M.; Song, L.; Nie, W.; Zhou, Y. Golf ball-like particles fabricated by nonsolvent/solvent-induced phase separation method. *J. Colloid Interface Sci.* **2013,** *391*, 168-71.
6. Gun, W. J.; Routh, A. F. Formation and characterization of pH-responsive liquid core microcapsules. *Langmuir* **2013,** *29* (40), 12541-12548.

7. Hanson, J. A.; Chang, C. B.; Graves, S. M.; Li, Z.; Mason, T. G.; Deming, T. J. Nanoscale double emulsions stabilized by single-component block copolypeptides. *Nature* **2008,** *455* (7209), 85-88.

8. Thiele, J.; Abate, A. R.; Shum, H. C.; Bachtler, S.; Forster, S.; Weitz, D. A. Fabrication of polymersomes using double-emulsion templates in glass-coated stamped microfluidic devices. *Small* **2010,** *6* (16), 1723-1727.

9. Wei, Y.; Wang, Y.-X.; Wang, W.; Ho, S. V.; Wei, W.; Ma, G.-H. mPEG-PLA microspheres with narrow size distribution increase the controlled release effect of recombinant human growth hormone. *J. Mater. Chem.* **2011,** *21* (34), 12691-12699.

10. Schmitz-Hertzberg, S.-T.; Mak, W. C.; Lai, K. K.; Teller, C.; Bier, F. F. Multifactorial design of poly(d,l-lactic-co-glycolic acid) capsules with various release properties for differently sized filling agents. *J. Appl. Polym. Sci.* **2013,** *130* (6), 4219-4228.

11. Wu, J.; Kong, T.; Yeung, K. W. K.; Shum, H. C.; Cheung, K. M. C.; Wang, L.; To, M. K. T. Fabrication and characterization of monodisperse PLGA–alginate core–shell microspheres with monodisperse size and homogeneous shells for controlled drug release. *Acta Biomater.* **2013,** *9* (7), 7410-7419.

12. He, T.; Liang, Q.; Zhang, K.; Mu, X.; Luo, T.; Wang, Y.; Luo, G. A modified microfluidic chip for fabrication of paclitaxel-loaded poly(l-lactic acid) microspheres. *Microfluid. Nanofluid.* **2011,** *10* (6), 1289-1298.

13. Wei, Q.; Wei, W.; Tian, R.; Wang, L. Y.; Su, Z. G.; Ma, G. H. Preparation of uniform-sized PELA microspheres with high encapsulation efficiency of antigen by premix membrane emulsification. *J. Colloid Interface Sci.* **2008,** *323* (2), 267-273.

14. Abraham, S.; Jeong, E. H.; Arakawa, T.; Shoji, S.; Kim, K. C.; Kim, I.; Go, J. S. Microfluidics assisted synthesis of well-defined spherical polymeric microcapsules and their utilization as potential encapsulants. *Lab Chip* **2006,** *6* (6), 752-756.

15. Wang, B.; Shum, H. C.; Weitz, D. A. Fabrication of monodisperse toroidal particles by polymer solidification in microfluidics. *ChemPhysChem* **2009,** *10* (4), 641-645.

16. Kanai, T.; Lee, D.; Shum, H. C.; Weitz, D. A. Fabrication of tunable spherical colloidal crystals immobilized in soft hydrogels. *Small* **2010,** *6* (7), 807-810.

17. Lee, D.; Weitz, D. A. Double Emulsion-Templated Nanoparticle Colloidosomes with Selective Permeability. *Adv. Mater.* **2008,** *20* (18), 3498-3503.

18. Chen, H.; Li, J.; Wan, J.; Weitz, D. A.; Stone, H. A. Gas-core triple emulsions for ultrasound triggered release. *Soft Matter* **2013,** *9* (1), 38-42.

19. Berkland, C.; Pollauf, E.; Varde, N.; Pack, D. W.; Kim, K. K. Monodisperse liquid-filled biodegradable microcapsules. *Pharm. Res.* **2007,** *24* (5), 1007-1013.

20. Utada, A. S.; Lorenceau, E.; Link, D. R.; Kaplan, P. D.; Stone, H. A.; Weitz, D. A. Monodisperse double emulsions generated from a microcapillary device. *Science* **2005,** *308* (5721), 537-541.

21. Tu, F.; Lee, D. Controlling the stability and size of double-emulsion-templated poly(lactic-co-glycolic) acid microcapsules. *Langmuir* **2012,** *28* (26), 9944-9952.

22. Amstad, E.; Kim, S. H.; Weitz, D. A. Photo- and thermoresponsive polymersomes for triggered release. *Angew. Chem. Int. Ed. Engl.* **2012,** *51* (50), 12499-12503.

23. Lensen, D.; van Breukelen, K.; Vriezema, D. M.; van Hest, J. C. Preparation of biodegradable liquid core PLLA microcapsules and hollow PLLA microcapsules using microfluidics. *Macromol. Biosci.* **2010,** *10* (5), 475-480.

24. Torza, S.; Mason, S. G. Three-phase interactions in shear and electrical fields. *J. Colloid Interface Sci.* **1970,** *33* (1), 67-83.

25. Amalvy, J. I.; Armes, S. P.; Binks, B. P.; Rodrigues, J. A.; Unali, G. F. Use of sterically-stabilised polystyrene latex particles as a pH-responsive particulate emulsifier to prepare surfactant-free oil-in-water emulsions. *Chem. Commun.* **2003,** (15), 1826-1827.

Chapter 4
Preparation of monodisperse PLA microcapsules encapsulating a single aqueous core by spontaneous emulsification

4-1 Introduction

In chapter 3, a simple process to prepare monodisperse PLA microcapsules with a liquid oil core using internal phase separation was elaborated. Although the process can be utilized to obtain core-shell microcapsules with different oil cores, it is challenging to encapsulate aqueous liquid core into the polymer microparticles since driving force for migration of phase-separated oil droplets to the centre in the microcapsules relies on hydrophobicity of the non-solvent co-dissolved in the organic phase.

As described in the previous chapters, biocompatible polymeric microcapsules with nano to micrometer in the diameter have been considerably studied in the world because of their ubiquitous applications especially for drug delivery carriers for sustained release. Most of drugs administrated in clinical therapy are actually hydrophilic ones. Hence, there have been increasing demands for development of the process to produce microcapsules with aqueous liquid cores using a simple process.

Various methods have been developed for the preparation of polymer microcapsules encapsulating hydrophilic compounds, including W/O/W emulsion formation, coupled with solidification techniques (*e.g.* solvent evaporation[1] and UV or heat polymerization[2]), miniemulsion polymerization,[3] layer-by-layer (L*b*L) assembly,[4] interfacial polymerization of polymer droplets,[5] supramolecular self-assembly,[6, 7] and surface-initiated atom transfer radical polymerization on template colloidal particles.[8] Although template methods with stepwise operations can fabricate microcapsules with hydrophilic cores, these techniques are not environmentally friendly because the step for core removal requires high energy and the whole process is time-consuming.

From the point of view of biocompatible polymer microcapsules, many reports have been carried out by solvent-evaporation method using W/O/W emulsion template. In this technique, the microcapsules are produced by removal of organic solvent from the prefabricated W/O/W complex emulsion. The complex emulsion droplets are generally produced in a two-step emulsification, which includes W/O emulsion formation by emulsifying the inner aqueous phase in the middle organic phase, and the second emulsification with the W/O emulsion and the external surfactant aqueous solution. Although this process circumvent denature of aqueous reagents encapsulated in the internal cores, it usually requires halogenated solvent and much time for polymer precipitation. Moreover, each emulsification step results in polydisperse emulsion droplets, giving rise to microcapsules with poorly controlled sizes and their structures.

Regarding the polydispersity, a recent developed microfluidic approach has enabled the production of highly controlled emulsion droplets and the resultant microcapsules in a continuous fashion. However, the technology does not solve the drawbacks in terms of complexity over the fabrication process. When using a microfluidic device that has several junctions, it is required to control the wetting properties of each section to produce precision droplets because the surface (wetting) property of the microchannels has a crucial impact on forming emulsion droplets.[9] For instance, to produce organic droplets, the wall of the channel should be tailored to be hydrophilic to avoid the wetting of the dispersed organic phase, whereas that of the channel should be hydrophobic when preparing aqueous droplets. Thus, to produce W/O/W emulsion, the microfluidic device must have both a hydrophobic section for the first emulsification and a hydrophilic section for the second one, meaning that the surface treatment prior to use is a bit complex. With capillary type microfluidic devices, preparation of monodisperse complex droplets can be easily generated without any wetting problems, but the control of the flow conditions has some limitations, which gives rise to difficulty in controlling over the resultant microcapsule size. Moreover, because of limitation in the inner capillary size, up to date, it is impossible to produce monodisperse microcapsules with less than 30 μm in the diameter.

In this study, a facile one-step process for fabrication of monodisperse PLA microcapsules with a single aqueous core has been developed. This process is based on “droplet to particle” technology consisting of microfluidic emulsification and subsequent solvent diffusion with some modification, shown in chapter 2. For this

process, an EA solution containing PLA and amphiphilic diblock copolymer, poly(D,L-lactide)-*b*-poly(2-dimethylaminoethyl methacrylate) (PLA-*b*-PDMAEMA), was utilized as a dispersed phase. The dispersed organic phase and a continuous aqueous surfactant solution saturated with EA were mixed in a Y-shaped microfluidic device to produce monodisperse O/W emulsion droplets. The resultant emulsion droplets flow towards the downstream of the channel. In this process, water was extracted from the continuous phase into the dispersed organic droplets through the EA/water interface *via* spontaneous emulsification induced by PLA-*b*-PDMAEMA that forms reverse micelles within each emulsion droplet, resulting in forming W/O/W emulsion droplets with multiple tiny aqueous cores. The complex droplets were then diluted with excess volume of pure water in the precipitation bath, facilitating extraction of EA into the external aqueous phase and coalescence of small water droplets within each emulsion droplet. Within a few second after onset of solvent diffusion, microcapsules with a single aqueous core were obtained as a result of complete coalescence of tiny internal droplets. This method has many advantages such as using non-toxic materials, simplification of the preparation process, and fine-tuning of their size. Similar to the previous chapters, EA that is non-toxic organic solvent with high solubility in water was used for the organic solvent, which makes it easy to remove by dilution with water. All materials used in this system (PLA, PLA-*b*-PDMAEMA and w-PEG-*b*-PLA) are biocompatible, thus resulting in biocompatible microcapsules that can be available in biological applications. The quick removal of EA from the droplets shortens precipitation time about hundreds times compared to a conventional emulsion-solvent evaporation technique using halogenated solvents. The one-step microfluidic emulsification using a simple device enables to reduce the microcapsule size up to 10 μm by changing broad range of flow conditions. As far as I know, there has been no report to fabricate monodisperse microcapsules with a single aqueous core using one-step emulsification. The effects of preparation parameters (such as PLA/PLA-*b*-PDMAEMA ratio, molecular weight of PLA, flow rates on the emulsification) on final structures of the microcapsules were investigated. In addition, the dual encapsulation of both hydrophobic and hydrophilic compounds within the microcapsules has been demonstrated.

4-2 Spontaneous emulsification

Spontaneous emulsification (in other words, self-emulsification) is a phenomenon that generates tiny droplets without the aid of any external or mechanical energy source when two immiscible liquids are brought in contact with each other. The phenomenon is generally induced by addition of highly surface-active species in the dispersed phase, leading to roughening of the interface between immiscible fluids and formation of small droplets. Such instabilities may occur whenever a ternary liquid/liquid/surfactant system whose equilibrium state is a microemulsion is first prepared in a macroscopically phase-separated state.[10, 11] The strong driving force for adsorption of the amphiphilic molecules to the interface between the immiscible liquids give rise to a vanishing or transiently negative interfacial tension between the two bulk phases, thereby triggering spontaneous creation of interface and allowing the system to evolve toward its equilibrium microemulsion structure.[12, 13] In recent years, Yu *et al.* have succeeded in preparation of biodegradable polymeric microcapsules *via* spontaneous emulsification-solvent evaporation method.[14, 15] They added sodium dioctyl sulfosuccinate (Aerosol OT or AOT) into the original polymer phase, which induced water diffusion into the polymer phase during solvent evaporation and formation of W/O/W emulsion, followed by generation of microcapsules with aqueous cores. This spontaneous process has enabled one-step formation of multiple emulsions without any specific equipment. However, AOT is a low molecular compound and removed during the formulation, thus it is just to help the microcapsule formation and is impossible to introduce any functionality on the resultant microcapsules. If amphiphilic copolymers playing a role in a co-surfactant as well as a surface modifier are utilized for the preparation, functional microcapsules should be obtained in a single step. In this study, considering addition of a high surface activity between EA and water saturated with EA phases as well as a high affinity to PLA homopolymer into the copolymer, PLA-*b*-PDMAEMA has chosen as the copolymer structure. The hydrophobic PLA block can be expected to have a high affinity to PLA homopolymer, whilst the hydrophilic PDMAEMA that is insoluble in EA has a cationic property, which makes it possible to induce spontaneous emulsification as a co-surfactant and simultaneously introduce a cationic amine surface on the microcapsules as a functional interface modifier.

4-3 Atom transfer radical polymerization (ATRP)

The new methodology in radical polymerization has been exploded in the late of 1990s, with the advent of controlled radical polymerization processes, including reversible addition-fragmentation chain transfer radical polymerization (RAFT),[16] nitroxide-mediated radical polymerization (NMP),[17] and atom transfer radical polymerization (ATRP).[18] These polymerization techniques allow one to synthesize polymers with controlled molecular weights and with well-defined structures. Among them, ATRP system utilizes a reversible halogen atom abstraction step in which a lower oxidation state metal (M_t^n complexed by ligands L and Y) reacts with an alkyl halide (P_m-X) to generate a radical (P_m) and a higher oxidation state metal complex ($XM_t^{n+1}LY$, k_a). This radical then adds monomer to generate polymer chain (k_p). Thereafter, the higher oxidation state metal can deactivate the growing radical to generate a dormant chain and the lower oxidation state metal (k_d), shown in **Scheme 4-1**. The molecular weight is highly controlled because both initiation and deactivation are considerably fast, allowing for all the chains to begin growing at the same time whilst maintaining a low concentration of active species. Termination reaction cannot be totally avoided, but can be extremely suppressed that is; the proportion of chains terminated compared to the number of propagating chains (the sum of active and dormant species) is smaller than 10%. In this chapter, ATRP has been applied to synthesis of amphiphilic PLA-*b*-PDMAEMA with controlled molecular structures in order to avoid undesirable effects of the structures on the interfacial phenomena.

Scheme 4-1 Equilibrium/propagation expression for ATRP.

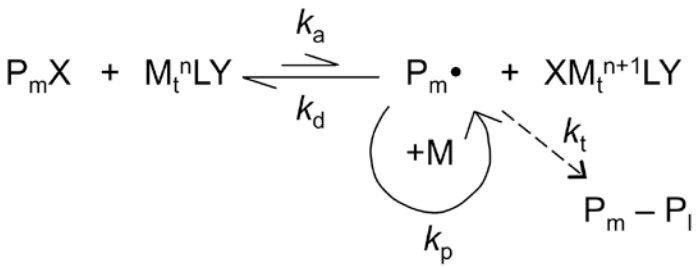

4-4 Experimental procedures

4-4-1 Materials

PLA and PEG-*b*-PLA were synthesized by a ring-opening polymerization of D,L-lactide in the presence of $Sn(Oct)_2$ as a catalyst using lauryl alcohol and poly(ethylene glycol) monomethyl ether (PEG, *M*n= 4,000, *M*w/*M*n= 1.06) as an initiator. The D,L-lactide was purchased from Purac (Netherland). The PEG was kindly supplied from NOF (Japan). $Sn(Oct)_2$, EA, ethylene glycol, triethylamine, chloroform, 0.1M HCl aqueous solution, sodium bicarbonate ($NaHCO_3$), anhydrous magnesium sulfate ($MgSO_4$), toluene, 2-propanol, *N*,*N*,*N'*,*N"*,*N"*-pentamethyldiethylenetriamine (PMDETA), tetrahydrofuran (THF), *n*-hexane, basic alumina, activated neutral alumina, dimethylformamide (DMF), CuCl(I), 2-(dimethylamino)ethyl methacrylate (DMAEMA) were obtained from Wako Pure Chemical Industries, Ltd. (Japan). 2-Bromoisopropionyl bromide was purchased from Sigma-Aldrich, Ltd. (Japan). DMAEMA was passed through a column of basic alumina to remove the stabilizing agents and stored under argon atmosphere at -20°C. CuCl(I) was purified by washing with glacial acetic acid until the liquid being colourless followed by ethanol in a Schlenk flask under argon atmosphere. The ultra pure water was produced by a Millipore Milli-Q purification system (EMD Millipore Corporation, USA).

4-4-2 Synthesis of 2-hydroxyethyl 2-bromopropionate (HEBP)

2-Bromoisopropionyl bromide (0.04661 mol) was added dropwise to a cold solution of ethylene glycol (0.99276 mol) and triethylamine (0.04357 mol) at 0°C for 1 h. The reaction was continued at 0°C for another 2 h and then heated to 40°C for 5 h. The reaction mixture was cooled, added to 200 mL of water, and extracted with chloroform five times, and then the organic layer was washed successfully with 0.1M HCl aqueous solution, saturated $NaHCO_3$ aqueous solution, and water. The organic layer was then dried over $MgSO_4$ and evaporated by a rotary evaporator to precipitate a product. The product was characterized with ^1H NMR (300 MHz, $CHCl_3$-*d*). The yield was 63%.

4-4-3 Synthesis of bromoisopropionate polylactide macroinitiator (PLA-Br)

PLA macroinitiator, PLA-Br, was synthesized by a ring-opening polymerization of D,L-lactide using HEBP as an initiator in the presence of $Sn(Oct)_2$ as a catalyst. D,L-lactide (12.0 g, 83.3 mmol), HEBP (230 mg, 1.17 mmol), and a toluene solution of

$Sn(Oct)_2$ (20.8 mg mL^{-1}, 50 μL) were placed into an glass ampule, which was sealed under reduced pressure and immersed in an oil bath at 130°C. The polymerization was conducted for 24 h. After cooling, the reaction mixture was dissolved in chloroform and excess 2-propanol was added. The precipitated polymer was recovered and washed with 2-propanol three times. The product was dried under reduced pressure over night. The yield was 80%.

4-4-4 Synthesis of polylactide-*b*-poly(2-dimethylaminoethyl methacrylate) (PLA-*b*-PDMAEMA)

The diblock copolymer, PLA-*b*-PDMAEMA was synthesized by ATRP of DMAEMA using the PLA-Br as a macroinitiator. The synthesis of the diblock copolymer was performed in DMF at 60°C in the presence of CuCl/PMDETA catalyst system under argon atmosphere. CuCl(I) (14 mg, 13.7 mmol) and PLA-Br (*M*n = 9,600, *M*w/*M*n = 1.15, 1.3286 g, 0.14 mmol) were placed in a Schlenk flask purged by three repeated vacuum / argon cycles. Six mL of degassed DMF was then added to the solution to dissolve the macroinitiator and the catalyst. After that DMAEMA (0.81 mL, 5.5 mmol) and PMDETA (28.9 μL, 0.14 mmol) were injected in the flask. The flask was immersed in an oil bath at 60°C. The polymerization was performed for 12 h. Then, the reaction flask was cooled down to room temperature and the solution was diluted with excess amount of THF. The copper catalyst was extracted by passing the diluted solution through a column of activated neutral alumina. The purified copolymer was precipitated in *n*-hexane three times, filtered off, and dried under reduced pressure at 40°C overnight. The yield was 71%.

4-4-5 Gel permeation chromatography (GPC) analysis

The molecular weight distribution (*M*w/*M*n) analysis of the synthesized polymers was performed with GPC (HLC-8220GPC, TOSOH, Japan) at 40°C, equipped with a refractive index detector and columns (TSKguardcolumn SuperH-H, TSKgel SuperHM-H, and TSKgel SuperH2000, TOSOH, Japan). DMF was used as the eluent at a flow rate of 0.6 mL min^{-1}. The calibration curve was prepared by using monodisperse polystyrene standards.

4-4-6 ^{1}H NMR Analysis

The synthesized polymer structures were determined from ^{1}H NMR spectra. The analysis was carried out using a JEOL FT NMR System (300 MHz, JMN-AL300, JEOL, Japan) at room temperature in $CHCl_3$-*d*. The number averaged molecular weights (*M*n) of PLA-Br and PLA-*b*-PDMAEMA were determined from ^{1}H NMR spectra.

4-4-7 Interfacial tension measurement

The interfacial tensions between EA solutions dissolving PLA-*b*-PDMAEMA at various concentrations and an EA-saturated aqueous solution were measured using a Wilhelmy plate interfacial tension meter (K100, Krüss, Germany). The EA-saturated aqueous solution (5 mL) was poured into a 50 mL vessel, and then EA (20 mL) solutions dissolving PLA-*b*-PDMAEMA with different concentrations were gently added into the aqueous solution. The measurements were performed at 20°C. The interfacial tension was accepted as an equilibrium value when it reached constant value regardless of time.

4-4-8 Preparation of monodisperse PLA microcapsules

A schematic illustration of the preparation procedure of monodisperse PLA microcapsules is shown in **Scheme 4-2**. A microfluidic device that was used for the microcapsule fabrication consisted of a Y-shaped channel (126 μm- and 136 μm-width channels with 75 μm in depth) made by SUS, a glass cover plate, Teflon tubing, and tubing connectors. The outer aqueous phase and the inner organic phase were pumped independently at various flow rates using syringe pumps connected to the device *via* Teflon tubing. An aqueous solution saturated with EA containing 1 wt% of w-PEG-*b*-PLA (*M*n = 4,400, *M*w/*M*n = 1.05, HLB = 18.2) was used as the continuous phase and an EA solution composed of PLA (*M*n = 7,300, *M*w/*M*n = 1.31) and PLA-*b*-PDMAEMA (*M*n = 16,200, *M*w/*M*n = 1.28) was used as the dispersed phase. The PLA to PLA-*b*-PDMAEMA ratio was varied from 10/0 to 5/5 (w/w). The flow rates of the dispersed phase and the continuous phase were 2 and 250 μL min^{-1}, respectively. For fluorescence microscopy, a trace amount of Nile red and 1 mg mL^{-1} of calcein were added to the dispersed phase and the continuous phase, respectively in order to visualize the location of these compounds. The obtained O/W emulsion was transferred into a bath filled with 100 mL of ultra pure water through Teflon tubing (Φ = 0.5 mm, *L* = 20 cm) whose exit tip was submerged in the water. The EA was then rapidly removed from

the droplet to the large volume of pure water by solvent diffusion with or without gentle stirring, leading to precipitation of PLA microcapsules. The microcapsules were washed with ultra pure water three times by centrifugation (himac CF 15R, Hitachi, Japan) at 3,000 rpm for 3 min to remove the excess surfactant, followed by freeze-drying overnight, resulting in dried PLA microcapsules.

4-4-9 Analysis of water extraction behaviour *via* oil-soluble PLA-*b*-PDMAEMA in the organic phase

As shown in **Table 4-1**, 4 kinds of two-phase systems were prepared to employ observation of water extraction behaviour *via* spontaneous emulsification. For the preparation, 6 mL of the continuous phase was placed into each vial and the dispersed phases were added into the vials. In this experiment, the continuous aqueous phase was dyed with Reactive Blue to enhance the visibility. The samples were shaken at 100 rpm for 24 hours and then the upper phase colour of the samples was observed with naked eyes. Size of aqueous droplet extracted in the upper phase was also analysed by using Zetasizer Nano (Malvern Instruments Ltd.) with a He-Ne laser beam at 633 nm at 25°C. The average value was obtained from three repeated measurements for each sample.

Scheme 4-2 Schematic illustration of monodisperse microcapsule fabrication process using microfluidic emulsification, spontaneous emulsification, followed by solvent diffusion.

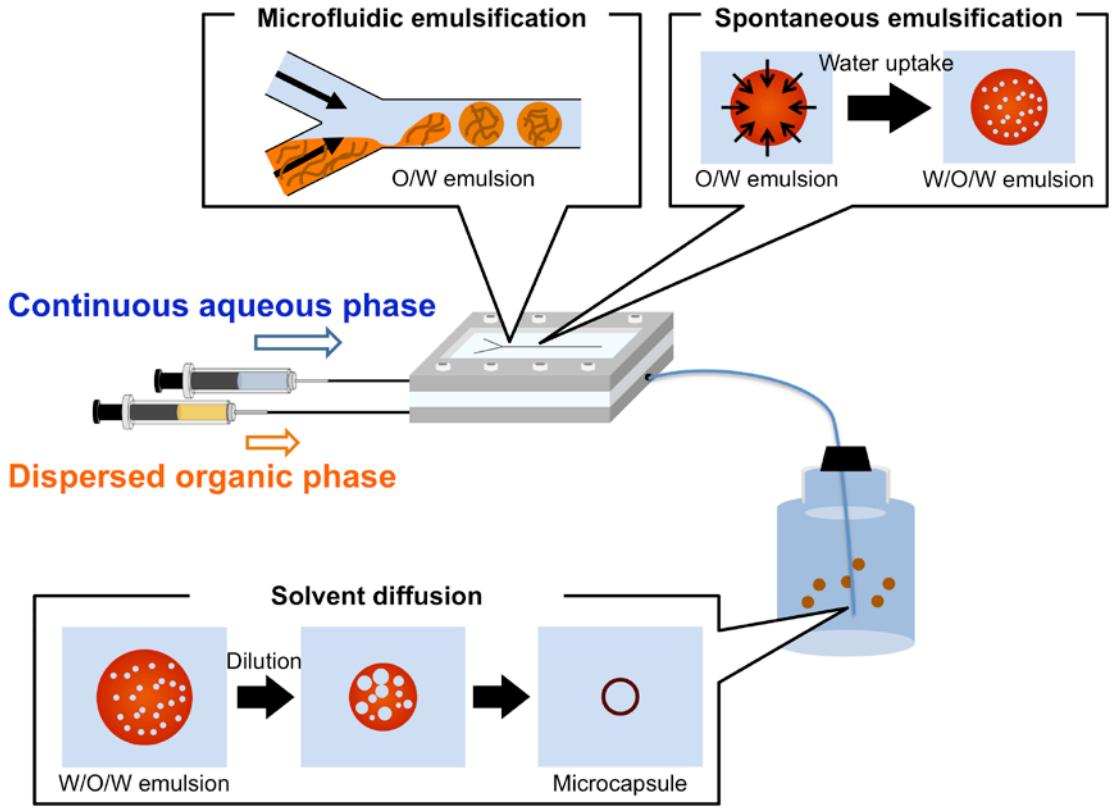

Table 4-1 Preparation conditions of two phase systems for extraction experiment.

Entry	Dispersed phase	Continuous phase
1	Ethyl acetate (EA)	Water saturated with EA
2	EA+4 mg mL^{-1} of PLA-*b*-PDMAEMA	
3	EA+6 mg mL^{-1} of PLA	
4	EA+4 mg mL^{-1} of PLA-*b*-PDMAEMA+6 mg mL^{-1} of PLA	

4-4-10 Optical microscopy

Microcapsule dispersion before washing was dropped on a glass slide and it was then observed with an optical microscope (BX50, OLYMPUS, Japan) equipped with a digital camera (CS230, OLYMPUS, Japan). This technique was used to estimate the size and observe the morphology of the microcapsules.

4-4-11 Fluorescence microscopy

Calcein and Nile red labelled-microcapsule dispersion was dropped on a glass plate. The sample was observed by a fluorescence microscope (All-in-one type BZ-8000, Keyence, Japan) to visualize the location of the encapsulated compounds. The red fluorescence derived from Nile red was observed with a TRITC filter (OP-66837, Keyence, Japan) (excitation wave length = 540 nm and absorption wave length = 605 nm). The green fluorescence derived from calcein was observed with a GFP-BP filter (OP-66836, Keyence, Japan) (excitation wave length = 470 nm and absorption wave length = 535 nm).

4-4-12 Scanning electron microscopy

Morphology of the microcapsules after freeze-drying was observed by a scanning electron microscope (SEM, S-4700, Hitachi Ltd., Japan) at intensity of 1 kV under various magnifications. A sputter-coater (E-1030 Ion-Sputter, Hitachi Ltd., Japan) was used to coat the samples with Pd-Pt to prevent the samples from charge up. Before the observation, the freeze-dried samples were stored in a desiccator.

4-4-13 Evaluation of size distribution of the microcapsules

The particle size and the distribution on the microscopic images were evaluated with an image analysis software (Winroof, Mitanishoji Co., Ltd., Japan). In the analysis, the size distributions were expressed by a coefficient of variation (CV) value, which was defined as follows:

$$\mathrm{CV} = 100\% \times \frac{((\sum(\mathrm{d_i} - \bar{\mathrm{d}})^2/\mathrm{N})^{\frac{1}{2}}}{\bar{\mathrm{d}}}$$

where d_i is the diameter of *i*th microsphere, $\bar{d}$ is the mean average diameter, and *N* is the total number of microcapsules counted. For each calculation, 200 microcapsules in the images were counted.

4-4-14 Observation of inner water droplets ripening and formation of microcapsules during solvent diffusion

The dispersed organic phase (100 μL) and the continuous aqueous phase (1 mL) were mixed and then emulsified by hand for a few seconds to prepare O/W emulsion. The dispersed phase was an EA solution containing PLA (*M*n = 9,600, *M*w/*M*n = 1.31), PLA-*b*-PDMAEMA (*M*n = 16,200, *M*w/*M*n = 1.28) at PLA/PLA-*b*-PDMAEMA ratio = 6/4 (w/w) and a trace amount of oil-blue N. The continuous phase was 1 wt% w-PEG-*b*-PLA (*M*n = 4,400, *M*w/*M*n = 1.05, HLB = 18.2) aqueous solution saturated with EA. After emulsification, a small portion of the emulsion was placed on a glass plate and immediately covered with a thin cover slip in order to suppress evaporation of EA. The sample was set up on the stage of optical microscope. To induce solvent diffusion of EA into aqueous phase, pure water was introduced into the gap between the glass slide and the cover slip using a disposal syringe. Using an optical microscope, ripening of inner water droplets and the following microcapsule formation process were observed.

4-4-15 Evaluation of the shell structure of the microcapsules

Surface analysis of the resultant microcapsules was employed using X-ray photoelectron spectroscopy (XPS) using Magnesium Kα radiation at a potential of 10 kV and an X-ray current of 20 mA. The pressure in the measurement chamber was ca. 5 x 10^{-8} Pa. Dried microcapsules were put on a plate and stored under reduced pressure by continuous operation of an oil rotary pump just before the measurement.

4-5 Results and discussion

4-5-1 Synthesis results of PLA-*b*-PDMAEMA

Amphiphilic poly(D,L-lactide)-*b*-poly(2-dimethylaminoethyl methacrylate) (PLA-*b*-PDMAEMA) was synthesized through a three-step approach consisting of a synthesis of a bifunctional initiator, 2-hydroxyethyl 2-bromopropionate (HEBP), followed by a ring-opening polymerization of D,L-lactide initiated by the initiator to produce bromoisopropionate polylactide (PLA-Br) macroinitiator, followed by ATRP of DMAEMA initiated by PLA-Br, as shown in Figure 4-1. This synthetic process of PLA-*b*-PDMAEMA enables a fine-tuning of both block lengths of PLA and DMAEMA. Using a ring-opening polymerization of D,L-lactide can design hydrophobic PLA block length by changing the molar ratio of D,L-lactide to HEBP, whereas the following ATRP of DMAEMA can control the hydrophilic PDMAEMA block length by varying the molar ratio of DMAEMA to PLA-Br macroinitiator.

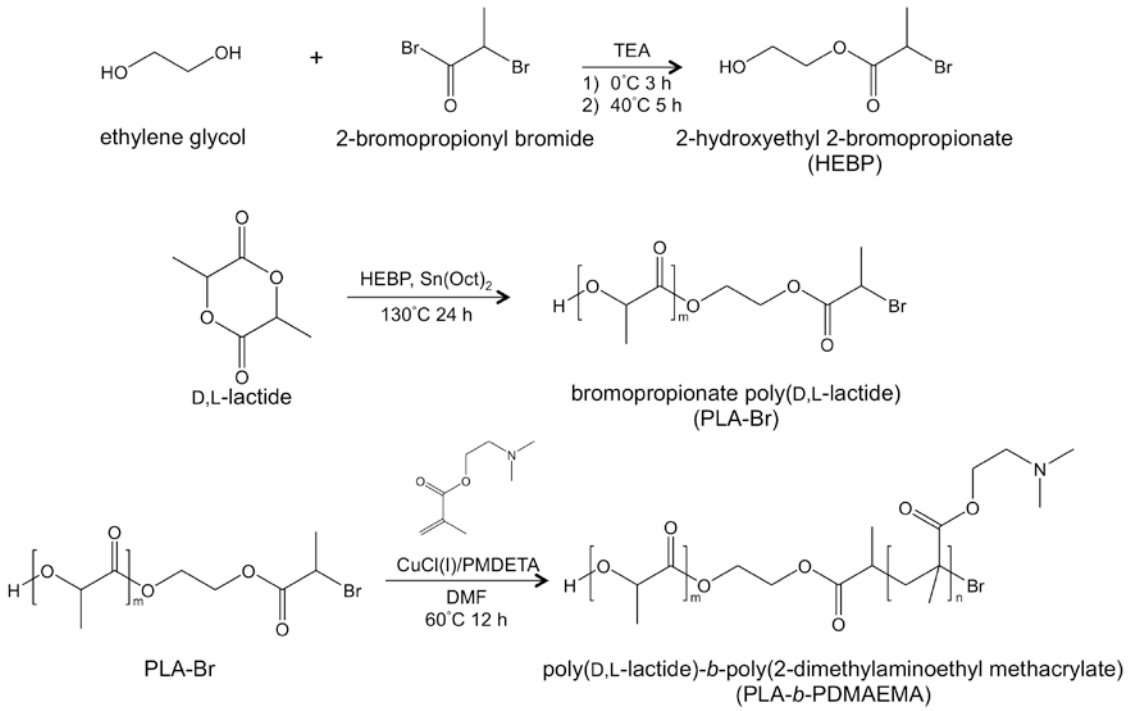

Figure 4-1 Synthetic procedure of PLA-*b*-PDMAEMA *via* three-step approach.

The first step was a synthesis of a bifunctional initiator, HEBP that has hydroxyl and bromine end groups. The hydroxyl group plays a role in an initiator of a ring-opening polymerization of D,L-lactide and the bromine works as an initiation site for ATRP in the last step. Figure 4-2 (a) shows ^{1}H NMR spectrum of the obtained HEBP. In Figure 4-2 (a), peaks of a (δ = 1.80), b (δ = 4.60), c (δ = 4.40), and d (δ = 3.90) were assigned to the methyl protons nearest bromine, the methine proton nearest bromine, the methylene protons closest to the ester bond, and the methylene protons nearest the hydroxyl termination, respectively. From the ^{1}H NMR spectrum, the synthesis of HEBP was confirmed. The product was liquid state at room temperature, which was used as a bifunctional initiator for a synthesis of PLA-*b*-PDMAEMA.

The second step was a ring-opening polymerization of D,L-lactide using HEBP as the initiator, leading to production of PLA-Br, which was used as a macroinitiator of ATRP for the third step. Similar to PLA homopolymer synthesis, the polymerization was carried out in an ampule containing D,L-lactide, the HEBP, and a trace amount of $Sn(Oct)_2$ at 130°C for 24 hours. The ^{1}H NMR spectrum of the synthesized polymer is shown in Figure 4-2 (b). The polymerization of D,L-lactide was confirmed by appearing a large peak e at 1.57 ppm for methyl protons of a lactic acid unit and a peak d at 5.15 ppm for a methine proton of a lactic acid unit. The methylene and methine peaks derived from the HEBP residue remained around 4.30-4.40 ppm with a slight peak shift, indicating that the polymerization has been initiated from the hydroxyl group of the HEBP. The *M*n of the PLA-Br reached 9,600 as determined from the spectrum by comparing the relative intensity of the methine groups of lactic acid units (δ = 5.15 ppm) and the methylene and the methine groups of HEBP (δ = 4.30-4.40 ppm), which is a bit smaller value than the theoretical molecular weight ($M\mathrm{n}_{\mathrm{theori.}}$) of the polymer, $M\mathrm{n}_{\mathrm{theori.}}$ = 12,200, estimated from the ratio of the initiator to the monomer and the molecular weight of the initiator but is close to the value, indicating that most monomer has been consumed during the polymerization. It was also confirmed that the polymerization proceeded in a controlled manner as evidenced by the narrow molecular weight distribution (*M*w/*M*n = 1.15) determined by GPC analysis.

The final step in the synthesis of the diblock copolymer was ATRP of DMAEMA using PLA-Br macroinitiator. The initial synthesis condition was $[CuCl(I)]_0/[PMDETA]_0/[PLA\text{-}Br]_0/[DMAEMA]_0$ = 1/1/1/39. The polymerization was carried out in DMF at 60°C in the presence of CuCl/PMDETA catalytic system under

argon atmosphere with Schlenk apparatus. After 12 h, the polymerization was stopped by introducing air in the Schlenk, followed by cooling the reaction mixture and diluting with an excess volume of THF. The product was recovered by precipitation in *n*-hexane after removal of CuCl(I) through an activated neutral alumina. The polymerization was confirmed from ^{1}H NMR spectrum, as described in Figure 4-2 (c). The polymerization degree of PDMAEMA block was calculated from the relative intensities of the amino methylene protons of DMAEMA residue from repeating units (δ = 2.30 ppm) and the methine protons of PLA (δ = 5.15 ppm) whose polymerization degree has already been determined from the spectrum of PLA-Br. The calculated polymerization degree of PDMAEMA was 42 units. The number was a bit bigger than the theoretical one, 39 units, calculated from the initial ratio of $[DMAEMA]_0$ to $[PLA\text{-}Br]_0$, however, it was very close value. The GPC measurement showed a narrow molecular weight distribution (the Mw/Mn = 1.28). Thus, the initiation efficiency of PLA-Br was quite high and the polymerization of DMAEMA initiated by PLA-Br also proceeded in a controlled manner. The overall molecular weight of PLA-*b*-PDMAEMA was about 15,900, including 9,600 for a hydrophobic PLA block and 6,300 for a hydrophilic PDMAEMA block. From the solubility test, it was found that the polymer was soluble in chloroform, THF, and EA, but the solubility in EA was not so good (the saturated concentration was about 10 mg mL^{-1}). PLA-*b*-PDMAEMA was used as a co-surfactant and a shell-forming compound in this system, as described in the following sections.

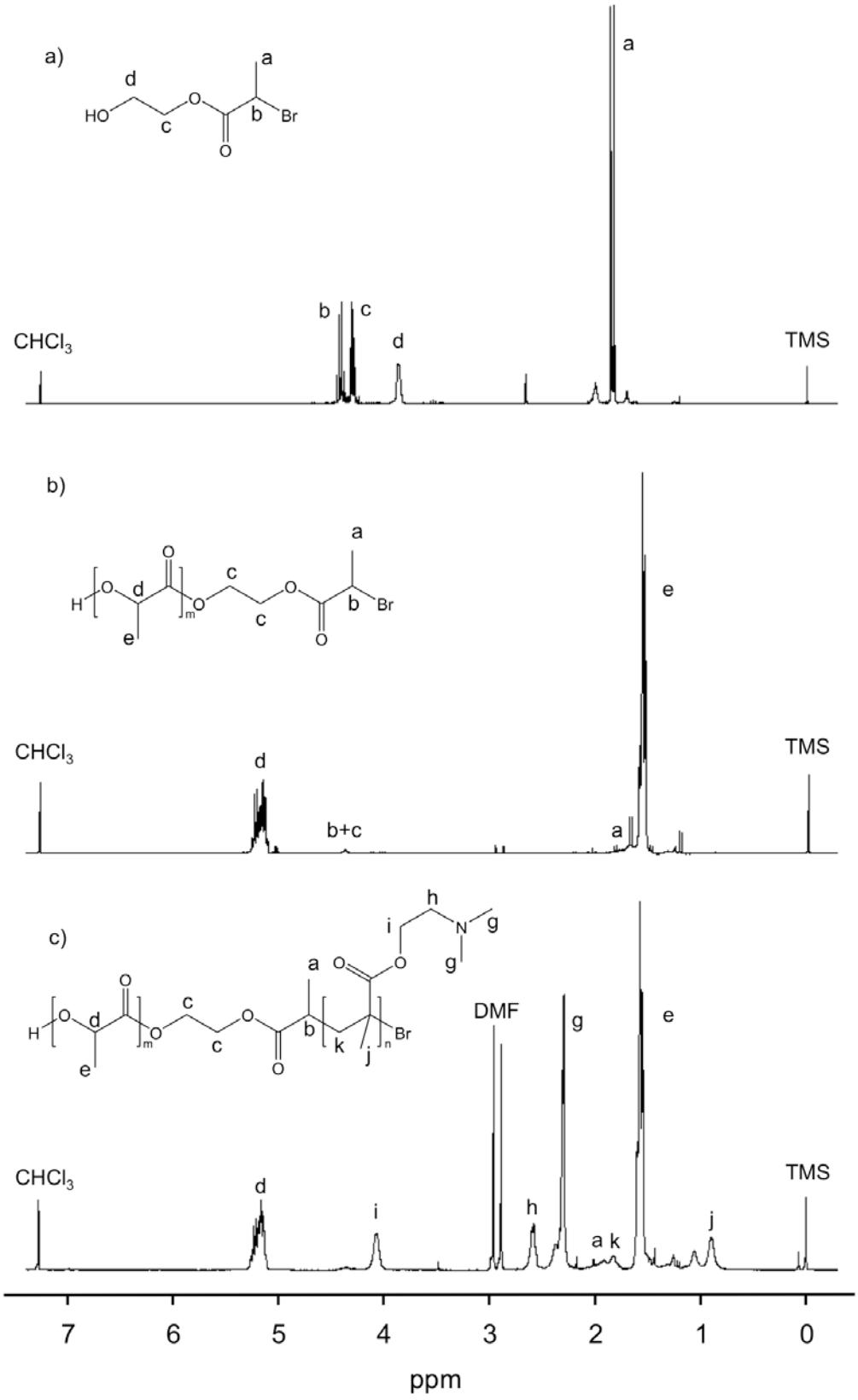

Figure 4-2 ^{1}H NMR spectra of (a) HEBP, (b) PLA-Br, and (c) PLA-*b*-PDMAEMA in $CHCl_3$-*d*.

4-5-2 Interfacial activity of oil-soluble PLA-*b*-PDMAEMA between EA and water saturated with EA

Interfacial activity of synthesized oil-soluble PLA-*b*-PDMAEMA between EA and water saturated with EA has been investigated. The copolymer was dissolved in EA and the interfacial tension was measured by varying the concentration of PLA-*b*-PDMAEMA in EA. Figure 4-3 depicts the interfacial tensions as a function of the copolymer concentration at 20°C. The graph represents that the interfacial tension dramatically decreases with an increase of the copolymer concentration and it reaches a constant value at the concentration around 0.01 wt%. From the figure, the CMC was determined at 0.004 wt%. It should be noted that the interfacial tension value in this system above the CMC is quite low less than 1 mN m^{-1}, which is out of detection threshold using the equipment. Therefore, the CMC determined here is just as reference. However, the results obviously revealed that oil-soluble PLA-*b*-PDMAEMA has a strong surface activity between EA and water saturated with EA.

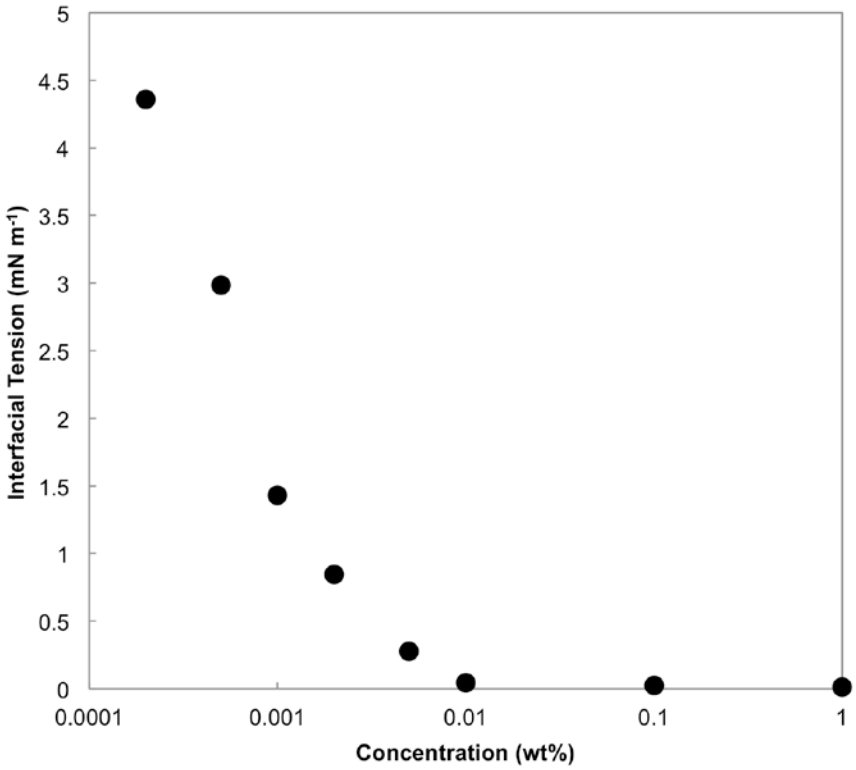

Figure 4-3 Interfacial tensions between EA and water saturated with EA as a function of concentration of oil-soluble PLA-*b*-PDMAEMA. The experiment was carried out using a Wilhelmy plate method at 20°C.

4-5-3 Water extraction behaviour of oil-soluble PLA-*b*-PDMAEMA in the organic phase

Similar to PEG-*b*-PLA, PLA-*b*-PDMAEMA is an amphiphilic copolymer, with a hydrophobic PLA block and a hydrophilic PDMAEMA block. Judging from solubility of each block, oil-soluble PLA-*b*-PDMAEMA molecules in EA form reverse micelles at the concentration above the CMC. So, it is expected that when preparing O/W emulsion in which the dispersed organic phase contains enough amount of oil-soluble PLA-*b*-PDMAEMA, the diblock copolymer would facilitate water-uptake from the continuous aqueous phase into emulsion droplets *via* spontaneous emulsification mechanism in order to form microemulsion. In other words, the copolymer extracts water from the continuous phase through the interface. From the speculation, the water extraction behaviour of the copolymer in the organic phase was investigated by shaking the emulsion systems for 24 hours. Figure 4-4 shows photographs of the O/W two-phase systems in which each dispersed organic phase has different components (**Table 4-1**). Because of low density of EA, the upper phases in Figure 4-4 represent the organic phase and the lower phases are the continuous aqueous phase dyed with Reactive blue. The dispersed phases of Sample 1 and 3 in Figure 4-4 are pure EA and an EA solution dissolving 6 mg mL^{-1} of PLA, respectively. It was found that both samples did not show any changes in colour after shaking for 24 hours, indicating that there was no obvious interfacial transport phenomenon and EA and PLA homopolymer could not extract the water partition from the continuous phase. On the contrary, the other two samples containing only PLA-*b*-PDMAEMA or both PLA-*b*-PDMAEMA and PLA showed change in the colour from transparent to light blue. These results indicate that PLA-*b*-PDMAEMA has extraction ability of aqueous phase.

It can be easily imagined that the water phases extracted into the dispersed phase after shaking disperse as a small droplet and are stabilized by amphiphilic PLA-*b*-PDMAEMA molecules, meaning that it will be possible to measure the diameter by dynamic light scattering (DLS). Therefore, DLS measurements of the organic phases after shaking for 24 hours about 3 samples (2, 3, and 4 in Figure 4-4) were employed. It was found that there was no peak in the dispersed phase of sample 3 but there were broad peaks in that of sample 2 and 4. No peak in sample 3 means that there is no extracted water droplet in the dispersed phase, supporting the photograph in Figure 4-4. The mean diameters of water droplets in sample 2 and 4 were 226.3 nm and 381.5 nm,

with polydisperse size distribution (PDI > 0.3), respectively (**Table 4-2**). These results revealed that the dispersed phases dissolving the diblock copolymer possessed tiny water droplets, although the sizes were polydisperse. It is also considered that the water droplets would be stabilized by the diblock copolymer.

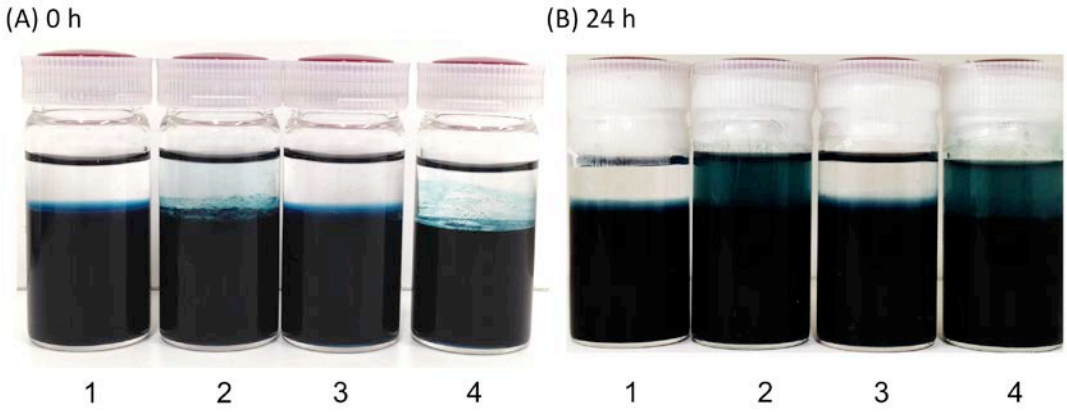

Figure 4-4 Photographs of two-phase systems consisting of organic phase and aqueous phase before and after shaking at 100 rpm for 24 hours. PLA (*M*n = 7,300, *M*w/*M*n = 1.31) and PLA-*b*-PDMAEMA (*M*n = 18,200, *M*w/*M*n = 1.46, HLB = 7.0) were used in the preparation.

Table 4-2 Summary of DLS measurements of the dispersed phase after shaking for 24 hours.

Entry	Dispersed phase	Ave. diameter (nm)	PDI
2	EA+4 mg mL^{-1} of PLA-*b*-PDMAEMA	226.3±1.3	0.34±0.01
3	EA+6 mg mL^{-1} of PLA	–	–
4	EA+4 mg mL^{-1} of PLA-*b*-PDMAEMA+6 mg mL^{-1} of PLA	381.5±2.0	0.36±0.02

4-5-4 Time course of microcapsule formation *via* spontaneous emulsification

In this study, a simple process for monodisperse PLA microcapsules with a single aqueous core through one-step emulsification was developed and the effects of preparation parameters on the microcapsule formation were investigated. This microcapsule formation process is based on microfluidic emulsification, followed by spontaneous emulsification and solvent diffusion, which includes W/O/W emulsion formation from O/W emulsion, induced by water uptake from the continuous phase *via* PLA-*b*-PDMAEMA. Herein, the effect of adding PLA-*b*-PDMAEMA to the dispersed phase on final structures of the microparticles was investigated. It should be noted that because of high volatility of EA and quick diffusion of EA into the aqueous phase within a few seconds, it was difficult to observe the ripening process using the microfluidic approach *in situ*. Therefore, instead of this, the monitoring was carried out on a glass slide covered with a thin cover slip using the model emulsion prepared by hand shaking. The dispersed organic phase was an EA solution dissolving PLA and PLA-*b*-PDMAEMA. The continuous aqueous phase was 1 wt% of w-PEG-*b*-PLA aqueous solution saturated with EA. Prior to the emulsification, a trace amount of Oil blue N was added to the dispersed phase in order to improve visibility of the phase. These solutions were transferred into a vial and then emulsified by shaking by hand. The portion of the resultant O/W emulsion was dropped onto a normal glass slide and subsequently covered with a cover slip to suppress evaporation of EA. Then a small volume of water was dropped adjacent to the cover ship on the glass slide, which was spread beneath the cover slip *via* capillary phenomenon. Due to high solubility of EA in water, EA diffused into the continuous aqueous phase, leading to the droplets to shrink and the concentration of polymers within each droplet to increase. Figure 4-5 shows optical microphotographs of transition from the emulsion to the microcapsules during solvent diffusion. In Figure 4-5 (a), it was found that small water droplets were observed within the emulsion droplets dyed blue even before the solvent diffusion, which indicates that the emulsion droplets extract water from the continuous phase on the emulsification. After diluting the emulsion by adding water, the emulsion droplets size gradually decreased and the tiny water droplets became bigger by coalescence, resulting in forming a single aqueous core within the emulsion droplets (Figure 4-5 (b-e)). Thereafter, further extraction of EA led to precipitating polymer from the

interface between outer aqueous phase and the emulsion droplets, yielding in the microcapsule with a single aqueous core (Figure 4-5 (f)). The series of the microcapsule formation process have completed within only a few seconds after dilution of the initial emulsion solution with pure water, which means that this proposed system has a potential to shortening fabrication time for the microcapsule, compared with the conventional emulsion-solvent evaporation technique that requires several tens minutes to hours to precipitate the polymer after the precursor emulsion preparation. From the result, it was found that it was possible to prepare double emulsion *via* one-step emulsification.

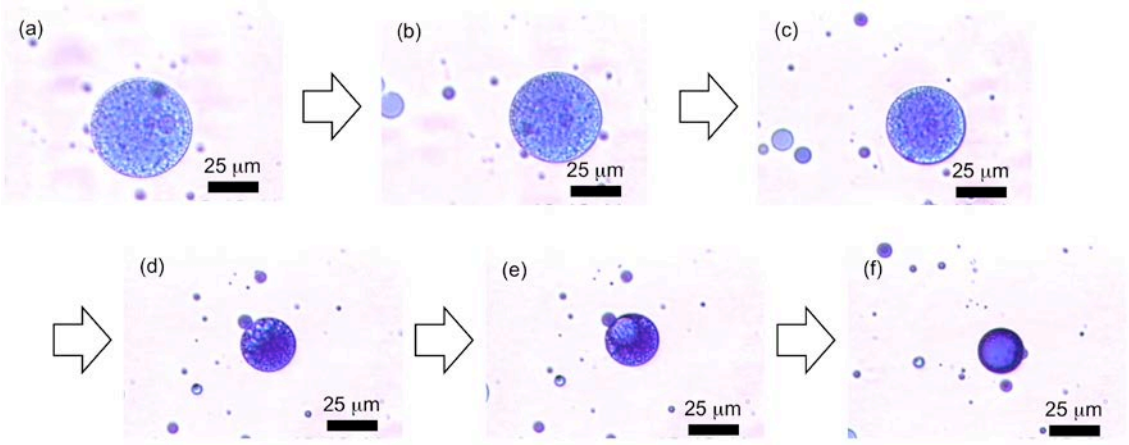

Figure 4-5 Optical micrographs of inner water droplets ripening, followed by formation of microcapsules during EA diffusion into the continuous phase. (a) Polydisperse model emulsion droplets after emulsification by shake by hand. The organic phase (blue region) already had many small water droplets (white dots). (b-e) After introduction of small amount of pure water from the left side of the image, rapid reduction of organic phase in size and evolution of inner water droplets were observed. (f) Microcapsule with a single aqueous core was eventually formed.

4-5-5 Effect of blend ratio of PLA to PLA-*b*-PDMAEMA on microcapsule structures

This process has been applied to the microfluidic approach so as to fabricate monodisperse emulsion droplets and the resultant monodisperse microcapsules. The dispersed organic phase and the continuous aqueous phase were pumped separately into the Y-shaped microfluidic device using syringe pumps to form precision polymer

droplets at the Y-junction. Thereafter, the O/W emulsion droplets travelled towards the downstream and were eventually transferred into a precipitation bath filled with excess volume of ultrapure water without stirring, where the polymer precipitation occurred. The effect of PLA to PLA-*b*-PDMAEMA ratio in the dispersed phase on final structures of the microcapsules was investigated. The monodisperse emulsion droplets were observed inside the Teflon tubing independent of the polymer compositions in the dispersed phase, as described in Figure 4-6. However, it was impossible to confirm the internal structure of the emulsion droplets from the image due to the low resolution.

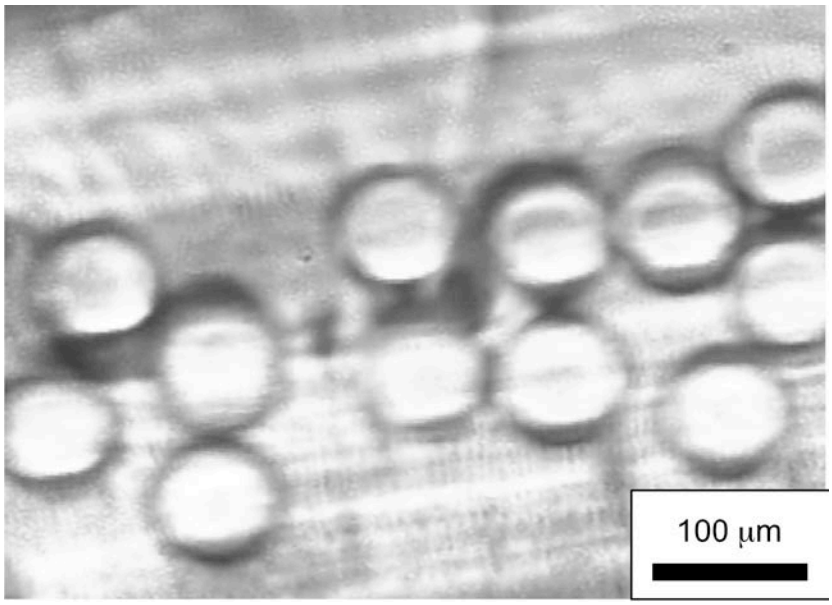

Figure 4-6 A representative optical microscopic image of monodisperse oil droplets dispersed in the aqueous phase before solvent diffusion, captured in the Teflon tube connected from the outlet of the microfluidic device to the vessel containing water for solvent diffusion. The dispersed phase were EA solution dissolving 6 mg mL^{-1} of PLA and 4 mg mL^{-1} of PLA-*b*-PDMAEMA. The continuous phase was an aqueous solution saturated with EA containing 1 wt% of w-PEG-*b*-PLA The flow rates were Q_d = 2 μL min^{-1}, Q_c = 50 μL min^{-1}.

Figure 4-7 shows optical micrographs of the resultant microcapsules after solvent diffusion prepared by changing the homopolymer to the diblock copolymer ratios. In the absent of PLA-*b*-PDMAEMA, monodisperse microspheres with a compact internal structure were obtained as shown in Figure 4-7 (a). With PLA/PLA-*b*-PDMAEMA at

9/1 (w/w), monodisperse microcapsules with dark contrast against the continuous phase were obtained (Figure. 4-7 (b)). The dark contrast means that there are many cores inside the microcapsules. In addition, the microcapsules had bigger diameter even though the preparation condition was the same except for the dispersed phase composition in comparison to the case of PLA microspheres, supporting that the microcapsules extracted water from the outer aqueous phase during the preparation process. With an increase of the ratio to 6/4 (w/w), it was found that almost all the microcapsules had a single aqueous core, as depicted in Figure 4-7 (c). The trend was seen that the microcapsule diameter increased with the increment of the block copolymer portion in the dispersed phase. From these results, it was found that adding PLA-*b*-PDMAEMA to the dispersed phase played an important role to induce transition of O/W emulsion to W/O/W emulsion by spontaneous emulsification. The internal structure of the microcapsules changed from a compact structure, a multi-core structure to a single core structure as increasing with the fraction of PLA-*b*-PDMAEMA in the dispersed phase.

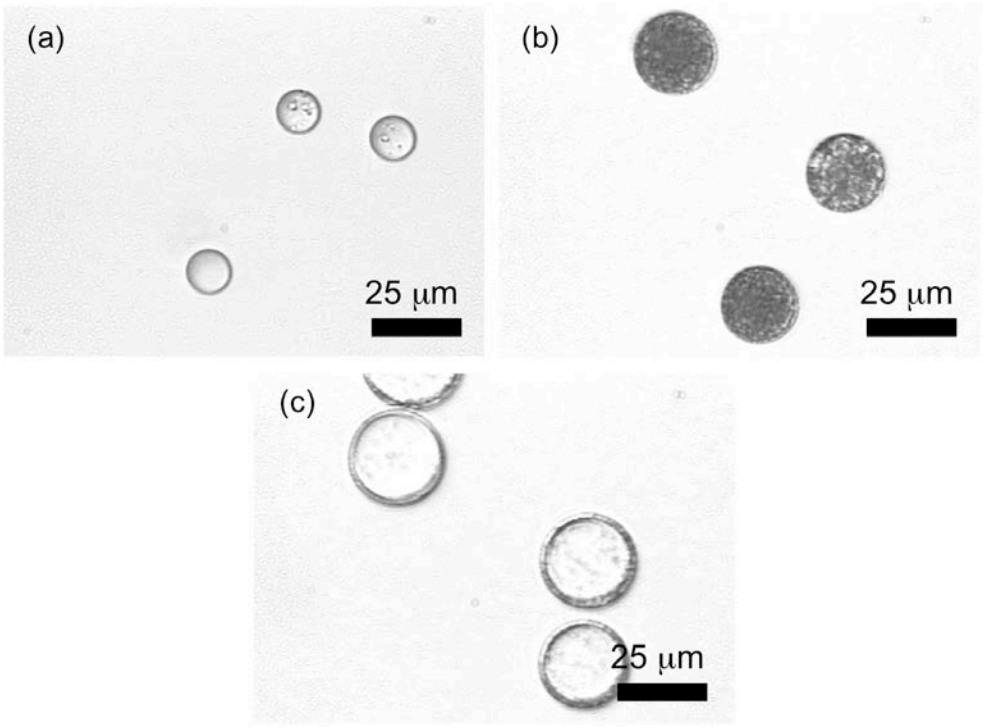

Figure 4-7 Optical microphotographs of monodisperse microcapsules prepared by varying the blend ratio of PLA/PLA-*b*-PDMAEMA. The ratio was (a) 10/0, (b) 9/1 and (c) 6/4 (w/w).

4-5-6 Effect of flow rate on the diameter of the microcapsules

Using the blend ratio at 6/4 (w/w), the microcapsules were prepared by changing the flow rate of the continuous phase (Q_c) whilst maintaining that of the dispersed phase (Q_d) constant. Figure 4-8 describes the change of diameter of the microcapsules and the CV value as a function of the flow rate of Q_c. The diameter of the microcapsules decreased from 32.6 to 10.3 μm with increasing the Q_c, which is the same trend as the previous studies on the microparticle fabrication. It was also found that the CV values were increased as an increment of the Q_c. Probably, this would be due to unstable emulsification in the microfluidic device upon higher Q_c. However, the CV values were kept at less than 10% regardless of the flow conditions, which indicated that the microcapsules had a relatively narrow size distribution.

Figure 4-9 shows optical microphotographs and SEM images of the microcapsules prepared by varying the flow rate of Q_c upon emulsification. The optical micrographs of the microcapsules have clearly proven the fact that the microcapsules have a single aqueous core in different to the microcapsules size, as shown in Figure 4-9 (a1-d1). For the SEM observation, it was found that most of the microcapsules were not collapsed even under a high vacuum condition during the observation. The cross sectional views of the microcapsules also revealed that interior of the shell of the microcapsules was a bit porous although the surface of the microcapsules was smooth regardless of the preparation condition, as shown in Figure 4-9 (a3-d3). This difference would be caused by too fast precipitation of the polymer during solvent diffusion. The microcapsule formation would involve coalescence of inner water droplets entrapped by spontaneous emulsification during solvent diffusion process. The rapid solidification of the droplets induced by EA extraction into the precipitation bath facilitates the polymer precipitation under the non-equilibrium configuration that has tiny water droplets before coalescence within the polymer droplet. The remaining small water droplets within the polymer matrix must be the origin of the porous in the shell of the microcapsules.

These results indicate that this system can tune microcapsule size in a controlled manner. In addition, it was found that the flow rates did not affect the morphology of the microcapsules. It is also important to note that with conventional techniques using microfluidics, it is almost impossible to prepare monodisperse microcapsules with smaller than 30 μm in the diameter since the microcapsule size is largely dependent on the size of the initial W/O emulsion droplets. From the point of view of the

microcapsules size, this proposed system would be a breakthrough to prepare single micron-sized or submicron-sized microcapsules by changing the microfluidic dimensions or the emulsion preparation conditions.

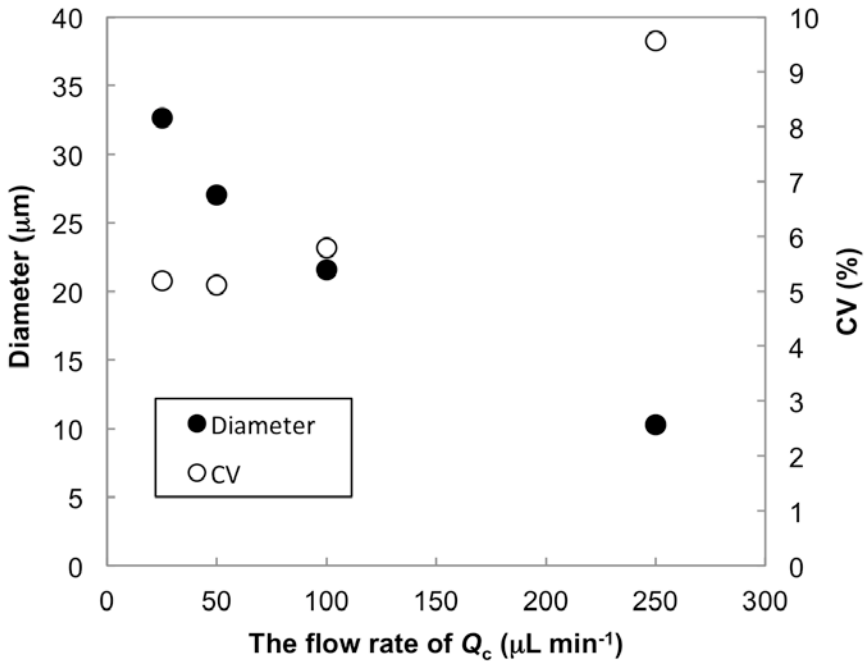

Figure 4-8 Effect of the Q_c on the diameter of the microcapsules and the CV value. The Q_c was (a) 25, (b) 50, (c) 100, and (d) 250 μL min^{-1}. The Q_d was kept at 2 μL min^{-1}.

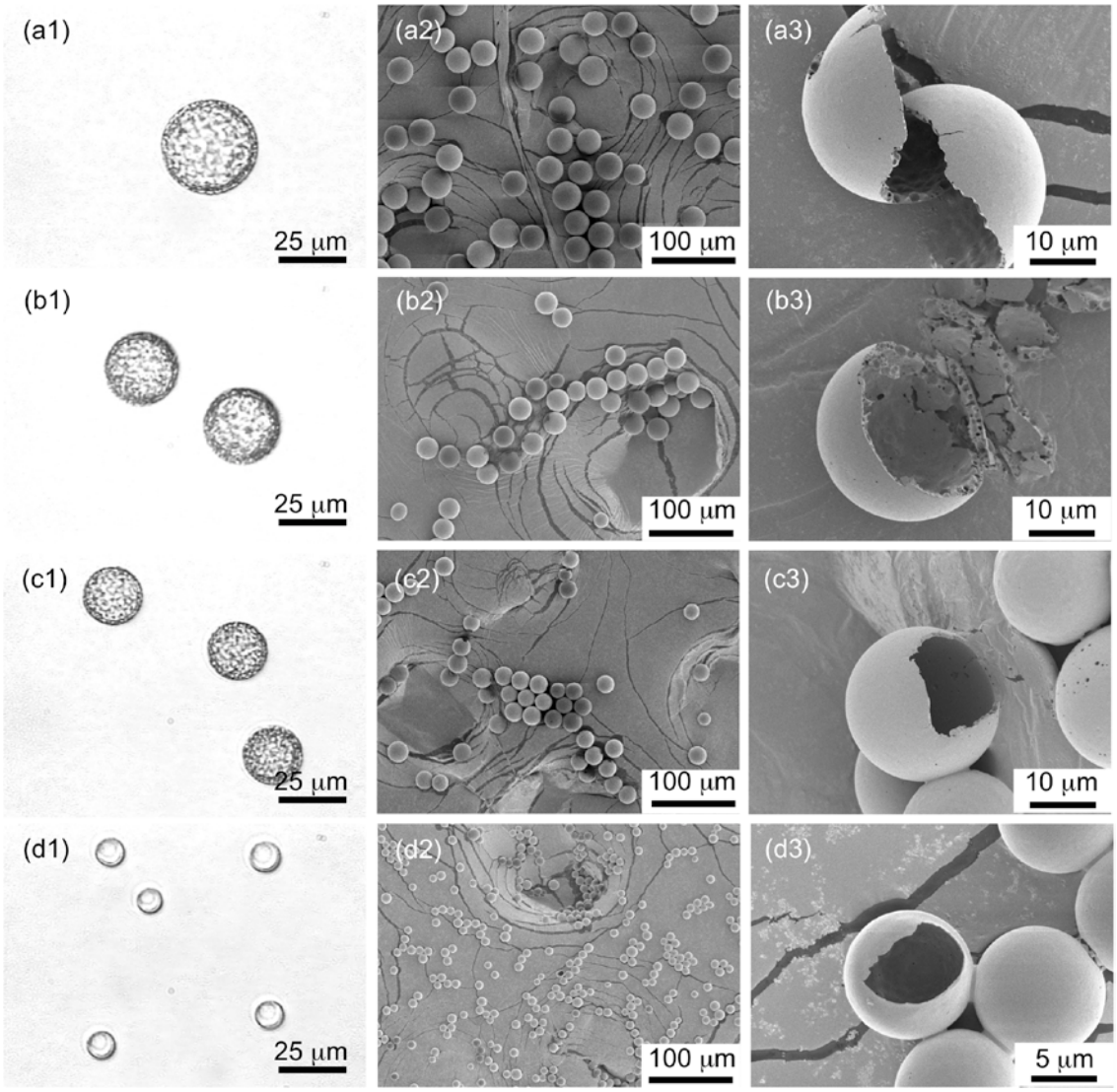

Figure 4-9 (a1-d1) Optical microscopic images and (a2-d2 and a3-d3) SEM images of microcapsules prepared by changing the flow rate of the Q_c. The Q_c was (a1-a3) 25, (b1-b3) 50, (c1-c3) 100, and (d1-d3) 250 μL min^{-1}. The Q_d was kept at 2 μL min^{-1}.

4-5-7 Effect of molecular weight of PLA homopolymer on the structure of the microcapsules

The effect of PLA molecular weight on the microcapsule structure was investigated. Figure 4-10 shows the microcapsules prepared using PLA with higher molecular weight (*M*n = 52,000, *M*w/*M*n = 1.29). From the optical microphotograph of the microcapsules after solvent diffusion shown in Figure 4-10 (a), monodisperse microcapsules with a single aqueous core were obtained, which is evidence that this system can be applied to PLA with different molecular weight at least in a range from 7,200 to 52,000 in the *M*n. It is interesting to note that when using PLA (*M*n = 52,000), the microcapsules deformed during drying process, leading to collapsed microcapsules that was not seen in the case using PLA (*M*n = 7,200) as shown in Figure 4-10 (b and c). Understanding the origin of the morphology difference, the time course of drying of the microcapsules dispersed in water was monitored on the stage of the optical microscope.

Figure 4-11 shows the time course of drying of the microcapsules prepared using different molecular weight of PLA and the same PLA-*b*-PDMAEMA. As shown in the arrow in Figure 4-11A, the morphology of the microcapsules prepared with PLA (*M*n = 7,200) did not change in the whole of the drying process, which just lost the water inside the microcapsules during the process. On the other hand, the morphological change in the microcapsules prepared with PLA (*M*n = 52,000) was observed during the drying, illustrating in Figure 4-11B. At the beginning of the drying, the continuous phase (water) in the system evaporated as shown in Figure 4-11B (a). Then, water inside the microcapsules started to evaporate accompanied with deformation of the microcapsules (Figure 4-11B (b)). The volume of the microcapsules declined as the inner water evaporated (Figure 4-11B (c-e)). As long as the water exists within the microcapsules, the deformation process continued. After complete evaporation of the inner water, the morphology change stopped (Figure 4-11B (f)). It was found that the morphology change was not reversible process, which means that the deformed microcapsules has never returned to the original spherical morphology even when the deformed microcapsules is re-dispersed in aqueous dispersant, although the inner vacant space of the microcapsules could be readily re-filled with water. From these results, it was revealed that the deformation of the microcapsules occurred not during SEM observation, but during the drying process after washing process. This deference may arise from the compactness of the shell structure. In the case using PLA (*M*n = 7,200),

the formed shell of the microcapsules does not have a rigid structure, which allows gas to go through the shell easily. On the contrary, when using PLA (*M*n = 52,000), the shell would possess a more compact structure and suppress the transport phenomena between the inner and the external aqueous phase. As the internal aqueous phase starts to evaporate from the microcapsules, in general, gas transportation from the external phase to the inner phase occurs in order to accommodate the volume reduction, however the gas transport would be restricted due to the rigid interfacial barrier, thus instead of this, the microcapsule would change the structure.

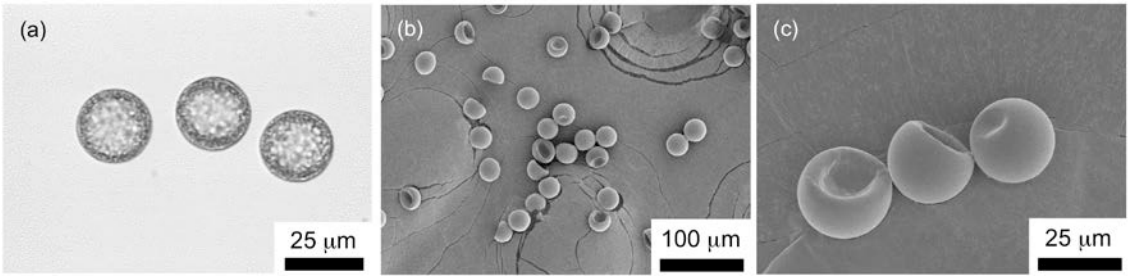

Figure 4-10 An optical microphotograph and SEM images of microcapsules prepared using relatively higher molecular weight PLA (*M*n = 52,000, *M*w/*M*n = 1.29) and PLA-*b*-PDMAEMA.

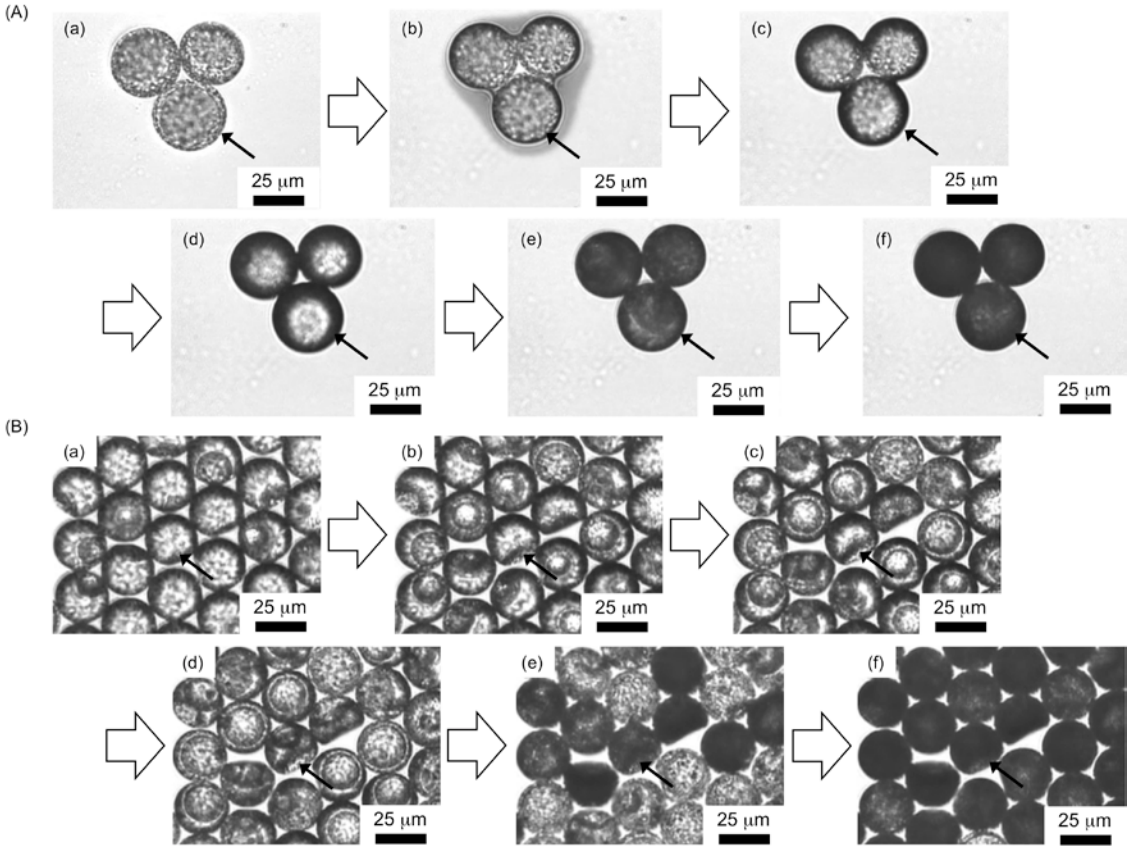

Figure 4-11 Time course of change of microcapsule structure during drying at room temperature. The microcapsules were fabricated using PLA with different molecular weights: (*M*n = (A) 7,200, (B) 52,000) and the same PLA-*b*-PDMAEMA. The blend ratio of PLA/PLA-*b*-PDMAEMA was fixed at 6/4 (w/w).

4-5-8 Encapsulation of both hydrophobic and hydrophilic compounds in the microcapsules using spontaneous emulsification

It was investigated whether the microcapsules encapsulated both a hydrophilic compound and a hydrophobic compound. In this experiment, “calcein” was dissolved in the continuous phase as a model hydrophilic compound. In addition, a model hydrophobic compound “Nile red” was dissolved in the dispersed phase. In this system, calcein must be encapsulated within the microcapsules through spontaneous emulsification after formation of O/W emulsion upon microfluidic emulsification. Figure 4-12 shows the fluorescence microphotographs of the resultant microcapsules after solvent diffusion, followed by washing with pure water to remove the unloaded calcein from the system. The core of the microcapsules clearly displayed green fluorescence derived from calcein, which indicates that in this system, the water-uptake from the continuous phase would occur during which the polymer droplets travel towards the downstream in the Teflon tubing as depicted in Figure 4-12 (b). The shell of the microcapsules showed red fluorescence attributing to Nile red, which indicates that hydrophobic substances dissolved in the dispersed phase can be easily entrapped within the shell of the microcapsules (Figure 4-12 (c)). From these results, this microcapsule formation technique is a promising way for dual encapsulation of a hydrophobic compound and a hydrophilic compound, as shown in Figure 4-12 (d, e).

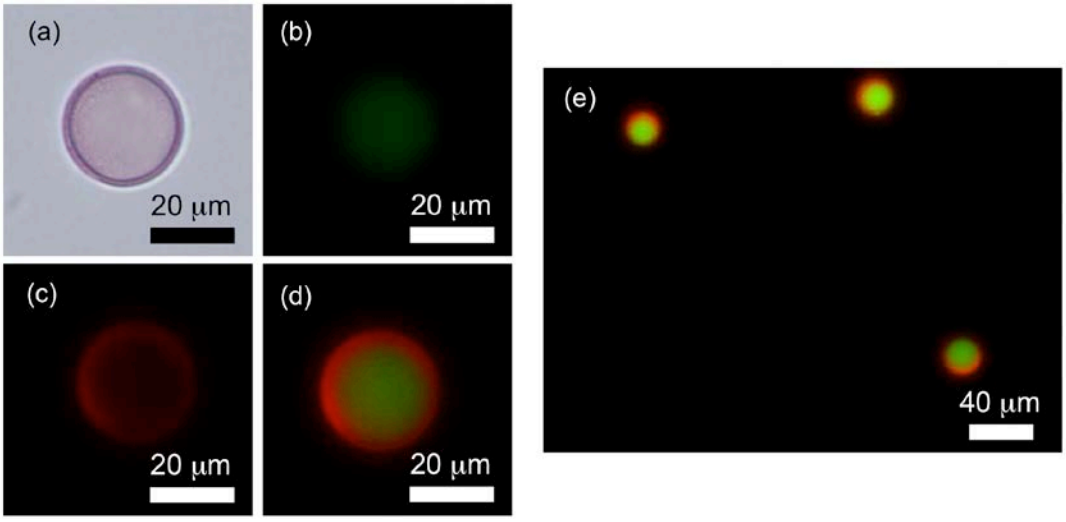

Figure 4-12 Fluorescence microphotographs of the microcapsules encapsulating calcein in the core and Nile red in the shell. (a) Bright image, (b) Green fluorescence filtered image, (c) Red fluorescence filtered image, (e) Low magnification overlay image of (b), (c), and (d).

4-5-9 Investigation of the shell structure of the microcapsules

Figure 4-13 shows XPS spectra of (a) the microcapsules consisting of PLA and PLA-*b*-PDMAEMA and (b) the microparticles composed of PLA. XPS is a surface chemical analysis technique that can be utilized to analyse the surface chemistry of materials. As shown in Figure 4-13 (a), the spectrum obviously describes a peak derived from bonding energy of N_{1s}, suggesting that there are amine groups of PDMAEMA block on the surface of the microcapsules. On the other hand, no peak was detected on the surface of PLA microparticles, as shown in Figure 4-13 (b). These results are a clue that PLA-*b*-PDMAEMA plays a role in a co-surfactant as well as a surface modifying reagent and this proposed process enables to tailor the surface property of the microcapsules during the formulation.

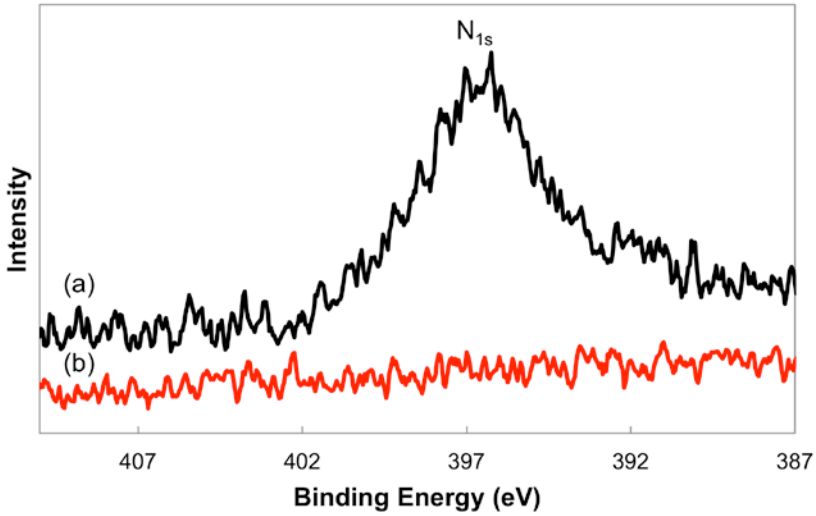

Figure 4-13 XPS spectra of microcapsules consisting of (a) PLA and PLA-*b*-PDMAEMA at (6/4, w/w) and microparticles composed of (b) PLA.

4-5-10 Proposed formation mechanism of microcapsules by spontaneous emulsification

Taking the above results into account, the microcapsule formation mechanism has been proposed. First, monodisperse O/W emulsion whose interface is stabilized by w-PEG-*b*-PLA is produced at the Y junction in the microfluidic device (Figure 4-14 (i)). Then, water molecule in the continuous phase is extracted to the emulsion droplets through the O/W emulsion interface during travelling towards the downstream of the microfluidics to form tiny water droplets stabilized by amphiphilic PLA-*b*-PDMAEMA molecules dissolved in the emulsion droplets (microemulsion) since PLA-*b*-PDMAEMA can dissolve in EA as a reverse micelle structure with PDMAEMA core and PLA shell so as to minimize the interfacial energy and the hydrophilic PDMAEMA core region of the reverse micelles is capable of entrapping aqueous molecules (in Figure 4-14 (ii)). After that, when the emulsion droplets enter into the precipitation bath filled with a great amount of pure water, EA diffusion from each emulsion droplet to the surrounding aqueous phase quickly occur due to its high solubility in water (8.7%, w/w at 20°C), which leads to the volume reduction of the emulsion droplets and the increase of polymer (PLA and PLA-*b*-PDMAEMA) concentrations within each droplet. Simultaneously, the increase in PLA-*b*-PDMAEMA concentration within EA droplets gives rise to microemulsion instability because of its low solubility in EA, facilitating coalescence of inner water droplets within each EA droplet, as shown in Figure 4-14 (iii). Further evolution of the inner water droplets results in bigger ones, and eventually forms double emulsion, as shown in Figure 4-14 (iv). Continuous diffusion of EA into the outer aqueous phase leads to precipitating polymers from the interface between the emulsion droplets and the continuous phase, thereby yielding in monodisperse microcapsules with a single aqueous core (Figure 4-14 (v)). Due to rapid diffusion of EA in the precipitation bath, the transition from the emulsion to the solid microcapsules has completed within a few seconds, which is a suitable for continuous production of the microcapsules.

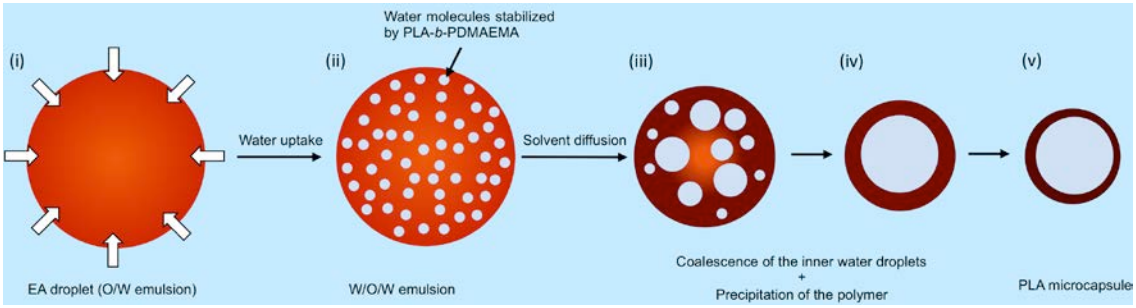

Figure 4-14 Proposed microcapsule formation mechanism using spontaneous emulsification and solvent diffusion. (i) EA droplets dissolving PLA and PLA-*b*-PDMAEMA are produced by emulsified with 1 wt% of w-PEG-*b*-PLA aqueous solution saturated with EA using microfluidic emulsification. (ii) While the emulsion droplets flow towards the downstream of the microchannel, water molecules are extracted from the continuous phase to the core of reverse micelles formed by PLA-*b*-PDMAEMA in the emulsion droplet. (iii) When the emulsion solution is transferred into excess volume of pure water, the concentration of PLA-*b*-PDMAEMA in the emulsion droplets starts to increase with decreasing the volume of the droplets induced by solvent diffusion of EA, leading to the coalescence of the tiny water droplets within the emulsion droplets because of precipitating the polymers. (iv) As a result of the coalescence, the emulsion droplets with a single aqueous core are formed. (v) The microcapsules are obtained after complete diffusion of EA into the external aqueous phase.

4-6 Conclusions

A simple process for fabricating monodisperse PLA microcapsules with a single aqueous core through spontaneous emulsification and solvent diffusion, coupled with a microfluidic approach has been elaborated. This process does not require any complex fluids operations. It was found that adding PLA-*b*-PDMAEMA to the dispersed phase was an essential element to induce water molecules extraction from the continuous phase to the polymer droplets and to form W/O/W double emulsion *via* one-step emulsification. The size of the microcapsules was readily tuned by the flow conditions on the emulsion preparation, resulting in monodisperse microcapsules with 10 to 33 μm in the diameter. In addition, the microcapsules could be fabricated using PLA with different molecular weights without any change in the preparation conditions. The fluorescence microscopy observation showed the microcapsules were capable of

encapsulating both hydrophobic and hydrophilic compounds in a single step. Surface chemical analysis based on XPS revealed that the surface of the microcapsules had amine groups derived from PDMAEMA block of the diblock copolymer. It was also found that the water-uptake from the continuous phase would occur when the emulsion was flowing in the Teflon tubing before entering in the precipitation bath. This facile preparation method for monodisperse microcapsules has great potential for producing polymeric microcapsules applied to biomedical applications.

References

1. Kim, S. H.; Kim, J. W.; Kim, D. H.; Han, S. H.; Weitz, D. A. Polymersomes containing a hydrogel network for high stability and controlled release. *Small* **2013,** *9* (1), 124-131.
2. Kim, B.; Soo Lee, H.; Kim, J.; Kim, S. H. Microfluidic fabrication of photo-responsive hydrogel capsules. *Chem. Commun. (Camb.)* **2013,** *49* (18), 1865-1867.
3. Li, W.; Matyjaszewski, K.; Albrecht, K.; Möller, M. Reactive Surfactants for Polymeric Nanocapsules via Interfacially Confined Miniemulsion ATRP. *Macromolecules* **2009,** *42* (21), 8228-8233.
4. Kondo, K.; Kida, T.; Ogawa, Y.; Arikawa, Y.; Akashi, M. Nanotube Formation through the Continuous One-Dimensional Fusion of Hollow Nanocapsules Composed of Layer-by-Layer Poly(lactic acid) Stereocomplex Films. *J. Am. Chem. Soc.* **2010,** *132* (24), 8236-8237.
5. Khopade, A. J.; Caruso, F. Two-Component, Ultrathin Microcapsules Prepared by a Core-Mediated Layer-by-Layer Approach. *Chem. Mater.* **2004,** *16* (11), 2107-2112.
6. Zhang, J.; Coulston, R. J.; Jones, S. T.; Geng, J.; Scherman, O. A.; Abell, C. One-step fabrication of supramolecular microcapsules from microfluidic droplets. *Science* **2012,** *335* (6069), 690-694.
7. Serra, C. A.; Cortese, B.; Khan, I. U.; Anton, N.; de Croon, M. H.; Hessel, V.; Ono, T.; Vandamme, T. Coupling microreaction technologies, polymer chemistry, and processing to produce polymeric micro and nanoparticles with controlled size, morphology, and composition. *Macromolecular Reaction Engineering* **2013,** *7* (9),

414-439.

8. Ma, Z.; Jia, X.; Hu, J.; Zhang, G.; Zhou, F.; Liu, Z.; Wang, H. Dual-responsive capsules with tunable low critical solution temperatures and their loading and release behavior. *Langmuir* **2013,** *29* (19), 5631-5637.

9. Nisisako, T.; Torii, T.; Higuchi, T. Novel microreactors for functional polymer beads. *Chem. Eng. J.* **2004,** *101* (1-3), 23-29.

10. Miller, C. A. Spontaneous Emulsification Produced by Diffusion — A Review. *Colloids and Surfaces* **1988,** *29* (1), 89-102.

11. Martin, C. A.; Magid, L. J. Carbon-13 NMR investigations of Aerosol OT water/oil microemulsions. *The Journal of Physical Chemistry* **1981,** *85* (25), 3938-3944.

12. Zhu, J.; Ferrer, N.; Hayward, R. C. Tuning the assembly of amphiphilic block copolymers through instabilities of solvent/water interfaces in the presence of aqueous surfactants. *Soft Matter* **2009,** *5* (12), 2471-2478.

13. Zhu, J.; Hayward, R. C. Interfacial tension of evaporating emulsion droplets containing amphiphilic block copolymers: effects of solvent and polymer composition. *J. Colloid Interface Sci.* **2012,** *365* (1), 275-279.

14. Yu, X.; Zhao, Z.; Nie, W.; Deng, R.; Liu, S.; Liang, R.; Zhu, J.; Ji, X. Biodegradable polymer microcapsules fabrication through a template-free approach. *Langmuir* **2011,** *27* (16), 10265-10273.

15. Xu, W.; Yu, X.; Liang, R.; Liu, S.; Tian, Q.; Deng, R.; Zhu, J. Generation of polymer nanocapsules via a membrane-extrusion emulsification approach. *Mater. Lett.* **2012,** *77*, 96-99.

16. Mayadunne, R. T. A.; Rizzardo, E.; Chiefari, J.; Chong, Y. K.; Moad, G.; Thang, S. H. Living Radical Polymerization with Reversible Addition−Fragmentation Chain Transfer (RAFT Polymerization) Using Dithiocarbamates as Chain Transfer Agents. *Macromolecules* **1999,** *32* (21), 6977-6980.

17. Guo, Y.; Tysoe, M. E.; Zetterlund, P. B. Rate enhanced nitroxide-mediated miniemulsion polymerization: effect of nitroxide water solubility. *Polymer Chemistry* **2013,** *4* (11), 3256-3264.

18. Wolf, F. F.; Friedemann, N.; Frey, H. Poly(lactide)-block-Poly(HEMA) Block Copolymers: An Orthogonal One-Pot Combination of ROP and ATRP, Using a Bifunctional Initiator. *Macromolecules* **2009,** *42* (15), 5622-5628.

Chapter 5

Summary and future outlook

5-1 Summary

In conclusion, the potential of the design of PLA particle structures has been successfully exploited by a combinatorial process of microfluidic emulsification and O/W emulsion-solvent diffusion, coupled with physicochemical phenomena based on interfacial chemistry. In the process, the quick removal of organic solvent from the droplets shortens the preparation time about several hundreds times as opposed to conventional techniques using halogenated solvents. In addition, all components used in the preparations are biocompatible, which is great advantageous to applications for biomedical fields.

The preparation of monodisperse PLA microparticles with a compact structure by microfluidic emulsification and subsequent solvent diffusion was presented and the structural control of the microparticles by introducing o-PEG-*b*-PLA was demonstrated. It was shown that the droplet sizes and the microparticle sizes were controlled from 6 to 50 μm with a narrow size distribution by altering the flow rate ratio of the continuous phase to the dispersed phase as well as PLA concentration in the dispersed phase. The final particle diameters were in good accordance with the theoretical sizes calculated from the sizes of droplets and the initial droplet compositions. Addition of o-PEG-*b*-PLA into the dispersed phase was found to lead to porous structures in the microparticles and the porosity was modulated by changing the blend ratio of PLA to o-PEG-*b*-PLA.

Rapid solidification induced by solvent diffusion from polymer droplets consisting of PLA, EA, and PFOB (non-solvent for PLA) in water was found to be a promising way to tailor microparticle structures. Monodisperse PLA microcapsules encapsulating a liquid oil core were successfully produced by internal phase separation within emulsion droplets during solvent diffusion. The diameter of the microcapsules as well as the core-shell ratio was finely tuned by altering the flow rates upon the emulsification and

the concentration of PFOB in the dispersed phase. In addition, it was found that higher molecular weight PLA used as a matrix retarded the coalescence of tiny PFOB droplets during internal phase separation and gave rise to structural complexity on the surface of the microcapsules, resulting in the microcapsules covered with tiny PFOB droplets, resembling colloidsome. Freeze drying of the microcapsules lead to formation of microcapsules with dimpled surface.

The preparation of monodisperse microcapsules encapsulating a single aqueous core has been generated by spontaneous emulsification from a simple O/W emulsion system during the formulation. The synthesized amphiphilic PLA-*b*-PDMAEMA was found to induce automatic formation of W/O/W double emulsion droplets from O/W emulsion droplets *via* spontaneous emulsification. The final morphology relied on the ratio of PLA-*b*-PDMAEMA to PLA in the dispersed phase, which varied from a compact, multiple cores to a single aqueous core structure as increasing the PLA-*b*-PDMAEMA composition. The diameter of the microcapsules was modulated in the range of 10 to 50 μm in the diameter whilst keeping a relatively narrow size distribution by changing the flow conditions upon emulsification. In addition, it was found that this process allowed dual encapsulation of a hydrophobic substance, Nile red in the shell and a hydrophilic substance, calcein in the core during the formulation. XPS analysis of the microcapsules revealed that PDMAEMA block of PLA-*b*-PDMAEMA existed on the surface of the microcapsules. These results suggest that the proposed microcapsule formation process enables not only to produce monodisperse microcapsules with a single aqueous core in a single step but also to modify the surface of the microcapsules.

The insights gained from this work should stimulate the exploration of novel applications of polymeric microspheres as well as scientific interests in structural control of polymeric microspheres.

5-2 Future outlook

Several important results have been obtained from this work, providing key insights into the parameters essential for design of polymer particle structures. Microfluidic rapid solidification of polymer droplets by solvent diffusion and interfacial phenomena such as internal phase separation and spontaneous emulsification enabled continuous

microparticle formation with well-defined sizes and controlled structures, thereby achieving the aims of this study. Nonetheless, avenues for future research work into applications of the prepared microcapsules as well as functional particle formation still exist.

Firstly, release studies of substances from the prepared microcapsules with different structures should be required to validate the effectiveness of the designed polymer particles as a drug carrier. The sizes of the microparticles as well as the structures of them would be important factors to control the release kinetics of the encapsulated reagents. The *in vitro* release studies will give a guideline how the structures affect the release behaviour.

In addition, this process can be extended to form composite materials with polymer and small additives including polymer/metal, polymer/inorganic material, which would impart the new functionality or enhance the physicochemical properties. One example, fabrication of monodisperse PLA/Fe_3O_4 composite microspheres was carried out using microfluidic emulsification and solvent diffusion and they exhibited magneto-responsive property. However, more studies in terms of the different compositions and the evaluation of their properties should be required.

Regarding microfluidic processing, there is still limitation in the minimum size of the resultant microparticles around 5 μm using microfluidic emulsification, which restricts the application of them as polymeric microspheres. One of the promising approaches is to make use of tip-streaming fluid dynamics formed in flow-focusing microfluidic devices, which makes it possible to create smaller droplets than usual droplets (d ~ 30 μm) in microchannels. Combination of tip-streaming flow and subsequent solvent diffusion would become a breakthrough to generate sub-micron sized polymer particles with a narrow size distribution. Some related works based on numerical and experimental approaches have been carried out in our lab and we have succeeded in preparing PLA nanoparticles around 800 nm in the diameter using tip-streaming and solvent diffusion, however, more sophisticated study is required to form stable tip-streaming and the nanoparticles.

Finally, another point is development of a process for mass production of the polymer microparticles using a microfluidic platform. The productivity of polymer particles in one microfluidic device was quite low, thus, the productivity should be increased by

using parallel type microfluidic devices or a new kind of microchannels, which is important to apply this system to industrial scale.

List of publications

The following papers and communications have been published or accepted during the course of this thesis.

1. Watanabe, T.; Ono, T.; Kimura, Y. Continuous fabrication of monodisperse polylactide microspheres by droplet-to-particle technology using microfluidic emulsification and emulsion–solvent diffusion. *Soft Matter* **2011,** *7* (21), 9894-9897.

2. Araki, T.; Kono, Y.; Ogawara, K.-i.; Watanabe, T.; Ono, T.; Kimura, T.; Higaki, K. Formulation and Evaluation of Paclitaxel-Loaded Polymeric Nanoparticles Composed of Polyethylene Glycol and Polylactic Acid Block Copolymer. *Biol. Pharm. Bull.* **2012,** *35* (8), 1306-1313.

3. Watanabe, T.; Kimura, Y.; Ono, T. Microfluidic Fabrication of Monodisperse Polylactide Microcapsules with Tunable Structures through Rapid Precipitation. *Langmuir* **2013,** *29* (46), 14082-14088.

4. Watanabe, T.; Kimura, Y.; Ono, T. Monodisperse polylactide microcapsules with a single aqueous core prepared via spontaneous emulsification and solvent diffusion. *RSC Adv.* **2014,** *4*, 4872-4877.

5. Watanabe, T.; Lopez, C. G.; Douglas, J. F.; Ono, T.; Cabral, J. T. Microfluidic Approach to the Formation of Internally Porous Polymer Particles by Solvent Extraction. *Langmuir* **2014** in press.